Altered cortical connectivity after experimentally induced long-term potentiation like pain amplification

Master Thesis

Aida Hejlskov Poulsen and Lea Tøttrup Jørgensen
Aalborg University, Biomedical engineering and Informatics

Spring 2017

AALBORG UNIVERSITY
STUDENT REPORT

AALBORG UNIVERSITY
STUDENT REPORT

School of medicine and health
Biomedical Engineering and Informatics
Niels Jernes Vej 12, A5
9220 Aalborg Øst
Telefon 9940 8752
http://www.smh.aau.dk/

Title:
Altered cortical connectivity after experimentally induced long-term potentiation like pain amplification

Theme:
Master's Thesis

Project period:
1st of February -
7th of June, 2017

Project group:
17gr10406

Participants:

Aida Hejlskov Poulsen

Lea Tøttrup Jørgensen

Supervisor:
Carsten Dahl Mørch

Co-supervisor:
Rosa Hugosdottir

Pages: 43 (including appendix: 93)

Concluded: 6th of June 2017

Synopsis:

Long term potentiation (LTP) is a strengthening of plastic synaptic connections. It is considered an underlying mechanisms of chronic pain and results in sensitization. LTP-like pain has previously been induced by conditional electrical stimulation and quantified by psychophysical and EEG data. Recent research in pain processing has been focusing on cortical connectivity, in order to display more complex brain processes. The aim of the present study was to investigate how cortical connectivity is affected by induced LTP-like pain. A 10 Hz increasing form of the exponential current decay pulse was applied for 50 seconds. Psychophysical data to mechanical pinprick stimuli and EEG in a rest recording and a recording during continuous mechanical pinprick stimulation were acquired. Cortical connectivity was assessed by coherence computed subsequent to source reconstruction, using sLORETA. No significant change in pain perception was detected in the psychophysical data or in coherence in the EEG recorded during pinprick stimulation. Significant interaction between time and connections was however observed for the rest recordings in the delta ($p=0.019$), theta ($p=0.0030$) and alpha ($p=0.0080$) bands. The decrease in coherence between the alpha waves in the parietal area and the orbitofrontal cortex was correlated to increase in pain perception. The fact that only EEG rest recordings revealed an effect of CES, may be due to the limited amount of subjects ($n=11$) and an insufficient standardization of stimuli intensity, as not all subjects perceived the CES as painful.

Preface

The report is a master thesis by group 17gr10406 at the 4th semester M.Sc in Biomedical engineering and informatics at Aalborg University, department of Health, Science and Technology. The semester lasted from 1st of February to 7th of June.

Reading guide

All references are cited according to the Harvard method as [author's last name, publication year]. Citations before period indicates the citation is for the particular sentence and citation after period indicates the citation is for the section or from last citation within the section.

Resumé

Langtidspotentiering (LTP) er blevet foreslået som en af mekanismerne bag overgangen mellem akut og kronisk smerte [Sandkühler, 2000, Kuner and Flor, 2017]. LTP er en synaptisk plasticitet, der øger den synaptiske effektivitet og resulterer i en sensibilisering af nociceptive nervebaner. LTP kan induceres ved intens aktivering af nociceptive C-fibre. [Kuner and Flor, 2017] LTP-lignende forstærkning af smerteopfattelse har tidligere været induceret med elektrisk stimulering af raske forsøgspersoner og manifesterede sig som en sensibilisering af stimuleringsområdet (homotopisk) og det nærvedliggende område (heterotropisk) [Klein et al., 2004]. Derudover har studier vist, at den heterotopiske sensibilisering er korreleret med den kortikale aktivitet [van den Broeke et al., 2010], og at plastiske ændringer i relation til LTP sker op gennem hele nervesystemet [Sandkühler and Gruber-Schoffnegger, 2012].

Til vores kendskab er LTP-lignende sensibilisering kun blevet undersøgt kortikalt gennem analyse af *event related potentials* (ERP). Denne type analyse tager ikke højde for den multidimensionale aktivitet, som er identificeret i forbindelse med eksperimentel induceret smerte og hos patienter med kronisk neuropatisk smerte [Friebel et al., 2011]. For at kunne klarlægge nogle af disse komplekse processer har nyere forskning haft fokus på analyse af forbindelserne mellem hjerneområder og hjernens kommunikationsmønstre [Reches et al., 2016]. Formålet med dette speciale var derfor at undersøge, hvordan kortikale interaktioner påvirkes af eksperimentelt induceret LTP-lignende smertesensibilisering.

Et forsøg blev udført, hvor elektroencefalografi (EEG) blev målt før og efter applikation af elektrisk stimulering til inducering af LTP-lignende forøgelse i smerteopfattelsen. EEG blev målt for to tilstande; hvile og under kontinuer mekanisk stimuli. Den elektriske stimulering havde en frekvens på 10 Hz, en længde på 50 sekunder og bestod af en eksponentiel pulsform. Denne stimulation blev givet på den højre arm med en pin-elektrode placeret med periferien 5 cm distalt for cubital fossa. Den venstre arm fungerede som kontrol. Udover EEG blev det psykofysiske respons evalueret ved subjektiv angivelse af smerteopfattelse under mekanisk pinprick stimulering via en visuel analog skala (VAS) fra 0 til 10, hvor 0 var ingen perception af stimulationen, 3 var grænsen mellem perception og smerte, mens 10 indikerede den værst tænkelige smerte. Den subjektive måling blev både foretaget under enkelt pinprick stimuli 10 og 20 minutter før og 10, 20 og 30 minutter efter elektrisk stimulering, samt under kontinuer stimuli, i forbindelse med EEG målingerne, 35 minutter før og 30 minutter efter elektrisk stimulering. Intensiteten af den elektriske stimulering blev sat efter den individuelle forsøgspersons smerteopfattelse. Det optagne EEG data blev projekteret til de bagvedliggende aktivitetskilder gennem sLORETA og kohærens blev beregnet mellem 9 interesseområder, fastsat gennem litteraturgennemgang. Ændringer i hvile og kontinuer stimuli målinger blev analyseret statistisk gennem henholdsvis to- eller tre-faktor repeated measures ANOVA for både den psykofysiske og EEG respons.

En ikke-signifikant tendens til øget sensitivitet til mekanisk stimuli efter elektrisk stimulering på normaliseret data blev observeret. Normaliseret VAS score for mekanisk kontinuer stimuli viste samme ikke-signifikante tendens, dog med stor varians, specielt for den stimulerede arm. Begge arme havde signifikant højere VAS score for de tre minutters stimuli (målt i areal under kurven), efter elektrisk stimulering. Der var ingen korrelation mellem hverken psykofysisk respons og smerteopfattelse under stimuli eller stimuli intensitet. Hverken for bagvedliggende kildeaktivitet i EEG målingen eller kohærens mellem de 9 interesseområder var der signifikant forskel mellem de to arme eller over tid under kontinuer mekanisk stimuli. For hvilemålingen var der derimod signifikant mindre aktivitet i delta frekvensbåndet i den inferiore parietale lap og den postcentrale gyrus. Derudover var der for kohærens en signifikant kohærens mellem tid og interaktivitet mellem interesseområder. Denne interaktion blev fundet for både delta, theta og alfa frekvensbåndene. De mest signifikante forbindelser i delta frekvensbåndet var mellem det orbitofrontale kortex og temporal pole, det primære somatosensoriske kortex og det parietale område. For theta frekvensbåndet var de mest signifikante forbindelser mellem det orbitofrontale kortex og det parietale område, mens

forbindelserne mellem det parietale område og orbitofrontale kortex og perigenual cingulate kortex var mest signifikante for alfa båndet. Endeligt var der, som den eneste forbindelse, signifikant korrelation mellem psykofysisk respons og forbindelsen mellem det parietale område og det orbitofrontale kortex i alfa båndet.

Alle resultater for både psykofysisk respons og EEG analyse skal ses i lyset af, at der kun var 11 forsøgspersoner inkluderet i forsøget. Det kom blandt andet til udtryk ved stor varians for den psykofysiske respons. Eftersom tidligere studier [Xia et al., 2016a, Klein et al., 2004] har observeret signifikante stigninger i smerteopfattelsen efter elektrisk stimuli og dette ikke har været tilfældet i dette speciale, spekuleres der i, hvorvidt LTP-lignende øgning i smerteopfattelse blev induceret. Årsagen til at LTP-lignende smerte ikke blev induceret i alle forsøgspersoner kan være, at der er anvendt en anden pulsform end i tidligere studier. Derudover fandt ikke alle forsøgspersoner den elektriske stimuli smertefuld, hvilket indikerer, at den individuelle intensitetfastsættelse ikke var optimal og dermed kan have været årsag til de ikke-signifikante psykofysiske resultater. At der alligevel var signifikant forskel for EEG hvileoptagelsen kan skyldes, at andre faktorer, som for eksempel forsøgspersonernes koncentration og forventning til stimuli, var ændrede mellem de to målinger.

Med flere forsøgspersoner, samt en mere optimal intensitetsfastsættelse kan analyse af bagvedliggende kilder, samt kohærens mellem interesseområder potentielt øge forståelsen af LTP-lignende smerteprocessering.

Table of contents

Resumé **v**

1 Introduction **1**
1.1 Preliminary question . . . 1

2 Problem analysis **3**
2.1 Long-term potentiation; a cellular model of pain . . . 3
2.2 Cortical processing of pain . . . 6
2.3 Experimental induction and evaluation of long-term potentiation . . . 6
2.3.1 Conditioning electrical stimulation . . . 7
2.3.2 Pain evaluation . . . 8
2.4 Connectivity analysis . . . 10
2.4.1 Linearity . . . 11
2.4.2 Volume conduction . . . 11
2.4.3 Common reference . . . 11
2.4.4 Signal-to-noise ratio . . . 12
2.4.5 Sample size bias . . . 12
2.5 Summary . . . 12
2.6 Problem statement . . . 13

3 Methods **15**
3.1 Experiment . . . 15
3.1.1 Setup . . . 15
3.1.2 Procedure . . . 16
3.2 Data processing . . . 20
3.2.1 Psychophysical data . . . 20
3.2.2 Preprocessing of EEG data . . . 20
3.2.3 EEG data processing . . . 22

4 Results **27**
4.1 Psychophysical data . . . 27
4.1.1 Single pinprick stimuli . . . 27
4.1.2 Continuous pinprick stimuli . . . 28
4.1.3 Relation between pain perception during CES, CES intensity and effect . . . 29
4.2 EEG data results . . . 31
4.2.1 Source reconstruction . . . 31
4.2.2 Coherence . . . 32
4.3 Correlation between coherence and perception increase . . . 35

5 Discussion **39**
5.1 Psychophysical results . . . 39
5.2 Source reconstruction and coherence analysis . . . 40
5.3 Limitations . . . 42

6 Conclusion **43**

References **45**

A Long-term potentiation **53**

B Electroencephalography **55**

C Pilot studies **57**

D Standard operating procedure **67**

E Case report file **73**

F Additional results **75**

G Connectivity analysis and source reconstruction **87**

H Standardized low resolution tomography analysis **93**

Chapter 1

Introduction

Physiological pain is an essential warning mechanism that alerts one to the presence of damaging stimuli. Initially, pain promotes removal of the limb in possible danger as a behavioral response. Subsequent to injury the tissue is more vulnerable and pain during the healing phase protects the tissue from further damage, and allows for rest and recuperation. Normally, the acute pain resolves in consistency with recovery of the initial injury. [Henderson and Di Pietro, 2016] After processing of acute pain, a reappraisal of the pain occurs and the pain may turn into memories, altering future actions [Garcia-Larrea and Peyron, 2013]. However, some individuals experience pain to persist even though the injury has healed, resulting in a chronic pain state, which is a disease on its own. [Henderson and Di Pietro, 2016] The definition of chronic pain varies, however most commonly it is categorized as pain persisting for at least six months [Eriksen et al., 2003]. The prevalence of chronic pain is approximately 19 % in Europe, being more prevalent with age, and more prevalent among women than men [Breivik et al., 2006]. Chronic pain can be either constant or intermittent and is often disabling both physically and mentally [Becker et al., 1997]. The disease is often accompanied by depression, anxiety, physical dysfunction, troubled sleep patterns and social isolation [Breivik et al., 2006]. The health related quality of life (HRQL) in chronic pain patients is consequently highly affected and is among the lowest observed HRQL for any medical condition [Becker et al., 1997].

The transition from acute to chronic pain has been suggested to involve long term potentiation (LTP). LTP is a persistent increase in synaptic strength, meaning the transmission of nerve signals between neurons becomes more effective. LTP of pain thus leads to enhanced excitation in the nociceptive pathways [Sandkühler, 2007]. Long term potentiation and depression (LTD) are believed to induce changes of the cortical map after nerve injury, by strengthening or weakening connections making cortical areas larger or smaller. [Navarro et al., 2007] LTP have been suggested as a model of synaptic plasticity in memory formation and chronic neuropathic pain. Previously, LTP have been investigated in several different types of animals, both in vivo and in vitro. In addition, LTP in hippocampus have been investigated in epileptic patients undergoing invasive surgery. Some of the mechanisms found in animals have been found when inducing an LTP-like state in awake human subjects by non-invasive stimulation. [Cooke and Bliss, 2006] LTP-like increase in pain perception has in several studies been experimentally induced in healthy volunteers, mimicking the sensitized pain condition [Klein et al., 2004, Cooke and Bliss, 2006, van den Broeke et al., 2010]. Electrical stimulation can induce LTP-like increase in pain perception at, and around the area of stimulation [Klein et al., 2004]. Increased sensitivity in the adjacent area have been proposed to be caused by central sensitization with LTP as the underlying mechanism [Klein et al., 2004]. In addition, altered cortical responses have been found after LTP-like increase in pain perception induced by electrical stimulation, indicating LTP to have an effect throughout the central nervous system [van den Broeke et al., 2011]. Both LTP-like pain increase induced experimentally, and chronic pain have previously been investigated using measures of cortical responses. [Martel et al., 2017, Gram et al., 2017, Case et al., 2017]

1.1 Preliminary question

How can experimental long-term potentiation be used as a model of chronic pain mechanisms and how can the long term potentiation-mechanisms be assessed?

Chapter 2

Problem analysis

LTP is a widely studied and well characterized synaptic plasticity [Cooke and Bliss, 2006]. In order to establish LTP as a cellular model of pain, the known mechanisms and important processes are initially described. Additionally, the involvement of LTP in the development of chronic pain is explained. The process of LTP involves both peripheral and central synapses, which should be taken into account when experimentally inducing and evaluating LTP-like pain. Thus the existing evaluation and induction methods are reviewed. Recently, cortical measures of LTP has been of increasing interest, mostly due to the objectivity of such measures and to better understand the central mechanism involved in chronic pain [van den Broeke et al., 2011]. Cortical activity can be analyzed in a number of ways each sufficient for certain types of analysis. Connectivity analysis is an analysis of complex brain activity and the interactivity in response to different environments [Bastos and Schoffelen, 2015]. Even though connectivity analysis has been widely used it has, to our knowledge, not yet been used to investigate the LTP-like increase in pain perception. Such an analysis could produce knowledge on changes in the central processing of pain leading to chronic pain disorders. Consequently, the basics of connectivity analysis are described.

2.1 Long-term potentiation; a cellular model of pain

Pain, and thus the nociceptive system, is essential in order to avoid potential damage and in the occurrence of inflammation or injury, to avoid further damage and allow for recovery. After the exposure to injurious or intense painful stimulation the nociceptive system sensitizes in order to protect the area of injury. This mechanism is mediated by synaptic plasticity. Synaptic plasticity is involved in regulation of synaptic strength and structure and is essential for the adaptive behavior of the nervous system. The synaptic plasticity processes are mostly activity-dependent and the nature of activity (intensity, frequency and duration) is a determinant as to whether a sensitization or a desensitization occurs. Sensitization can be the result of windup or LTP, while desensitization often is a resultant of LTD. [Ji et al., 2003]

Windup is characterized by an increase in the generation of action potentials from dorsal horn neurons, when repeated stimulation is applied [Woolf, 2011]. It is thus a summation of slow synaptic potentials, that produce a cumulative depolarization resulting in sensitization, where the pain to identical repeated noxious stimuli increases for each successive stimulus (see figure 2.1) [Ji et al., 2003]. Windup is a homosynaptic activity-dependent plasticity, which means the sensitization only occurs at the site of stimuli [Woolf, 2011]. The manifestation of windup only takes place during the eliciting stimuli [Ji et al., 2003].

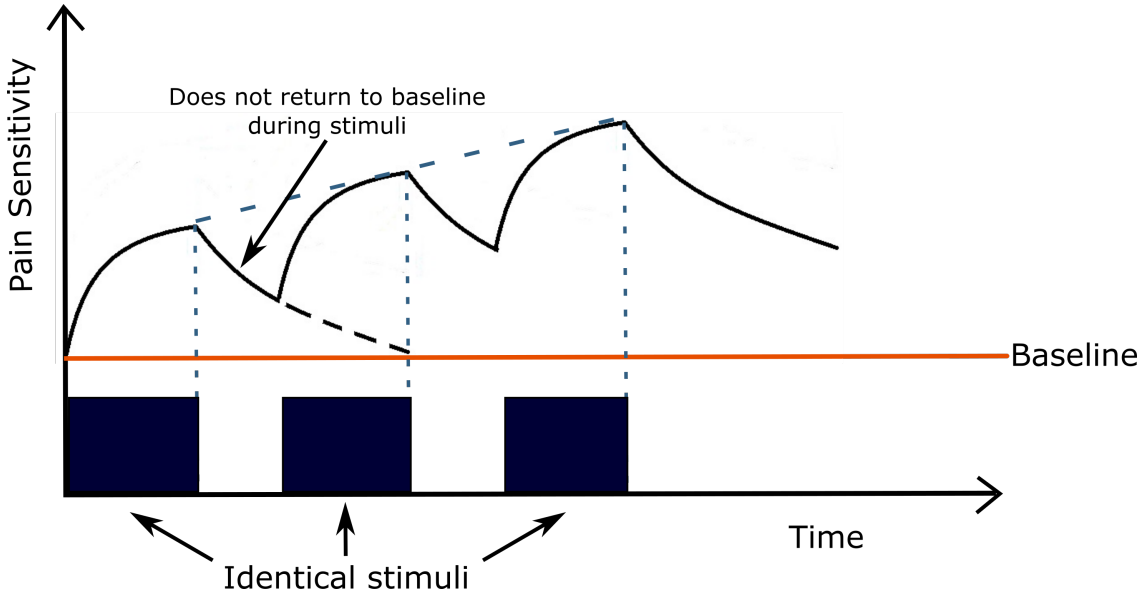

Figure 2.1: Illustration of windup, modified from [Staud, 2006]. When repeated identical stimuli are applied the pain sensation will not return to baseline during the interstimulus interval resulting in increased pain sensation to the same intensity stimulus.

LTP and LTD are more complex processes that involve both homo- and heterosynaptic plasticity and manifest over a longer time period than the windup phenomenon [Ji et al., 2003]. LTP and LTD are opposite mechanisms and convey a long lasting increase or decrease in synaptic efficiency [Cooke and Bliss, 2006]. LTP was firstly discovered in the hippocampus of anesthetized rabbits. Several in vitro studies and later in vivo studies have suggested LTP in the hippocampus to be an underlying mechanism of memory formation and learning. [Bliss and Collingridge, 1993] Subsequent to the discovery of LTP at hippocampal synapses additional animal studies have identified LTP in several different synapses throughout the central nervous system, both at the brain level and the spinal cord [Cooke and Bliss, 2006], including spinal dorsal horn synapses between ascending neuron projections and C-fiber nociceptors [Kuner and Flor, 2017]. LTP is an input specific process in which a single neuronal pathway can be potentiated without affecting inactive input to the same cell. Apart from being long-lasting and input-specific, LTP is likewise characterized by associativity. Associativity is when a nerve is potentiated by a weak stimulus, because a strong stimulus occurs simultaneously, even though the weak stimulus is not strong enough to result in the potentiation by itself. [Cooke and Bliss, 2006]

The initial induction of LTP is considered to be caused by calcium influx activating calcium sensitive enzymes, mediating the persistent pre- and post-synaptic modifications that lead to increased synaptic strength (see figure 2.2). The contribution of pre-synaptic modifications to potentiation is an increased release of neurotransmitters, which is suggested to be mediated by retrograde messengers released at the post-synaptic terminal. [Bliss and Collingridge, 1993] Apart from intercellular signaling, the post-synaptic modifications include altered gene expression (increase or decrease in production of specific gene products) and phosphorylation of receptors. Phosphorylation of receptors results in altered receptor properties in most cases increasing the excitability of the post-synaptic neuron. [Cooke and Bliss, 2006] The gene transcription and protein synthesis may contribute to synaptic remodeling. This remodeling includes a possible increase in the amount of receptors and dendritic spines at the synapse, which like phosphorylation results in increased post-synaptic response to pre-synaptic activity [Kuner and Flor, 2017] (for further elaboration of the physiologic mechanism of LTP see appendix A).

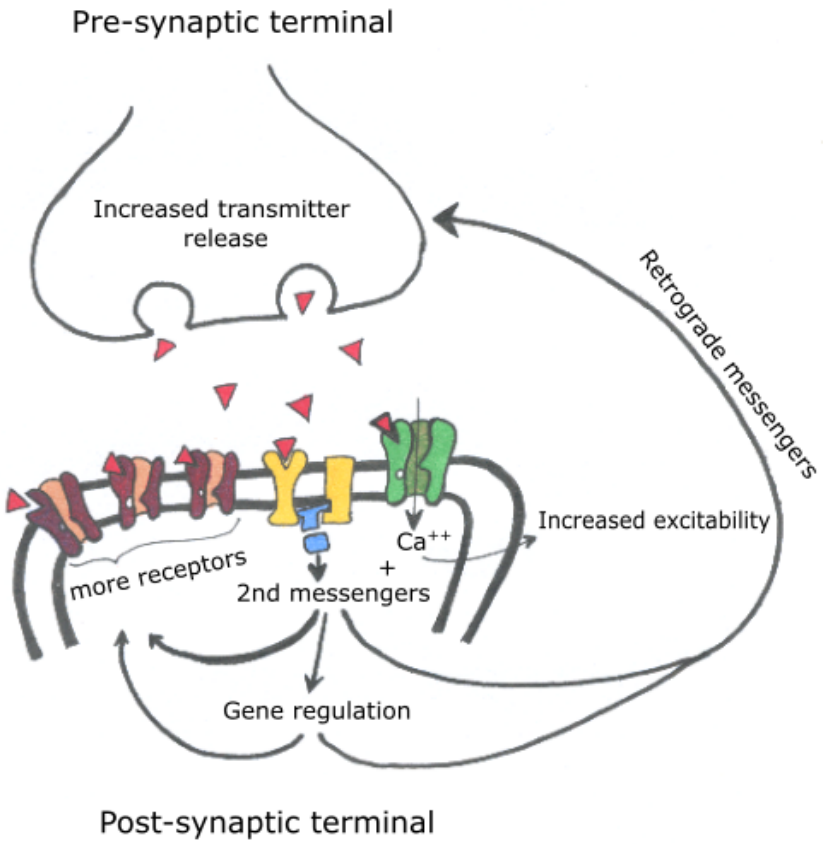

Figure 2.2: Mechanisms in LTP. The activation of the post-synaptic nerve results in the activation of second messengers, that regulate the gene transcription, and contribute to the synaptic remodeling and the increase in transmembrane receptors. Additionally, second messengers may act as retrograde messengers, that signal the pre-synaptic cell to increase the neurotransmitter release when activated. Gene regulation may also play a part in the release of retrograde messengers. All these mechanism mediated by the influx of calcium are contributing to the increase in synaptic strength.

LTP in the nociceptive pathways introduces an enhanced responsiveness of spinal dorsal horn neurons and develops after activating C-fiber nociceptors in an intense fashion [Kuner and Flor, 2017]. Because of the enhanced sensitivity of spinal neurons, LTP of pain has been suggested to be an underlying mechanism of chronic pain [Klein et al., 2004], and an attractive cellular model of central sensitization and the perceptual correlates hyperalgesia (increased pain perception) and allodynia (decreased pain threshold) [Sandkühler, 2007]. The LTP induced hypersensitivity is considered to be a result of increased dendritic spine density, mediated by suppressed expression of proteins that normally acts as a pruning factor at spinal and hippocampal synapses [Kuner and Flor, 2017]. This structural remodeling of spinal dendritic spines leads to the hypersensitivity seen in inflammatory pain states [Kuner and Flor, 2017] and experimentally induced LTP [Sandkühler, 2009]. In neuropathic pain other, not entirely known, mechanisms are involved. Regardless of how spine remodeling is mediated it seems to have a major role in the maintenance of chronic nociceptive hypersensitivity across different types of chronic pain. [Kuner and Flor, 2017] ling is mediated it seems to have a major role in the maintenance of chronic nociceptive hypersensitivity across different types of chronic pain. [Kuner and Flor, 2017]

Several studies have found experimentally induced LTP-like pain in humans to manifest as a sensitization of the conditioned area (homotopic hyperalgesia) as well as the area adjacent to the conditioned area (heterotopic hyperalgesia) [Klein et al., 2004, Lang et al., 2007, Klein et al., 2008,

Pfau et al., 2011]. The homotopic hyperalgesia is characterized by sensitization of nociceptive Aδ- and C-fibres. However, Henrich et al. [2015] concluded that the C-fibre sensitization is predominant in relation to the homotopic effect, since nerve blockers targeting Aδ-fibers did not alter the perceptual correlates. The homotopic area is sensitized to mainly mechanical and thermal stimuli and thus considered to primarily result from an enhanced responsiveness of peripheral nociceptors [Woolf, 2011]. The heterotopic hyperalgesia is characterized is thought to predominantly be a result of central sensitization. [Lang et al., 2007, Woolf, 2011]. When A-fibres were blocked, Henrich et al. [2015] found the heteoropic hyperalgesia after induction of LTP-like pain to be reduced compared to LTP-like pain induced without A-fibre blockage. Thus Aδ-fibres are involved in pain perception of the heterotopic area [Henrich et al., 2015]. These heterosynaptic responses to LTP-like pain are possibly correlated with a neurophysiological response in the cortex [van den Broeke et al., 2010]. Adaptation in the nociceptive, system following pain, occurs along the entire neuroaxis, from synapses to cortical areas [Sandkühler and Gruber-Schoffnegger, 2012].

2.2 Cortical processing of pain

Pain is processed at different levels starting with nociception, to conscious experience of pain ending with pain memory. In the first order pain processing network, the earliest responses to nociceptive stimuli from the spinothalamic system is the posterior insula, medial parietal operculum, and mid-cingulate cortex. When the first response to nociceptive stimuli turns into conscious pain, a second order pain processing network is activated. The most consistent areas in the second order networks, and also often being related to the pain matrix, are mid and anterior insula, the anterior cingulate, and prefrontal and posterior parietal areas. Additionally, although not as consistently, the striatum, supplementary motor area, hippocampus, cerebellum, and temporoparietal junction. All the areas in the second order network are also involved in processes not involving pain and does not evoke pain when stimulated directly. In the third order pain processing network, a reappraisal of the pain happens through activation of perigenual cingulate cortex, orbitofrontal cortex, temporal pole, and anterolateral prefrontal area (see all three levels on figure 2.3). In this reappraisal, the pain is related to emotions and experiences and turns into pain memories. [Garcia-Larrea and Peyron, 2013]

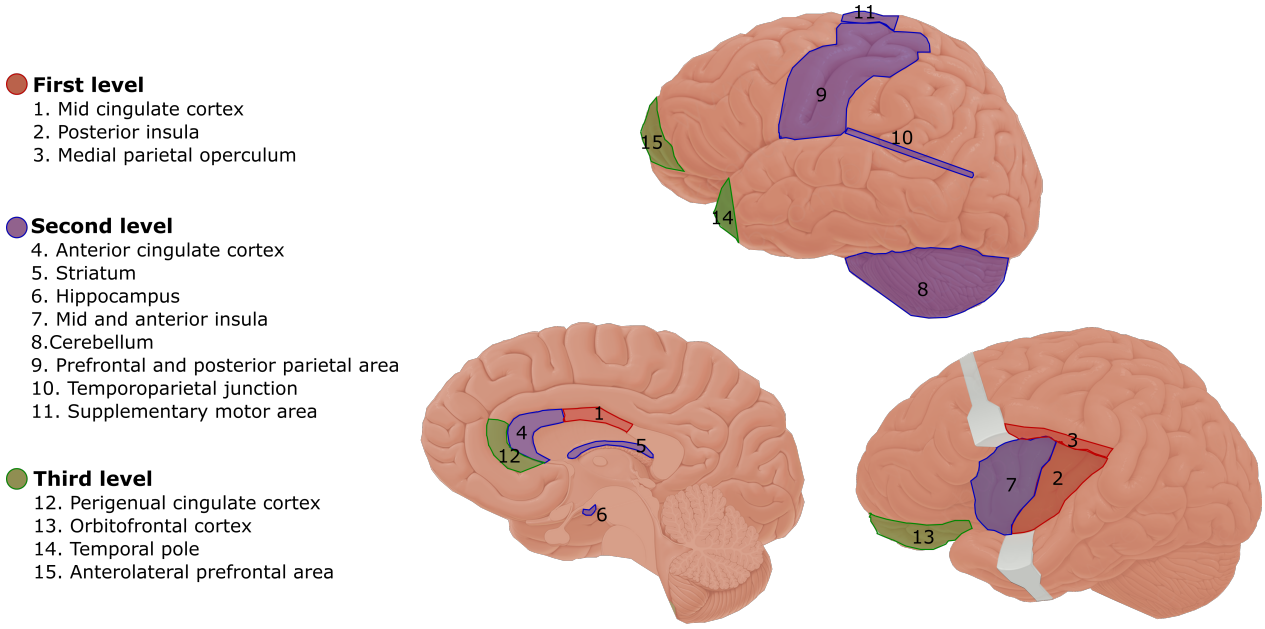

Figure 2.3: First, second, and third pain processing level.

2.3 Experimental induction and evaluation of long-term potentiation

An LTP-like central sensitization have previously been induced in healthy subjects with capsaicin injection [Jutzeler et al., 2015, Mohr et al., 2009, van den Broeke et al., 2015], and electrical stimulation [Klein et al., 2004, Xia et al., 2016b, van den Broeke et al., 2011]. The injection of capsaicin causes central sensitization and mimics an injury and the patterns of homotopic and heterotopic hyperalgesia through activation of peripheral transduction mechanisms of nociceptive afferents. Electrical stimulation of afferent C-fibres have similar hyperalgesia patterns, however modulations are different from the capsaicin, as electrical stimulation directly elicits action potentials and does not depend on intracellular signal transduction processes. [Lang et al., 2007, Weidner et al., 2000] Using capsaicin as a model of pain has its limitations according to some types of hyperalgesia related to central sensitization. For example the capsaicin model does not induce hyperalgesia of some of the nociceptors mediating sensations such as mechanical pain, itch and pleasant touch. [Henrich et al., 2015] Additionally, capsaicin induces a relatively slow rising LTP [Sandkühler, 2007]. Consequently, the following will focus on experimentally induced LTP-like increase in pain perception by conditioning electrical stimulation (CES).

2.3.1 Conditioning electrical stimulation

CES have been used to induce LTP-like pain amplification with different frequencies showing both high (100-200 Hz) and intermediate (10 Hz) frequency stimulation sufficient for LTP-like pain induction [Xia et al., 2016b].

High frequency stimulation (HFS), in the form of 5 trains of 100 Hz rectangular pulses (2 ms) applied for 1 second and with an inter-train interval of 10 seconds, have previously been shown to induce LTP-like increase in pain perception both in C-fibres [van den Broeke et al., 2014] and A$\boldsymbol{\delta}$-fibres [van den Broeke et al., 2011]. [Klein et al., 2004] The intensity of the applied HFS have been investigated by Klein et al. [2004], showing no difference in induced LTP-like pain for intensities of 10 or 20 times the perception threshold. Likewise Hansen et al. [2007] found no differences in induced LTP-like pain connected to the intensity of the stimulation. The HFS experimentally induced LTP-like pain has been expressed both by homotopic hyperalgesia to electrical stimuli [Klein et al., 2004, Pfau et al., 2011] and heterotopic hyperalgesia to mechanical stimuli [van den Broeke et al., 2010, Klein et al., 2006, Hansen et al., 2007, Xia et al., 2016b]. In relation to these findings Klein et al. [2004] only investigated the heterotropic hyperalgesia to mechanical stimuli, and the homotopic hyperalgesia observed by Klein et al. [2004] and Pfau et al. [2011] to electrical pinprick could not be replicated by van den Broeke et al. [2010] and Xia et al. [2016b].

Since the homotopic LTP-like increase in pain to electrical stimuli found by Klein et al. [2004] could not be replicated by Xia et al. [2016b] amongst others, it is speculated that a different stimulation paradigm could optimize the reproducibility. It has been investigated if other pulse shapes are more sufficient for selective activation of small nerve fibres. A model by Hennings et al. [2005a] indicated that small fibres are activated at a lower threshold than thick fibres when using an exponentially rising pulse shape, which corresponds to the findings of Hennings et al. [2005b] who found that exponentially rising pulses can be used to selectively activate thin fibres. Additionally, Hennings et al. [2005b] found indications of pre-pulses to square waves, having an effect on the recruitment order of small and large fibres. This is however in contradiction to the model by Hennings et al. [2005a] who found rectangular pulses with rectangular or ramp pre-pulses to be insufficient in relation to selective thin-fibre activation.

In a study by Hugosdottir et al. [in press] four different pulse forms were investigated in relation to perception threshold when applied with either a pin electrode or a patch electrode. The ratio between perception threshold for the two electrode types and for each pulse form was considered an estimate of the pulse forms ability to selectively activate nociceptors. The highest ratio was observed for the 50 milliseconds increasing form of exponential current decay, suggesting this pulse form to be better for selective activation of nociceptors, than the traditional rectangular pulse form. [Hugosdottir et al., in press] Besides the pulse shape, the pulse width differed from the traditional

HFS paradigm as the best pulse forms in Hugosdottir et al. [in press] were of 50 milliseconds duration, whereas the pulse width in conventional HFS is 2 milliseconds [Klein et al., 2004].

2.3.2 Pain evaluation

Assessing the hypersensitivity brought about by induction of LTP-like pain can help understand the pathophysiologic mechanisms and to investigate the time course and nature of LTP. Such assessment measures can be both subjective and objective. [Fillingim et al., 2016]

Subjective evaluation

Pain is an internal, subjective feeling which make the use of self-report important [Fillingim et al., 2016]. Psychophysically, LTP-like pain is most commonly assessed through ratings of the sensory intensity [Fillingim et al., 2016], using pain scales such as the numerical rating scale (NRS), and visual analog scale (VAS), following electrical stimuli [Klein et al., 2004], mechanical stimuli by pinpricks [van den Broeke et al., 2010, Klein et al., 2004, 2006] and thermal stimuli by laser [Vo and Drummond, 2016, van den Broeke and Mouraux, 2014a,b]. These subjective pain ratings are thus used to asses the sensitization and has been used to identify the degree and the time frame of experimentally induced LTP-like pain [Klein et al., 2004, Pfau et al., 2011, Klein et al., 2008, Lang et al., 2007].

HFS induced LTP-like pain leads to increased pain ratings in the heterotopic area and thus a mechanical sensitization to pinprick stimuli for at least 60 minutes after induction [Klein et al., 2004, Xia et al., 2016b, Pfau et al., 2011]. Klein et al. [2004] and Pfau et al. [2011] tested a longer time frame and found the mechanical sensitization to persist after 3.2 (n=3) and 8 hours (n=55), respectively. In addition Klein et al. [2004] found heterotopic effects to light touch (allodynia) after HFS. For homotopic sensitivity, Klein et al. [2004] and Pfau et al. [2011] found the increased pain ratings to electrical stimuli to last for at least 60 minutes after LTP-like pain induction. Like the heterotopic mechanical sensitization, Klein et al. [2004] found increased sensitivity to homotopic electrical stimuli for 3.2 hours for a subset of subjects and Pfau et al. [2011] found above baseline sensitivity for 8 hours. Sensitivity to thermal stimulation have been found to be enhanced for at least 45 minutes after HFS [van den Broeke and Mouraux, 2014a,b].

Several factors can affect the subjective pain ratings. Dowman [2001] found subjective ratings to change with attention and Clark et al. [2008] found alterations in pain ratings relative to stimulus unpredictability. Opposed to the subjective ratings the objective potentials measured from the brain were unaffected in both studies.

Objective evaluation

Subjective pain ratings have been the standard of pain evaluation, however such ratings only account for perceptual correlates of LTP-like pain. Recent research has introduced objective methods for measurements of the neuronal correlates of LTP-like pain, central sensitization and chronic pain. Manresa et al. [2014] and Manresa et al. [2013] assessed central sensitization through reflex receptive fields. After capsaicin sensitization healthy subjects as well as spinal cord injured patients presented expansion of the reflex receptive field and a lowered nociceptive withdrawal reflex threshold [Manresa et al., 2014]. Similar tendencies has been shown in patients suffering from chronic neck pain and chronic low back pain (LBP) [Manresa et al., 2013]. Other objective approaches include functional image modalities such as functional magnetic resonance imaging (fMRI), magnetoencephalography (MEG), and electroencephalography (EEG) [Wartolowska, 2011]. The method of evaluating the central plasticity through brain activity has been suggested to be highly relevant in the understanding of the central mechanisms of LTP and may be more sensitive and reliable than VAS scores [van den Broeke et al., 2011].

Pain evaluation through brain activity has included analysis of both latency and amplitude of evoked potentials in EEG studies, investigating LTP-like pain. An amplitude increase of event

related potentials (ERP) following LTP-like pain induction has been observed when stimulating the heterotopic site with electrical stimuli [van den Broeke et al., 2010, 2011, 2013], pinprick stimuli [van den Broeke et al., 2016a], vibrotactile stimuli [van den Broeke and Mouraux, 2014a] and selective thermal stimuli of mechano-insensitive C-fibres [van den Broeke and Mouraux, 2014b]. van den Broeke et al. [2016a] found the time course of the brain response elicited in the heterotopic area after HFS by pinprick stimulation to follow the general time course of the increased sensitivity to pinprick. Hence both the sensitivity and ERP amplitude was significantly increased 20 minutes after LTP-like pain induction and remained enhanced for at least 45 minutes. The EEG response to the same pinprick stimulation at the control arm showed a significant decrease in mean amplitude both 20 and 45 minutes after induction of LTP-like pain compared to baseline [van den Broeke et al., 2016a]. Maihöfner et al. [2010] likewise observed increased brain activity to pinprick stimulation after electrically induced heterotopic hyperalgesia. This increased activity was located at the contralateral posterior parietal cortex and the bilateral secondary somatosensory cortex. No difference in activation was observed in the primary somatosensory cortex. [Maihöfner et al., 2010]

In a meta-analysis, Friebel et al. [2011] found 22 and 18 local maxima in brain activity when analyzing experimentally induced pain and chronic neuropathic pain respectively, indicating pain analysis in the brain to be a complex process. In addition, both primary and secondary processes were found. [Friebel et al., 2011] Traditional analysis of ERPs cannot account for this multidimensional activity, as it is focused on a single brain area and most often evaluation of magnitude and latency. Recent research has consequently been focusing on the interactions within the brain to identify communication patterns and to evaluate the contribution of different brain areas in the processing of pain. [Reches et al., 2016] This brain-mapping approach enables an extended display of some of the complex processes.

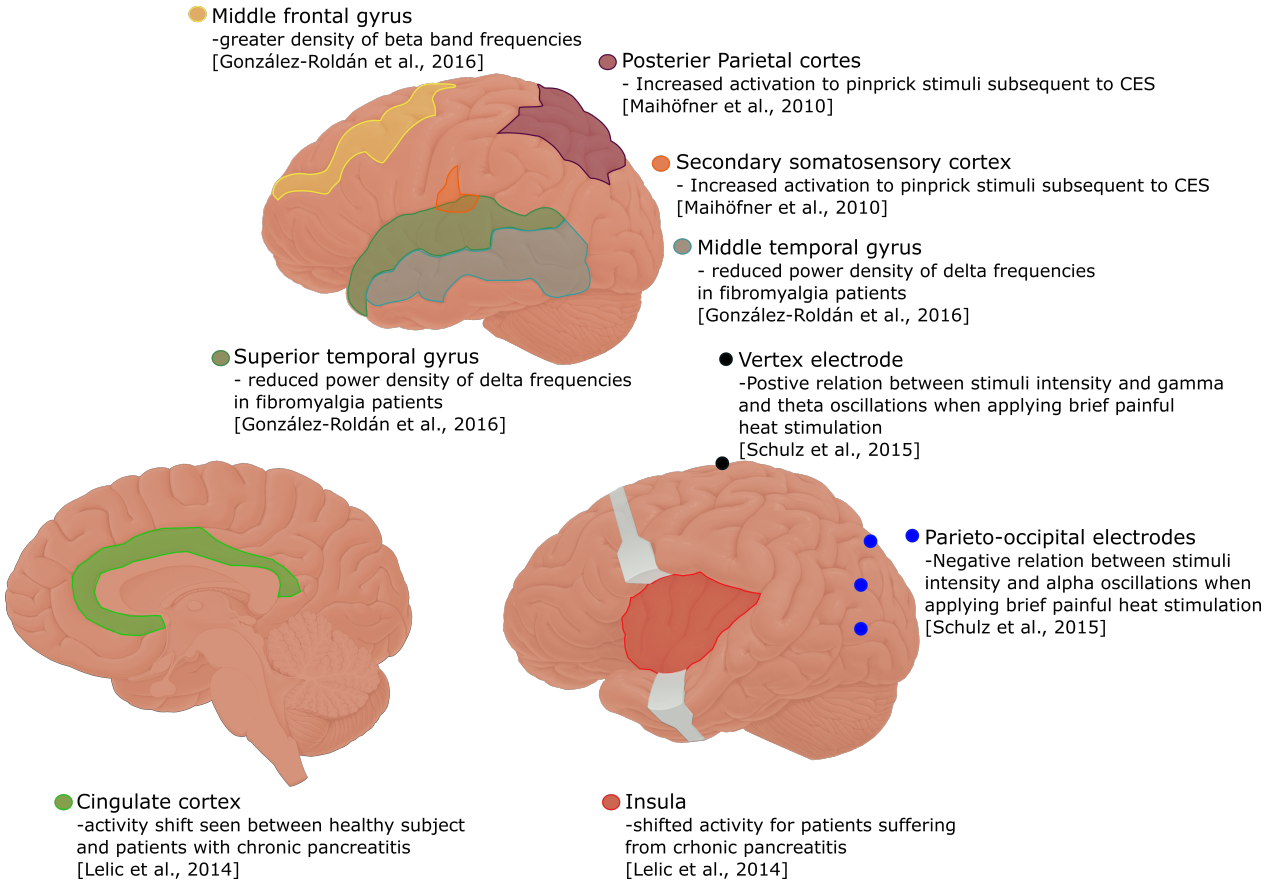

Figure 2.4: Illustration of the brain areas in which pain studies have found significant correlations to pain perception and stimulus intensity.

Lelic et al. [2014] performed both traditional EEG analysis of ERPs and brain source connectiv-

ity analysis to investigate the pain processing in patients suffering from chronic pancreatitis, when stimulating the pancreatic area. The amplitude and latency of ERPs showed no difference between patients and healthy volunteers. The brain source connectivity analysis however, revealed a significant shift of activity in the opercular-insular area and the cingulate cortex in the patient group. The experienced pain correlated to the degree of shift, showing a greater shift in patients with greater pain. [Lelic et al., 2014] González-Roldán et al. [2016] likewise, found alterations of connectivity of the pain network in chronic pain patients. Patients with fibromyalgia exhibited a reduced power density of the delta frequencies at the insula, the right superior and the middle temporal gyri. The power of delta frequencies in the insula were furthermore negatively correlated to the duration of pain. In addition, a greater density of beta band frequencies over the right middle frontal lobe and the midcingulate gyrus together with increased coherence in the left hemisphere was observed in patients when compared to healthy controls.

Connectivity measures has also been used in experimentally induced tonic pain. For brief painful heat stimulation Schulz et al. [2015] found a positive relation between intensity of stimuli and brain oscillation at theta and gamma frequencies, observing the strongest response in at these frequency bands at the vertex electrodes. Additionally, they observed a negative relation of intensity to oscillations at alpha frequencies, strongest at the left parieto-occipital electrodes. The changes in oscillations were found to correlate with the pain perception, suggesting the theta, gamma and alpha responses to be related to the intra-individual variations in the subjective experience of pain. However, the inter-individual variation in pain experience was found to only be related to the theta activity (the reported findings of pain evaluation through brain activity are summarized in figure 2.4). [Schulz et al., 2015]

2.4 Connectivity analysis

Connectivity analysis is focused on the interaction of different brain regions. This type of analysis convey information about the cortical infrastructure of function, where a single functionality may involve a number of specialised regions. The connectivity analysis thus seek to determine the nature of distributed and connected processing in the brain. [Friston, 2011]

Two major subgroups of connectivity analysis exist; functional and effective connectivity. Functional connectivity analysis is a probability distribution over responses [Friston, 2011]. When performing functional connectivity analysis the aim is to capture interdependency between signals, providing information on the temporal correlation between brain regions. The direction of influence is not referenced in functional connectivity measures. [Sakkalis, 2011] Effective connectivity however, aims at describing causal interactions among regions, making such measures more dynamic compared to functional connectivity. [Friston, 2011] A wide range of both functional and effective connectivity measures has been used to quantify neuronal interactions of the brain. When performing connectivity analysis it is important to consider the number and length of epochs, and thus the amount of recorded data, since it has an effect on the stability of the analysis [van Diessen et al., 2015]. For two widely used connectivity measures, phase lag index and amplitude envelope correlation, Fraschini et al. [2016] found the analysis to stabilize at epoch lengths of 6 and 12 seconds, with six epochs, constituting a total data length of 36 and 72 seconds. The sample frequency did not seem to have a substantial effect on the connectivity analysis. The length needed to avoid bias depend on the connectivity measure and whether the analysis is performed in the signal or source space. Performing source reconstruction prior to connectivity analysis decreases the needed epoch length. [Fraschini et al., 2016]

When performing connectivity analysis all channels can be taken into account or each pair of channels can be analyzed separately. The pairwise bivariate approach often provides more stable results, however it is with such an approach not possible to distinguish between direct and indirect interactions. Consequently, spurious measures could be obtained in the situation of a third source providing a common input (indirect interaction) to the signal pair under analysis. [Bastos and Schoffelen, 2015]

In addition to the problem of common input, some general challenges exist when performing con-

nectivity analysis. Mostly these challenges are experimental biases that influence the connectivity measures and their interpretation. In addition to experimental biases a number of assumptions must be made, for instance about linearity. When choosing which connectivity measure to use, the experimental design and the corresponding challenges must be accounted for. [Bastos and Schoffelen, 2015]

2.4.1 Linearity

Linear approaches are widely used, and compared to non-linear measures, straightforward to compute and interpret. However, neural processes and neural activity in general have non-linear characteristics that will not be quantified by linear methods [Sakkalis, 2011]. Consequently, a number of non-linear connectivity measures have been suggested making it possible to identify non-linear dependencies within the brain. [van Diessen et al., 2015] These non-linear approaches are however more complex and highly susceptible to noise. Additionally, the linear methods are more robust than non-linear methods and since the linear methods often perform well even in non-linear cases, the non-linear methods are often used to compliment linear methods in order to add information not accessible by linear methods. [Sakkalis, 2011]

2.4.2 Volume conduction

Volume conduction is basically the current flow in tissues adjacent to an active neuronal source which, especially when using surface electrodes, causes several electrodes to record activity from the same source, and thus when several sources exist the electrodes pick up activity from multiple sources. This is due to the fact that surface electrodes are placed far away from the actual neural source and that the scull introduces spatial blurring of the electrical potentials. [Bastos and Schoffelen, 2015] The spatial signal spreading is a challenge, since it may cause misleading results stating a non-existing neuronal interaction among regions. The results would then be due to the channels picking up the same neuronal source, rather than reflect true interactions. [Bastos and Schoffelen, 2015, Stam and van Straaten, 2012]

The effect and influence of volume conduction cannot be completely removed, however it can be minimized either through the application of source reconstruction prior to connectivity analysis or by using phase-based connectivity measures that discard signal contributions of 0 or 180 degree phase differences. When performing source reconstruction, the signal is projected back to the underlying sources and some volume conduction is thereby canceled. Only signals from the same source will have a 0 or 180 degree phase differences and by discarding these, only signals from different sources is compared in a connectivity analysis. [van Diessen et al., 2015] Such connectivity measures take advantage of the instantaneity property of volume conduction, which means a dominant neuronal source visible on several channels will result in similar phase observations at those channels. [Bastos and Schoffelen, 2015] Source reconstruction often adds complexity to the data analysis and may influence obtained correlations between source-based signals [Stam and van Straaten, 2012]. Source reconstruction is an inverse problem that only provides a unique solution when constraints and assumptions are made. Additionally, even though mapping to the source space does account for volume conduction it cannot remove the effect completely. [van Diessen et al., 2015] The phase-based connectivity measures may detect true interactions between signal components, however the measures are unable to detect interactions near zero-phase difference [Bastos and Schoffelen, 2015].

2.4.3 Common reference

Using a common reference may cause spurious connectivity estimates due to signal fluctuation at the reference electrode, which will be reflected at all electrodes [Bastos and Schoffelen, 2015]. The effect of the common reference is both spatial and temporal. If a substantial amount of noise is present the choice of reference may affect the signal-to-noise ratio at some electrode sites. The location of the reference is also important in relation to the regions of interest, since different reference locations will add or subtract a constant value, which may result in mistaking the activity of interest as noise

or vice versa. When fluctuations occur at the reference electrode, it is reflected in the remaining electrodes and thus add a non-constant temporal component to the signal. [Yao, 2001] This may yield faulty correlations at zero time lag. Connectivity measures that are sensitive to zero time lag correlations are thus highly affected by fluctuations at the reference electrode. The extent of influence is dependent on the power of fluctuations and the chosen location for the reference electrode. When the reference fluctuations are strong, and a weak neuronal coupling exist, the artefactual coherence caused by the common reference may dominate making it difficult to detect the true interaction. [Bastos and Schoffelen, 2015]

Using separate references for all channels would eliminate the artefactual coherence component, however it may not be practically feasible [Bastos and Schoffelen, 2015]. Methods of re-referencing the signal prior to analysis is thus often used in order to overcome the common reference problem [Bastos and Schoffelen, 2015, van Diessen et al., 2015]. The aim of re-referencing is to minimize the influence of fluctuations at the reference, by either removing the reference signal from the channels or by introducing a new reference with neutral potential [Bastos and Schoffelen, 2015, van Diessen et al., 2015].

2.4.4 Signal-to-noise ratio

All measured signals contain signal-of-interest and noise. When analysing the signal, it is important to be certain that a difference between two conditions is due to changes in the signal-of-interest and not merely changes in noise resulting in a different signal-to-noise ratio (SNR) between measurements or subjects. Some connectivity measures can be corrupted by SNR if this changes between measurements. Methods comparing signals at different times or two time series' ability to predict one another are vulnerable to changes in SNR. When affected by changes in SNR, a found connectivity can be a result of an asymmetric relation between signals if one signal is more affected by noise than the other. [Bastos and Schoffelen, 2015] In addition when one signal is affected more by noise a change in correlation can be found when comparing signals [Friston, 2011].

Methods exists that are more robust to changes in SNR when SNR-problems cannot be addressed experimentally. These methods takes both the signal-of-interest and noise into account by modeling the two parts of the signal. [Bastos and Schoffelen, 2015]

2.4.5 Sample size bias

Sample size can bias the connectivity analysis both when the sample size differ between measures and for some methods, when the sample size is small. When the sample size is too small the connectivity may be overestimated and the result may show non-present interactions. For this reason it is sometimes necessary to normalize to the number of measures. [Bastos and Schoffelen, 2015] To which degree the results are affected by the sample size bias depends on the type of connectivity measure used. [van Diessen et al., 2015]

The bias on the results can be decreased with a larger sample size. In addition, sample size bias can be reduced with a bootstrap procedure by repeatedly performing the analysis on randomly selected trails. [Bastos and Schoffelen, 2015] In addition to larger sample size an equal number of measures in the compared groups and epochs of equals length reduces the sample size bias. [van Diessen et al., 2015]

2.5 Summary

LTP is a strengthening of the synapses which leads to sensitization. This sensitization is often helpful in order to avoid further damage after injury and to allow for recovery at the injury site. [Ji et al., 2003] Sustained LTP of pain is considered an underlying mechanism of chronic pain [Woolf, 2011].

LTP is induced at the cellular level and is initially mediated by calcium influx at the post-synaptic neuron. The calcium influx contribute to the synaptic changes by activation of second messengers and subsequent gene regulation. At the post-synaptic neuron new dendritic spines are

formed and additional receptors emerge at the cell membrane. Additionally, retrograde messengers are released into the synapse and cause modifications at the pre-synaptic neuron, leading to increased neurotransmitter release, whenever the neuron is activated. All these mechanisms are involved in the strengthening of synapses along the entire neuromatrix. [Kuner and Flor, 2017] The synapse strengthening manifest as hypersensitivity, which is present both at the conditioned area and adjacent to the conditioned area [Woolf, 2011]. LTP-like increase in pain perception can be induced experimentally by intense activation of C-fibre nociceptors [Kuner and Flor, 2017]. The homotopic sensitization after peripheral LTP-like pain induction is considered a peripheral sensitization, whereas the heterotopic sensitization is considered a central mechanism which is correlated to neurophysiological responses in the cortex. Consequently, LTP-like increase in pain perception can be evaluated both subjectively by the use of pain scales and objectively by recordings of the cortical response. [van den Broeke et al., 2010] It has been suggested that plastic changes at the brain level is a contributing cause of chronic pain [Navarro et al., 2007]. It is thus particular interesting to investigate the cortical response to LTP of pain.

Previous studies have analyzed ERP to painful stimuli before and after experimentally inducing LTP-like pain. [van den Broeke et al., 2016b] The traditional ERP analysis can however not account for the multidimensional activity and several local maxima, which has been identified in experimentally induced pain and chronic neuropathic pain [Friebel et al., 2011]. In order to enable an extended display of some of the complex brain processes recent research has been focusing on connectivity analysis as a way to quantify interactions within the brain and to map communication patterns between brain regions [Reches et al., 2016]. However, to our knowledge connectivity analysis has not previously been used to investigate the cortical response in LTP.

2.6 Problem statement

How is the cortical interactivity affected by experimentally induced long-term potentiation-like pain?

Chapter 3

Methods

The aim of the present study was to investigate the effect of experimentally induced LTP-like pain on cortical interactivity. Accordingly, an experiment was conducted measuring brain activity prior and subsequent to an experimentally induced LTP-like increase in pain perception. Psychophysical data were likewise recorded to be able to combine subjective and objective evaluation and thus get a wider perspective on the induced LTP-like pain. Subsequent to data acquisition, the psychophysical data and the cortical data were analyzed separately. The psychophysical data for different conditions were analyzed and tested statistically. The cortical data however were initially preprocessed to account for both noise and physiologic artefacts. The main data processing of cortical activity included three steps; source reconstruction, connectivity analysis, and statistical analysis.

3.1 Experiment

The experiment was conducted according to the Helsinki Declaration and approved by the local ethics committee (Approval no.: VN-2016/76).

3.1.1 Setup

The subject was seated comfortably in a chair with both arms placed on a table in a supine position. An EEG cap with 64 active EEG electrodes was placed upon the subject's head according to the 10-20 standard. EEG was sampled with 1200 Hz and the impedance kept under 30 kΩ. For a more selective activation of nociceptors a punctuate electrode with small diameter cathodes placed in a circular frame and with a steel anode outside the pin area was used, based on the method used in Lelic et al. [2012], Xia et al. [2016b], and Petrini et al. [2014]. Electrodes were placed on both arms in order to be able to account for the effect of the electrode pins, however only the electrode on the right arm was connected to the stimulator. The electrodes were placed with the periphery 5 cm distal to the cubital fossa and the VAS meter was placed between the subject's hands, for easy scoring with both hands (see electrode placement on figure 3.1). The VAS ranged from 0 to 10, where 0 was no pain, 3 was the border between pain and no pain, and 10 was unbearable pain. The acquisition and stimulation equipment was placed turning away from the subject (see setup on figure 3.2) to minimize possible bias of expected stimulation or seeing results.

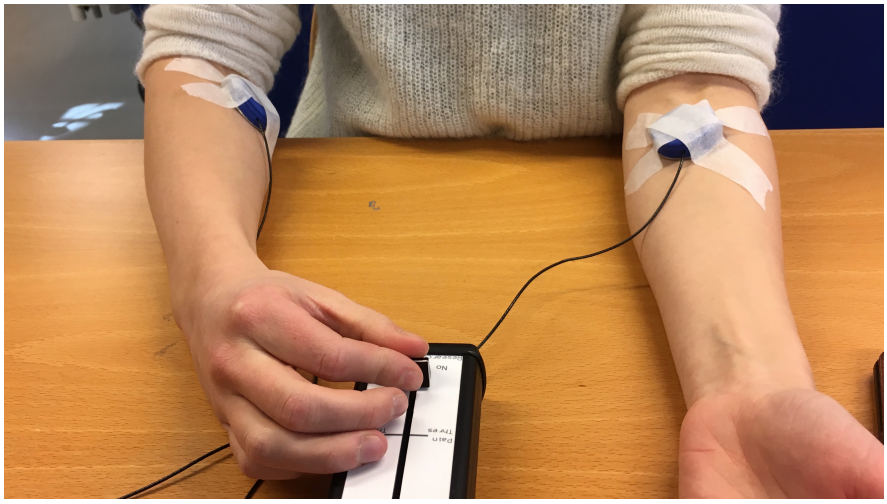

Figure 3.1: The electrodes were placed on both arms with the periphery of the electrode 5 cm distal to the cubital fossa and the VAS meter was placed between the subject's hands.

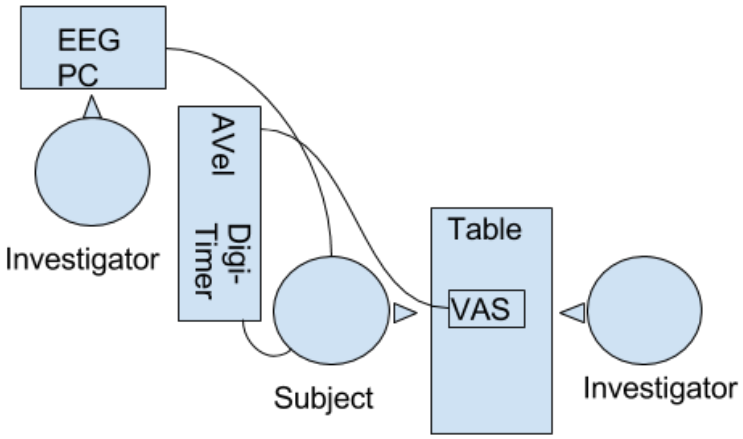

Figure 3.2: Experimental setup. One experiment investigator controlled the computers, and stimulator used in the experiment. The other investigator instructed the subject and performed pinprick stimuli. AVel was the software used for electrical stimulation and recording of psychophysical data.

3.1.2 Procedure

The experiment consisted of one session with two EEG recording blocks, 6 single pinprick blocks and a CES block (see figure 3.3).

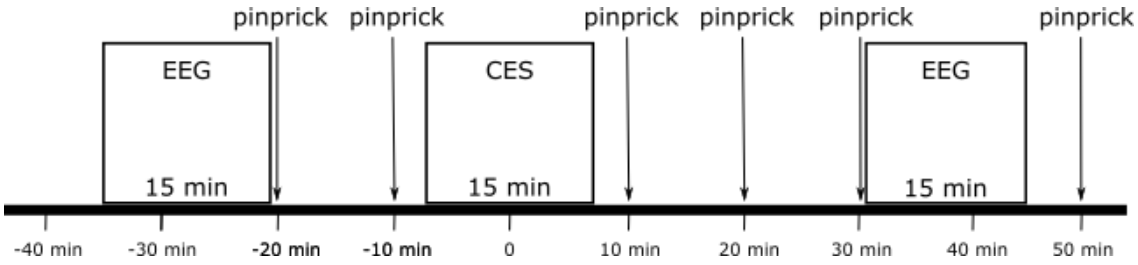

Figure 3.3: Experimental time line. EEG recordings were performed 35 minutes prior and 30 minutes subsequent to CES, while single pinprick test stimuli were applied 10 and 20 minutes prior and 10, 20, 30, and 50 minutes after application of CES.

EEG recording block

The first EEG block was performed 35 minutes prior to CES, while the second block was performed 30 minutes subsequent to CES. The EEG measurement 30 minutes after CES was chosen based on the findings by Klein et al. [2006], showing punctuate hyperalgesia to develop immediately after CES and increase slightly before peaking between 40 and 60 minutes subsequent to CES. Even though the stimulation paradigm differed from that by Klein et al. [2006], it was assumed the induction and time course of hypersensitivity would be similar. Each of the EEG blocks contained one rest recording and two recordings during continuous pinprick stimulation, one on each arm (see figure 3.4 and for further elaboration of procedure see appendix D).

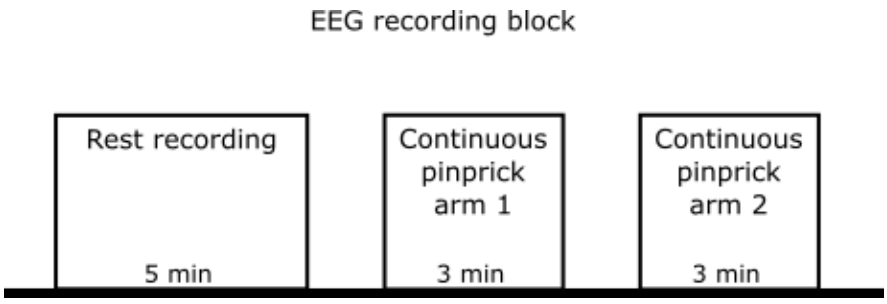

Figure 3.4: Time line for the two EEG recording blocks. Each block started with a five minute rest recording followed by two three minute recordings during continuous pinprick stimulation, one on each arm.

Resting state EEG has been of increasing interest as a network analytical approach [van Diessen et al., 2015] and was consequently acquired prior to and subsequent to CES to analyse possible potentiation. EEG recordings during continuous pinprick stimulation was performed in order to evaluate the the processing of painful stimuli and the CES induced LTP-like pain effect on the cortical pain processes. Continuous pinprick stimulation was performed manually with a relatively low frequency of 0.5 Hz, to minimize the possible windup effect. Additionally, to avoid windup the stimulation site was randomized within an area 2-2,5 cm from the center of the electrode. This test stimulation zone, adjacent to the conditioned site, was chosen in order to evaluate the the central mechanism involved in the CES response. van den Broeke et al. [2010] found the sensitivity to be different proximal, distal, lateral and medial to the electrode. Consequently, the stimulation area was further divided into four sections, two in which continuous stimulation was performed and two for single pinprick test stimuli, according to dermatomes (see stimulation areas and dermatomes on figure 3.5). The division of single pinprick stimulation zone and continuous stimulation zone additionally made sure that the continuous pinpricking procedure would not affect the area and thus the results of single pinprick. The subject was instructed to continuously rate the sensation of the continuous pinprick stimuli on the VAS meter in order to evaluate the perception of the stimuli and to be able to correlate neural effects and perception.

The weight of the pinprick used for continuous pricking was determined prior to the initial EEG recording, through an average of VAS ratings. In order to be able to evaluate the cortical effect of CES on pain processing the weight determination aimed at a VAS rating between 3 and 4 (for further elaboration of the weight determination see appendix D).

To ensure a sufficient data amount for the connectivity analysis five minutes of recording for each condition (rest and continuous pinprick) was preferred. However, to avoid substantial sensitization due to pinprick the continuous pinprick recording was abbreviated to three minutes (see preliminary study in appendix C).

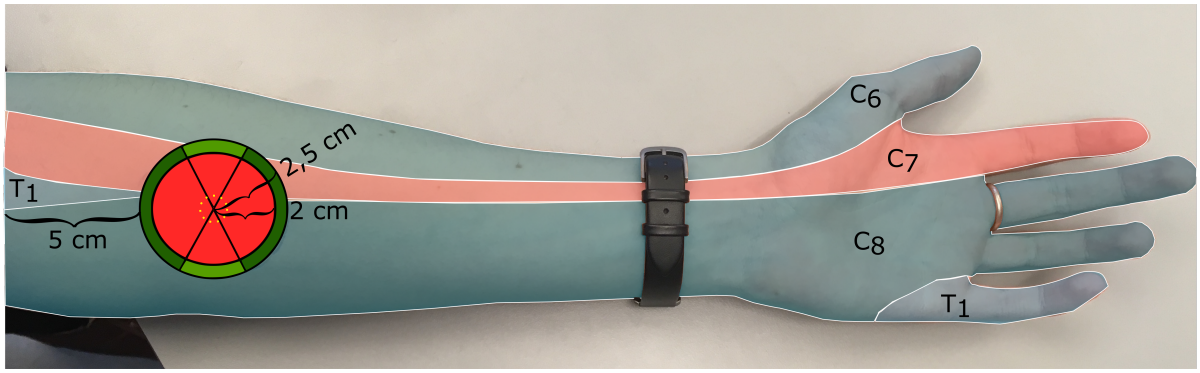

Figure 3.5: Stimulation sites. The stimulation area was placed with the electrode periphery 5 cm distal to the cubical fossa. The red area was the stimulation site for CES (radius of 2 cm). The yellow dots represent the electrode pins. The green areas were used for pinprick stimulation. The dark green area was the stimulation site for continuous pinprick, and the light green area was the stimulation site for single pinprick. The division of the arm indicates different dermatomes [Martini et al., 2012].

Single pinprick block

A total of six blocks of single pinprick were performed in order to evaluate the psychophysical response to CES adjacent to the conditioned zone (see light green area on figure 3.5). In order to analyse the time course of the CES response, single pinpricks were performed 10 and 20 minutes prior to CES and 10, 20, 30, and 50 minutes subsequent to CES. For each of the six blocks, the subject was asked to rate eight single test stimuli with a pinprick weight of 25.6 g on each arm. The choice of pinprick weight was based on findings of Xia et al. [2016a] and on a preliminary study. Xia et al. [2016a] found the 30 g and 50 g pinprick weights to be more suitable for quantifying sensitization than the 12.8 g weight. Additionally, the preliminary study testing available weights of 6.4, 12.8, 25.6, and 50,1 g (see appendix C) indicated the 25.6 g weight to be most suitable. The pinpricks were performed in a randomized fashion within the defined stimulation zone to avoid windup (see elaboration of procedure in appendix D).

Conditional electrical stimulation

The CES block included a training period, a determination of perception threshold, a determination of stimuli intensity, and finally the application of CES (see figure 3.6).

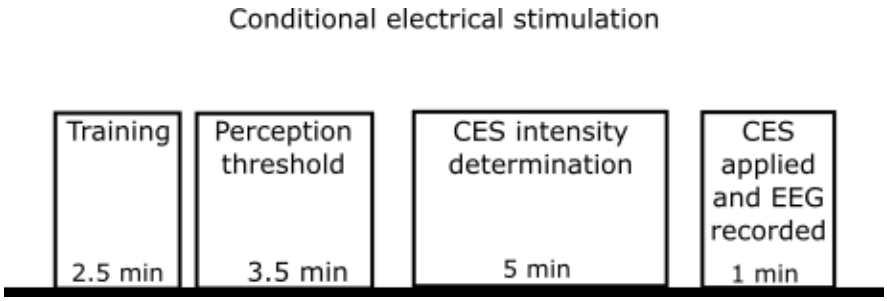

Figure 3.6: The block of CES contained an initial training period followed by a perception threshold determination. Subsequently, the stimulation intensity was determined and CES applied.

The pulse shape and duration of CES were chosen based on a preliminary study (see appendix C) and findings by Hugosdottir et al. [in press]. In both Hugosdottir et al. [in press] and the preliminary study, a 50 miiseconds exponential current decay pulse with a trailing phase was more sufficient than the conventional rectangular pulse shape. A exponential pulse shape activated nociceptive fibres more selectively [Hugosdottir et al., in press]. In the preliminary study, investigating the LTP-like increase in pain, sensitivity induced by either conventional HFS or an exponential pulse, the exponential current decay pulse induced a slightly larger increase in pain perception. Additionally,

a decreased stimulation intensity was needed for the exponential current decay pulse to induce LTP-like increase in pain perception. Consequently, the CES was applied as a 50 seconds stimulation of a 10 Hz increasing form of the exponential current decay with an exponential trailing phase (see pulse equation 3.1 and shape on figure 3.7).

$$i(t) = \begin{cases} \frac{I_s}{1-e^{\frac{-T_s}{\tau}}} \cdot (1 - e^{\frac{-t}{\tau}}), & 0 \leq t < T_s \\ I_s \cdot e^{\frac{-t}{\tau_{tr}}}, & T_S \leq t \leq T_{tr} \end{cases} \tag{3.1}$$

$\boldsymbol{T_s = 0.4}$, $\boldsymbol{I_s}$ - *intensity, current controlled by stimulator* $\boldsymbol{\tau = (T_s/2)}$ - *time constant for the increasing current,* $\boldsymbol{T_{tr} = 0.5}$, $\boldsymbol{\tau_{tr} = \tau/6.6}$ - *time constant for the trailing phase*

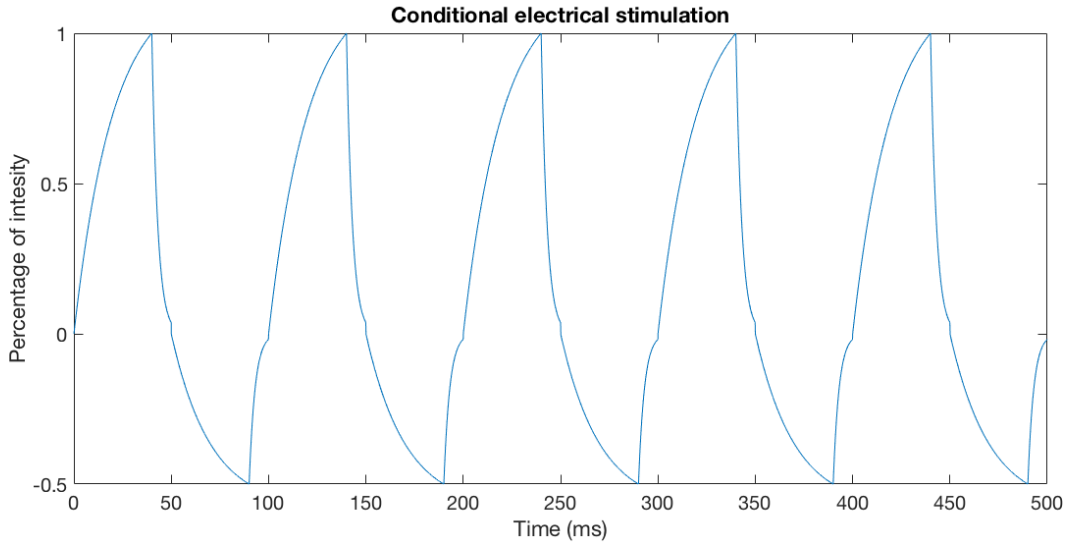

Figure 3.7: A representation of the CES stimulation with 0.5 second pulses

The training period was performed to familiarize the subject to the stimuli sensation, in order to get a better determination of the perception threshold and the stimulation intensity (see procedure in appendix D). Subsequent to training the perception threshold was determined through the method of limits, with three ascending and three descending measures and a step size of 5 %. To minimize the number of stimuli needed for determination and thus minimize possible sensitization from the determination stimuli, the perception threshold was used as starting point for the intensity determination. Single stimuli pulses were used for each step (see elaboration of procedure in appendix D).

The CES intensity determination was performed as a staircase method targeting a VAS of 4. A VAS score of 4 was expected to result in a VAS score of 6-7 with the 50 second stimulation. The staircase methodology was chosen in an attempt to minimize the number of stimuli given prior to the application of CES and the standardization of intensity to a VAS of 4 was selected based on a preliminary study (see appendix C) and preliminary testing of the CES pulse shape for different stimulation lengths. In order to mimic the sensation produced by the CES and to make the stimulation easier for the subjects to rate a 0.5 second stimuli of the CES pulse form was used. The intensity was initially increased in steps of 50 % till a VAS rating of 4 was achieved. Subsequently, the intensity was decreased with a step size of 20 % till the VAS score was below 4. Two additional measures, one ascending and one descending was performed, with intensity step sizes of 10 % and 5 %, respectively. The stimulation intensity for the CES was determined by the average value of the two ascending and two descending measures (see further elaboration of procedure in appendix D).

3.2 Data processing

For both the psychophysical data and EEG, the analysis were performed in *MATLAB R2017a* and *IBM SPSS statistics 24*. Unless otherwise mentioned, all statics were performed in *IBM SPSS statistics 24*. In addition *KEY-LORETA* was used for source reconstruction of EEG data.

3.2.1 Psychophysical data

The VAS ratings for single pinprick stimulation and continuous pinprick stimulation were processed separately using different methods. Additionally, the continuous VAS rating during CES was analyzed.

The increase in perception caused by CES was computed as the percentage difference between VAS scores of the condition and control arm for the four single pinprick measurements subsequent to CES. In order to investigate if the number of subjects was sufficient, a power analysis was performed using the standard deviation ($\boldsymbol{\sigma}$) of the percentage increase in perception, an alpha level of 5 %, and a desired power (1-$\boldsymbol{\beta}$) of 90 % (see equation **(3.2)**).

$$\boldsymbol{n = 2 \cdot \frac{(Z_{\alpha/2} + Z_{\beta})^2 \cdot \sigma^2}{d^2} = 2 \cdot \frac{(1.96 + 1.2816)^2 \cdot \sigma^2}{d^2}} \tag{3.2}$$

with Z being a table value, and d being the effect size [Kadam and Bhalerao, 2010]

Single pinprick stimuli

An average of the eight VAS ratings during the single pinprick stimulation for each time point was used for the data processing. The purpose of the statistical analysis was to identify significant differences in VAS ratings over time and between the condition and control arm. Prior to this analysis a Shapiro-Wilk test was performed to test for normality. Since the Shapiro-Wilk test could not reject the null-hypothesis of normality ($\boldsymbol{\alpha} = 0.05$) a two-factor repeated measures ANOVA was performed with time (a total of four time points; 10, 20 30, 50 minutes, after CES) and arm (to levels; condition and control) as the within-subjects factors. Baseline measurements (-10, -20 minutes relative to CES) were averaged and included as a co-variant.

Continuous pinprick stimuli

The first three seconds of VAS scores during the continuous pinprick stimulation was excluded from the analysis, due to the initial trailing phase. The area under the curve (AUC) was calculated for each arm before and after CES using the integral function *trapz*. To check for significant differences in time and between the AUC of the condition and control arm a repeated measures ANOVA was performed. The within subject factors were time (six time points) and arm (to level; condition and control). For significant ANOVA results, post hoc testing was performed as a paired t-test with Bonferroni correction.

3.2.2 Preprocessing of EEG data

An EEG signal is subject to both non-physiological and physiological noise. Non-physiological artefacts include line noise from the external electrical equipment (50 Hz noise) and possibly noise from the EEG system itself raised by poor electrodes or poor electrode contact, electrode position, cables, and the amplifier. [Cao et al., 2015] The EEG system was checked and impedance kept under 30 k$\boldsymbol{\Omega}$ prior to and during each experimental session and thus the noise originating from the equipment could be neglected in the data processing. The line noise was evaluated by spectral analysis (see figure 3.8), which indicated the need for a notch filter in the preprocessing of the EEG. Additionally the spectral analysis showed an influence of a DC component, illustrating the need for a high pass filter. The high pass filter was implemented as a second order butterworth filter with a cutoff-frequency of 0.05 Hz. Subsequent to filtration of the DC component, the data were passed

through a second order butterworth notch filter with cutoff frequencies of 49 Hz and 51 Hz (see the effect of the high pass and notch filter in figure 3.8).

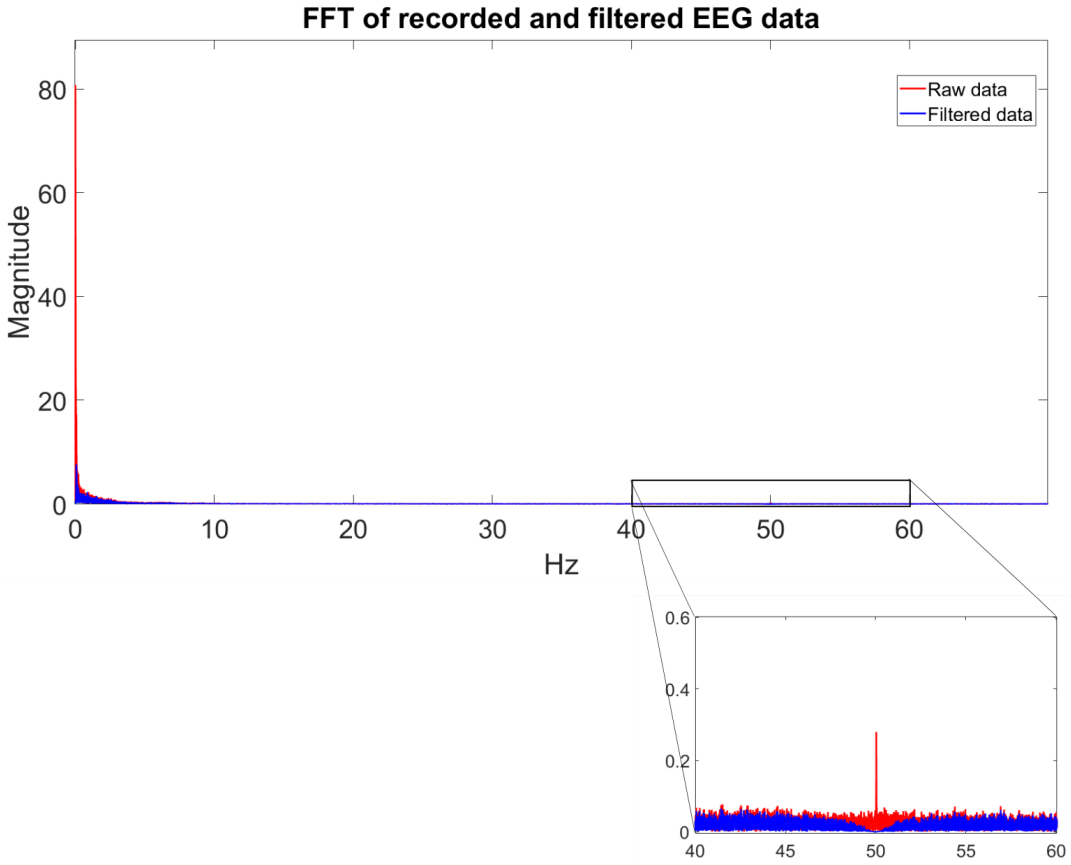

Figure 3.8: FFT of raw and filtered EEG data (subject 2, post CES rest recording). Red is the FFT of the raw EEG recording. Blue is the FFT subsequent to filtering.

The physiologic artefacts can be divided into three subgroups [Cao et al., 2015]:

- **Movement artefacts** caused by movement of the head and body.
- **Bioelectrical potential artefacts** that include bioelectric signals caused by blinking and movement of the eyes and facial muscles. Electrical potentials generated by the heart may also interfere with the recorded signal.
- **Skin resistance** may change during the recording session due to sweating and vasomotor activities and thus influence the signal.

Physiological artefacts such as blink, and larger head and body movements and movements of facial muscles can be identified by visual inspection of the EEG, since the bioelectrical potential artefacts are of greater amplitude than brain signals. These artefacts were rejected through visual inspection as the recordings were sufficiently long, for rejections of data not to affect the stability of the connectivity analysis. Rejection was performed using the *MATLAB* toolbox *EEGLAB*. Pulse artefacts were considered negligible and skin resistance artefacts were considered small and partly accounted for by impedance check during the experiment.

After the artefact rejection, the data were truncated to an equal amount of epochs of 12 seconds for all subject and for each of the two conditions; rest and recording during continuous pinprick stimuli.

3.2.3 EEG data processing

When performing connectivity analysis the method should to some extend account for volume conduction, since it is a significant factor that can distort the results. Mainly two approaches exist being; source reconstruction or a specialized connectivity measure. [van Diessen et al., 2015] The choice of reference electrode however greatly influence connectivity analysis performed in the signal-space, making signal-space analysis less suitable than source-space analysis. Additionally, the source-space based analysis has the advantage of interpretability, enabling the possibility of anatomical interpretation. [Mahjoory et al., 2017] Consequently, source reconstruction was performed prior to the connectivity analysis. The choice of source reconstruction was made with a comparison of existing methods (see appendix G) and through the following criteria;

- The method should be validated and used with experimental data
- The method should be implemented in an existing available toolbox
- The method should have a reasonable localization error and the ability to detect deeper lying sources
- The method should have a reasonable resolution and the ability to detect multiple sources

Based on the literature and the identified criteria the method standardized low resolution tomography analysis (sLORETA) was chosen for source reconstruction and implemented through the *KEY-LORETA* software by Pascual-Marqui [2015a]. After investigating connectivity methods used in relation with source reconstruction techniques (see table G.1 in appendix G), coherence were chosen. Coherence has previously been used with success after source reconstruction with both sLORETA and several other source reconstruction methods.

sLORETA

The goal of source reconstruction is to identify anatomical and functional structures of activity within the brain [Michel et al., 2004]. The electric fields recorded at the scalp can in theory be generated by an infinite number of sources and combinations thereof. This inverse problem of mapping the signal-space to the source-space has thus no unique solution and a priori assumptions based on physiological and biophysical knowledge must be introduced in order to reduce the number of unknowns and thereby make the problem solvable. The accuracy of the results are consequently dependent on the accuracy of the assumptions and thus the inverse solution method used. [Michel and Murray, 2012] Additionally, the accuracy of the reconstruction is dependent on the head model that is initially selected to compute the inverse problem [Michel et al., 2004].

In the *KEY-LORETA* software a three-shell spherical head model is used. The model is based on MRI images and the electrode coordinates are achieved by cross-registration between spherical and realistic head geometry. The spatial resolution of the implemented head model is 5 mm, dividing the head in a total of 6239 voxels. [Pascual-Marqui, 2015c]

The sLORETA algorithm is a tomographic based reconstruction method with the assumption that the biological signal is independent and uniformly distributed. This assumption makes the approach linear with exact zero-localization error. The algorithm is based on the standardization of the minimum norm solution (MNS). This standardization solves the issue of locating deep sources, which the MNS method in it self is incapable of. [Jatoi et al., 2014] In order to standardize the current density estimate ($\hat{\boldsymbol{J}}$) the variance should be estimated. The sLORETA algorithm takes both the actual source variance and the noise variance into account. In order to simplify the calculations and to adjust for the reference problem, the sLORETA procedure initially performs an average reference transform of the scalp electric potentials and the lead field matrix. [Pascual-Marqui, 2002] The final estimate obtained by the sLORETA algorithm is described by equation **(3.3)**, in which $\mathbf{l}$ denotes the $\mathbf{l}$'th voxel and $\boldsymbol{S}_{\hat{\boldsymbol{J}}}$ is the source variance estimate obtained by the electric potential variance and the MNS (for further mathematical background of sLORETA see appendix H). [Pascual-Marqui, 2002]

$$\text{standardized estimate of current density} = \hat{\boldsymbol{J}}_l^{\boldsymbol{T}} \cdot [\boldsymbol{S}_{\hat{\boldsymbol{J}}}]_{ll}^{-\mathbf{1}} \cdot \hat{\boldsymbol{J}}_l \tag{3.3}$$

Coherence

Coherence is one of the most commonly used measures of connectivity in the frequency domain [van Diessen et al., 2015]. Coherence, is an analysis of linear connectivity. The coherence measure provides information about the stability of power asymmetry and phase relationship between two signals rather than providing information on the relationship itself. [Sakkalis, 2011] It is the frequency domain equivalent to the cross-correlation function and is normalized, bounding the coherence coefficient by 0 and 1 [Bastos and Schoffelen, 2015]. For a coefficient of 0, no linear dependence is present between the to investigated signals and for a coefficient of 1 a complete correspondence is present [Niso et al., 2013]. When calculating the coherence it is assumed the signals are stationary (mean and variance of the signal does not change over time). This assumption may be relaxed if a Short Time Fourier Transform is used. [Sakkalis, 2011] In the sensor space coherence is calculated directly on the time-varying signal recorded at the electrodes. In the source space however, the strength of connectivity is determined through the magnitude of activity of the underlying sources [Bowyer, 2016].

To avoid calculating the coherence between each of the voxels and thus to limit the amount of coherence measures, regions of interest (ROI) were defined within the source space. ROI were defined using Brodmann areas (BA) [Trans Cranial Technologies Ltd., 2012] corresponding to the areas involved in pain processing in the contralateral side. For analysis of the resting state, coherence within both hemispheres were calculated. Pain processing occurs at different levels in the brain [Iannetti and Mouraux, 2010, Garcia-Larrea and Peyron, 2013] and the included ROIs were cortical areas from all levels. The following BA were used (see figure 3.9):

- BA 1-3 (Primary somatosensory cortex)
- BA 5,7 (Parietal areas)
- BA 9 (Anterolateral prefrontal area)
- BA 11 (Orbitofrontal cortex)
- BA 13-16 (Insula)
- BA 20-22 (Temporal pole)
- BA 23-32 (Cingulate cortex)
- BA 33 (Perigenual cingulate cortex)
- BA 43 (Parietal operculum)

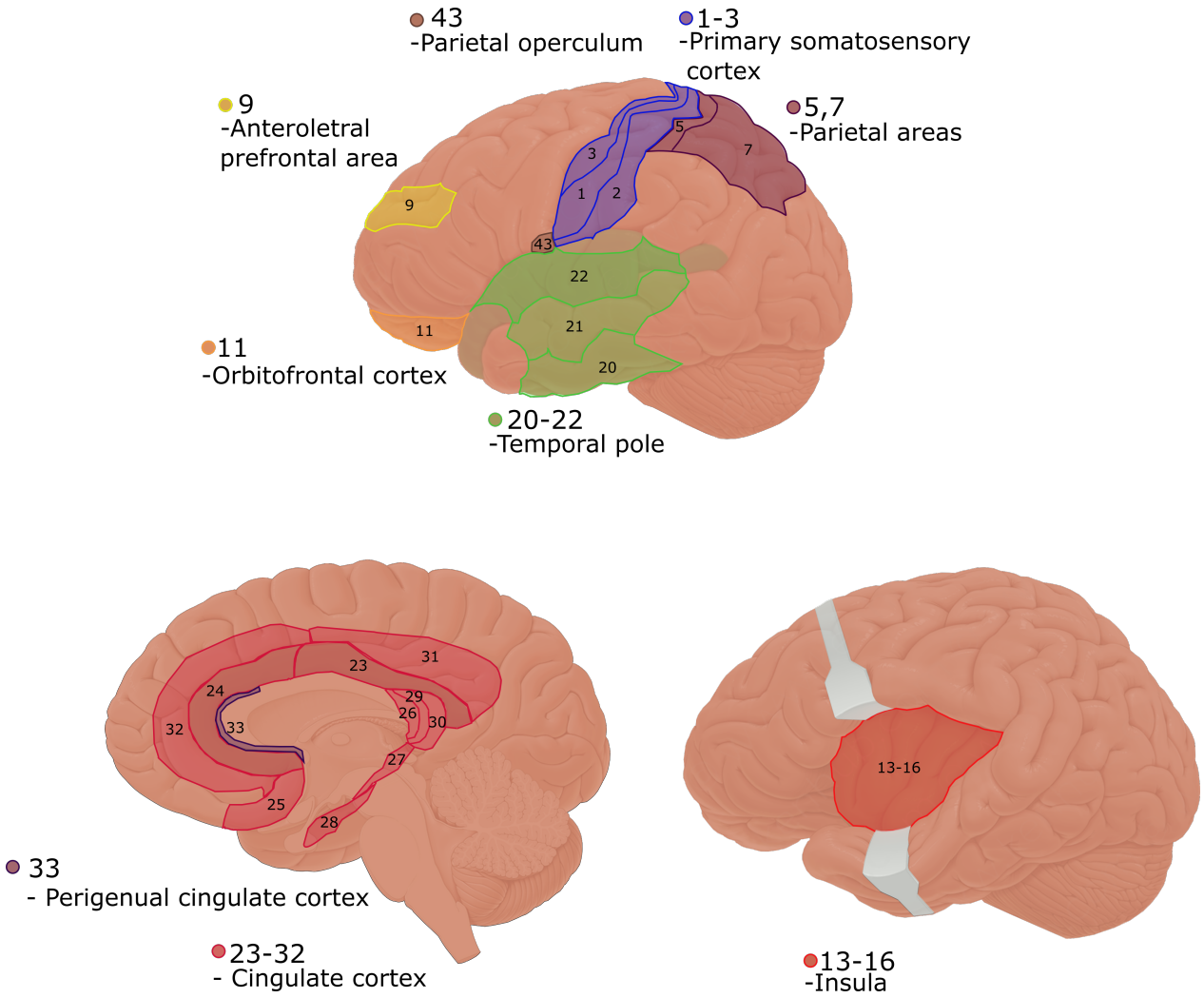

Figure 3.9: The brodmann areas defined as regions of interest wihtin the LROETA-Key software.

Coherence between ROIs for a given frequency (f) was thus measured on the ROI-time courses ($\boldsymbol{\sigma(f)}$) estimated by the source reconstruction. The coherence ($\boldsymbol{\eta(f)}$) between two regions ($\boldsymbol{r_1}$ and $\boldsymbol{r_2}$) is obtained by calculating the correlation of the region-time course spectra (see equation **(3.4)**, with * denoting the complex conjugate and $\langle\cdot\rangle$ the average over epochs). [Sekihara et al., 2011]

$$\eta(f) = \frac{\langle \sigma_{r1}(f) \cdot \sigma^*_{r2}(f) \rangle}{\sqrt{\langle |\sigma_{r1}(f)|^2 \rangle \cdot \langle |\sigma_{r2}(f)|^2 \rangle}} \tag{3.4}$$

The coherence analysis resulted in a coherence matrix in which each entry value indicated how strong the coherence between two ROIs was at each frequency. The analyzed frequency bands were delta (2-4), theta (4-8), alpha (8-12 Hz), beta1 (12-16 Hz), beta2 (16-23 Hz), and beta3 (23-30).

EEG statistics

The recorded and processed EEG data were analyzed statistically with two purposes. It was investigated if the source activity differed before and after CES and between arms. In addition, it was investigated if the calculated coherence differed before and after CES and between arms.

To test the statistical differences between sources the *KEY-LORETA* software was used to perform voxel-by-voxel comparison for each frequency band of paired groups. The statistical test was a non-parametric permutation test, with 5000 Monte Carlo permutations, corrected for multiple comparison [Pascual-Marqui, 2015b]. The basis of permutation testing is to pool the groups under investigation and subsequently test the statistical difference of every possible way (or a relatively large fixed number) of dividing the pooled samples into two groups of the original group sizes. When

all possible permutations have been tested the distribution of test results is compared to the test of original groups. If the original group difference is contained in the middle 95 % of permutation mean differences the hypothesis that the two groups are from the same distribution cannot be rejected. [Pesarin and Salmaso, 2010] The test statistic used for the permutation test was a log of F-ratio with a significance level of 0.05.

In total four statistical tests were performed in relation to sources:

- Comparison of rest recordings before and after CES
- Comparison of continuous pinprick recordings on the condition arm before and after CES
- Comparison of continuous pinprick recordings on the control arm before and after CES
- Comparison of continuous pinprick recordings for the condition and control arm, subsequent to CES

For statistical analysis of the coherence, a three-factor repeated measures ANOVA was performed for each frequency band for the continuous pinprick recordings. The within-subject factors were arms (two levels; condition and control), time (two levels; prior and post CES), and connections within the contralateral hemisphere (36 levels; 9 ROIs with connections to each other). For the rest recordings a two-factor repeated measures ANOVA was conducted for each frequency band with time (two levels; prior and post CES) and connections of both hemispheres, however not between hemispheres (72 levels; 9 ROIs with connections to each other), as within-subject factors. The residuals for the ANOVA tests were tested for normality through the Shapiro-Wilk test and evaluation of skewness and kurtosis, in order to check the assumptions of the ANOVA were kept.

Chapter 4

Results

Eleven healthy volunteers participated in the experiment, all giving informed consent prior to participation. The subject group consisted of 7 females and 4 males, all right handed and with an average age of 24.73 (± 1.68). Additional demographic data on the subjects are presented in appendix F.

4.1 Psychophysical data

On average, the subjects' perception threshold were 0.054 (±0.031) mA and the average stimulation intensity during CES was 0.31 (±0.28) mA. The perception threshold were multiplied by 6.72 (±6.067) times on average. The average VAS scoring and standard deviation during CES is presented in figure 4.1, where a slight increase in VAS score was present within the first 5 seconds, whereupon the VAS score slowly decreased up until the end of stimulation.

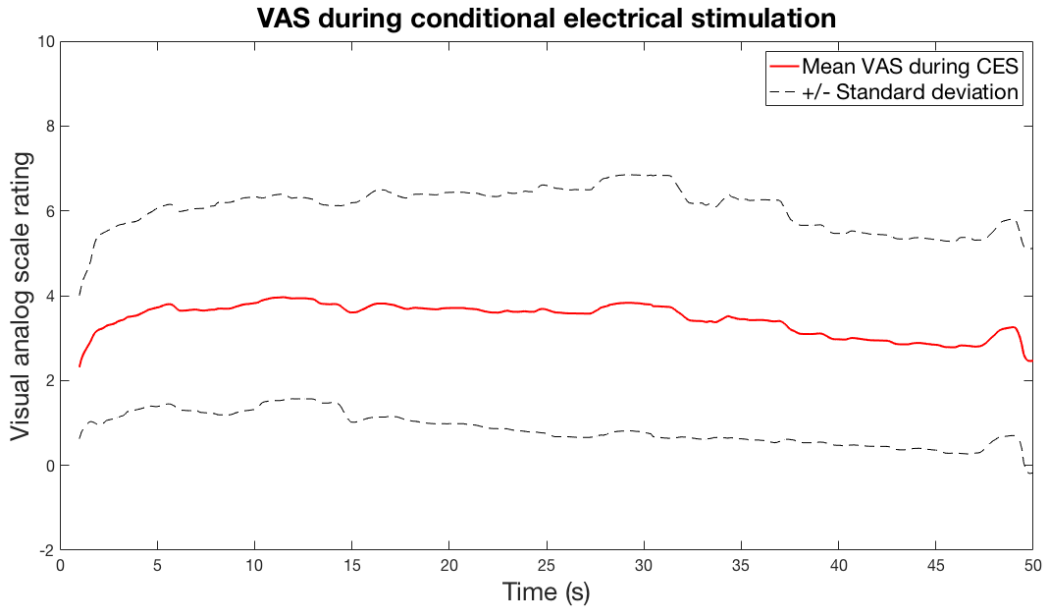

Figure 4.1: Visual analog scale ratings for all subjects during CES.

The average increase in perception of the condition arm, when compared to control was 14 % and the standard deviation was 11.51 %. In sample sizes calculations the effect size (**d**) was set to 10 % and the resultant number of subjects needed was 28 (see equation **(4.1)**)

$$n = 2 \cdot \frac{(1.96 + 1.2816)^2 \cdot 0.1151^2}{0.1^2} \simeq 28 \tag{4.1}$$

4.1.1 Single pinprick stimuli

The VAS scores during single pinpricks normalized to baseline are presented in figure 4.2. The variance was greater for the conditioned arm compared to the control, subsequent to the application of CES. VAS scores for both arms increased from baseline, subsequent to CES, however for the normalized VAS scores the increase was slightly larger for the condition arm. This trend was

however not significant (p=0.29). The VAS scores of the control arm was more stable over time, whereas the VAS scores for the the condition arm increased 10 minutes subsequent to CES and a decreased at 20 minutes subsequent to CES, after which it increased again. Changes over time was however not significant for either of the arms (p=0.72) and likewise no significant condition-time was present (p=1).

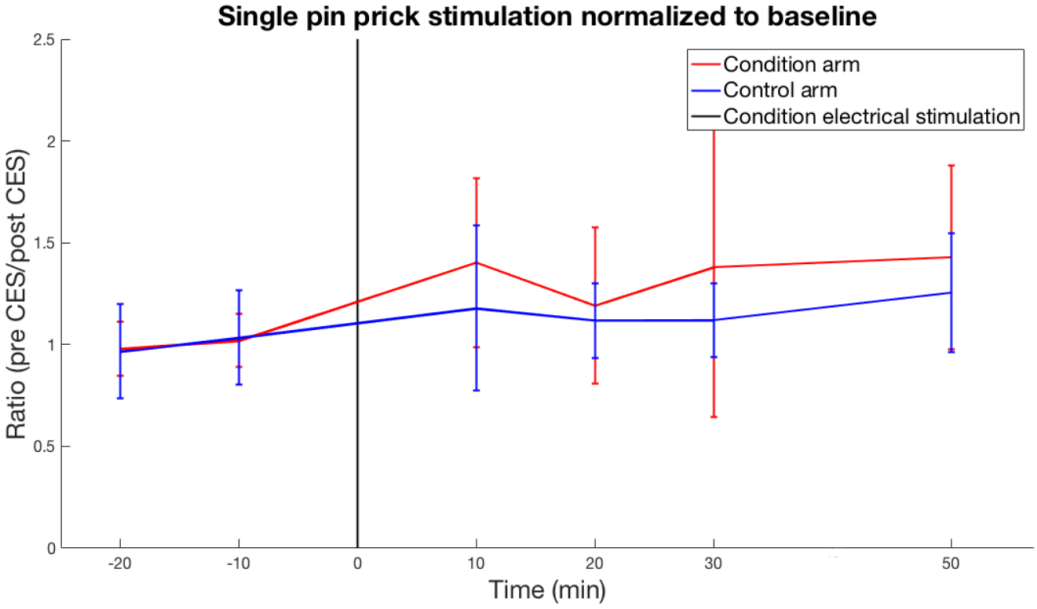

Figure 4.2: Single pinprick VAS scores. Average for all subjects normalized to baseline measurement (20 and 10 minutes before CES).

4.1.2 Continuous pinprick stimuli

As for the single pinprick stimuli the VAS scores during continuous pinprick showed a greater variation among subjects for the conditioned arm compared to the control (see figure 4.3). The normalized VAS scores for the control arm were relatively stable over the entire three minutes period, whereas normalized VAS scores for the condition arm started at a maximum and then decreased. This indicates the VAS measurements had a similar time course before and after CES for the control arm, whereas the condition arm subsequent to CES started well above the measurement prior to CES and at the end of the three minutes the difference between before and after was no longer present.

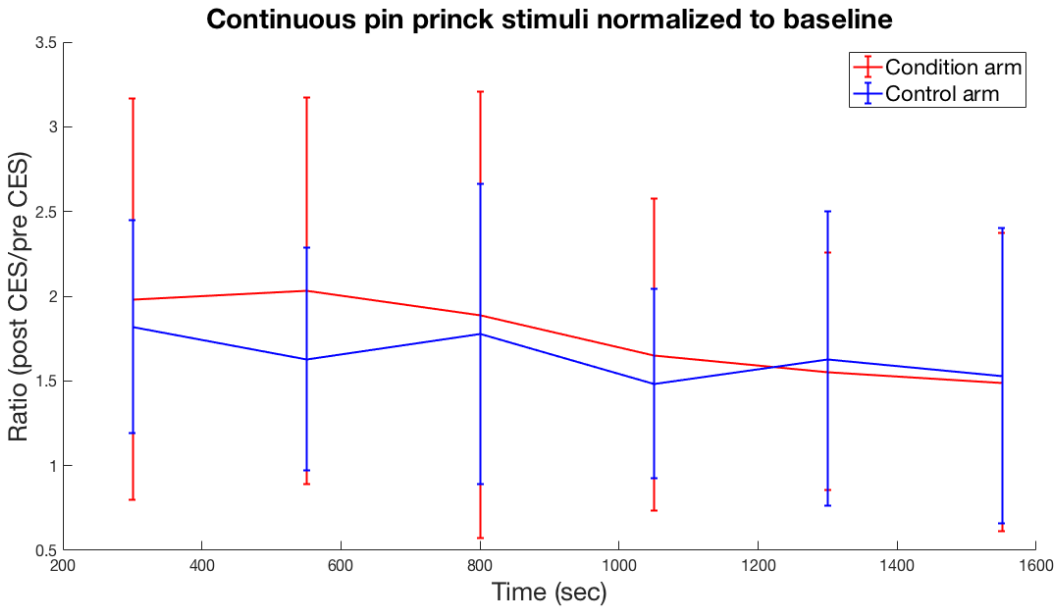

Figure 4.3: Continuous pinprick results. Average for all subjects measured 40 minutes after CES and normalized to baseline measured before CES.

The difference, in area under the curve (AUC), between the two arms for all subjects and the time-arm interaction was not statistically significant (p=0.85, p=0.64). The main factor time was significantly different (p=0.004) and post hoc testing revealed the AUC for both the condition and control arm to be increased subsequent to CES (see table 4.1).

Table 4.1: Table of values of AUC for both condition and control arm. The values are based on an average of all subjects and p-values are presented for the post hoc statistical paired t-test, comparing time before and after CES. Bold font p-values indicate significance. For significance after Bonferroni correction p<0.025.

Arm	time relative to CES	AUC	p-value post hoc time comparison
condition	prior	3930.45	**0.022**
	subsequent	5377.12	
control	prior	3492.97	**0.017**
	subsequent	5310.03	

4.1.3 Relation between pain perception during CES, CES intensity and effect

In order to investigate if the increase in pain perception subsequent to CES was related to the pain perception during CES, a relational plot (presented in figure 4.4) and the correlation coefficient was computed. The plot and the correlation coefficient showed the relation to be individual and random between subjects and no significant correlation existed (see table 4.2).

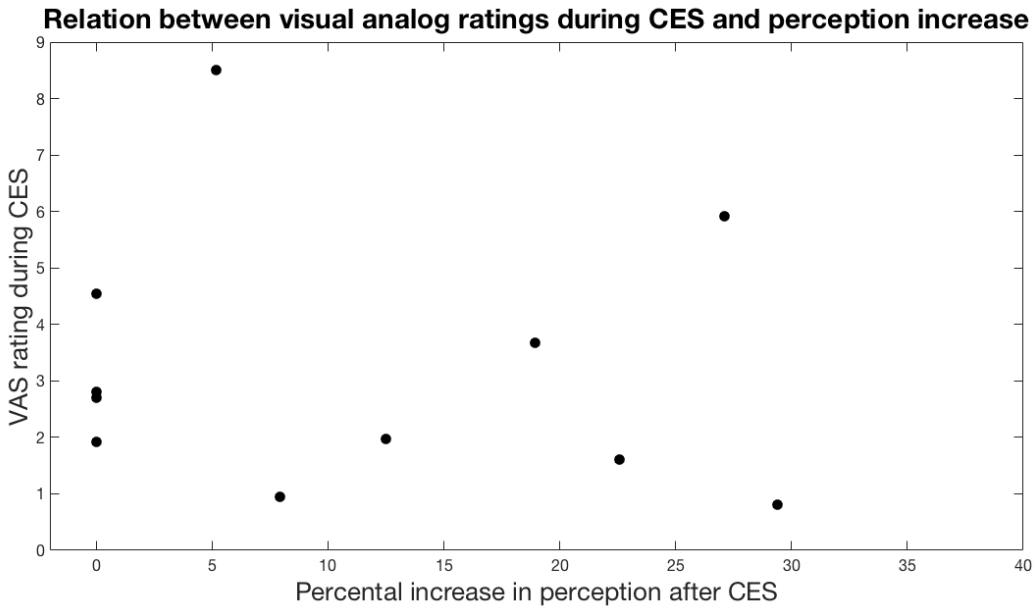

Figure 4.4: Relation between visual analog score during conditioning electrical stimulation and percentage difference in single pinprick VAS ratings between the condition and control arm.

An additional relationship between the intensity of CES and the perception increase was investigated. The results were not significant and random among subjects (see figure 4.5 and table 4.2).

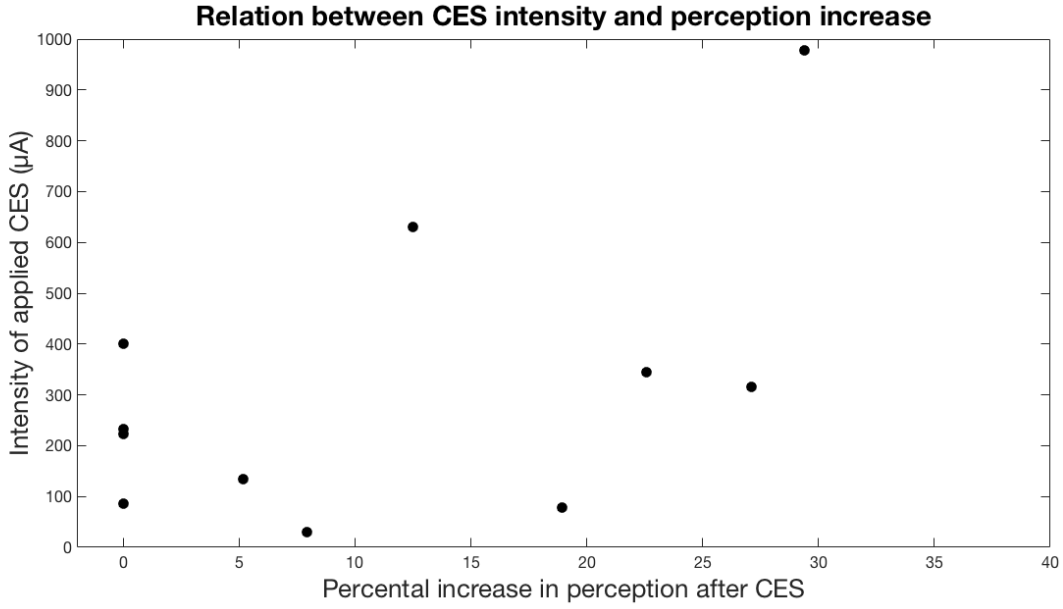

Figure 4.5: Relation between the percentage difference in single pinprick VAS scoring for the condition and control arm after application of CES and the intensity of the applied CES.

Table 4.2: Table of correlation coefficients and corresponding p-values for the tested relations between VAS rating during CES or CES intensity and the overall percentage increase in pain perception after CES.

Relation tested	**Correlation coefficient**	**p-value**
VAS during CES and effect	-0.12	0.73
CES intensity and effect	0.51	0.11

4.2 EEG data results

4.2.1 Source reconstruction

The overall average voxel activity among subjects for the conditioned arm before and after CES primarily showed source activity in the frontal and parietal lobe. All frequency bands showed activity concentrated at the middle frontal gyrus and the inferior frontal gyrus. For the theta band, additional activity was located in the superior frontal gyrus and the medial frontal gyrus. Apart from the middle frontal gyrus and the inferior frontal gyrus the beta1 and beta2 band activity was located at the superior temporal gyrus and middle temporal gyrus. Alpha band activity was additionally present at the precuneus.

For the control arm source activity were for all beta bands in the inferior frontal gyrus and middle frontal gyrus. These areas were also active for the alpha and theta band with an addition of the precuneus and the superior temporal gyrus, respectively (see alpha band activity post CES in as example figure 4.6 and activity in remaining frequency bands in appendix F). For the delta band, source activity was located at the superior temporal gyrus and the middle temporal gyrus.

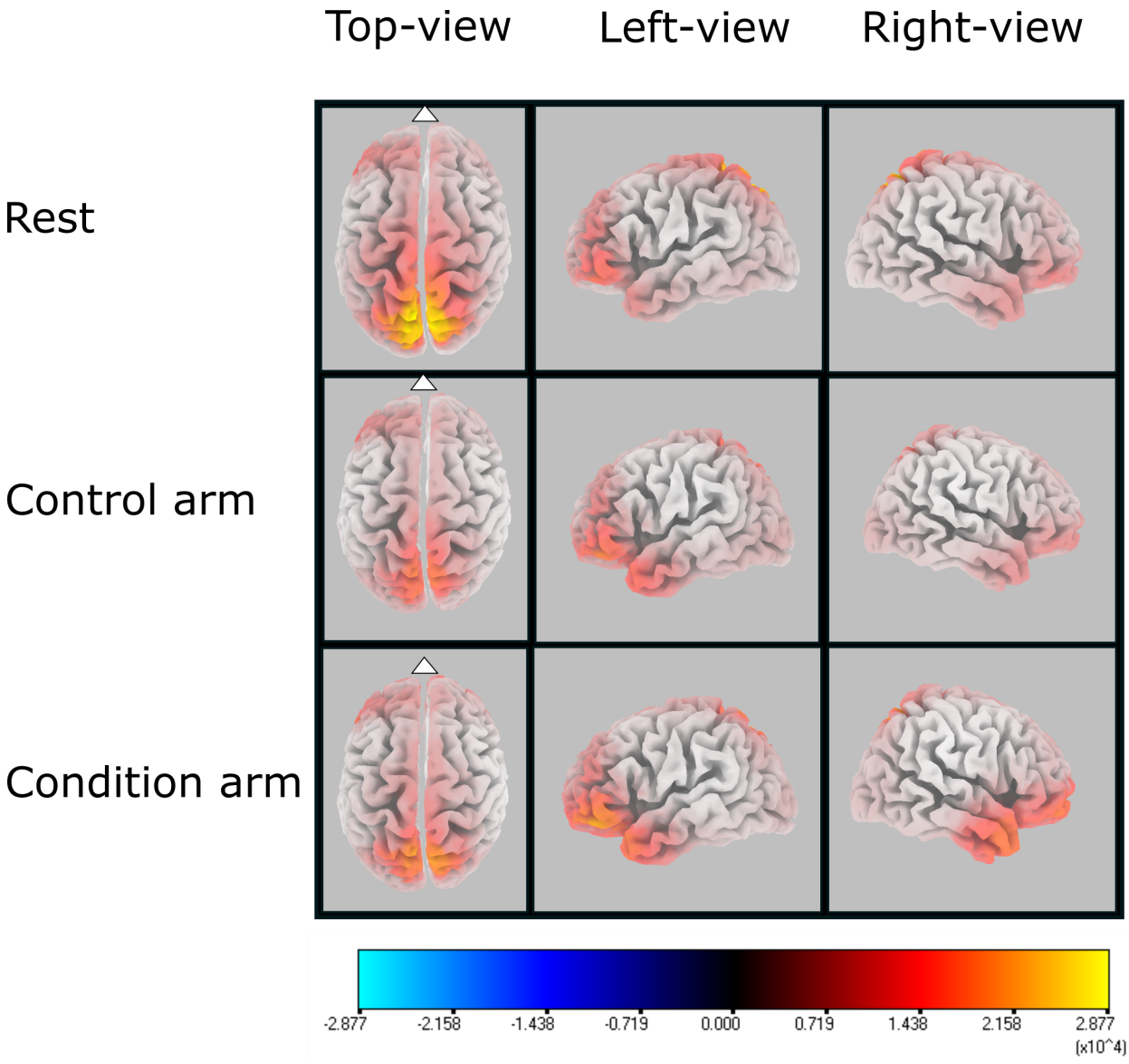

Figure 4.6: Source activity post CES in the alpha band frequency for the rest recording, and the continuous pinprick recording on the control and condition arm.

No significant differences were found for either the condition or control arm when comparing

recordings before and after CES. Likewise, no significant difference in source activity was present between the arms. Only the comparison of EEG rest recordings prior and subsequent to CES showed significant differences ($p<0.05$). These differences were present in the delta frequency band in the inferior parietal lobule and the postcentral gyrus. At these areas the activity in the rest recording prior to CES was significantly higher than subsequent to CES (see difference map in figure 4.7)

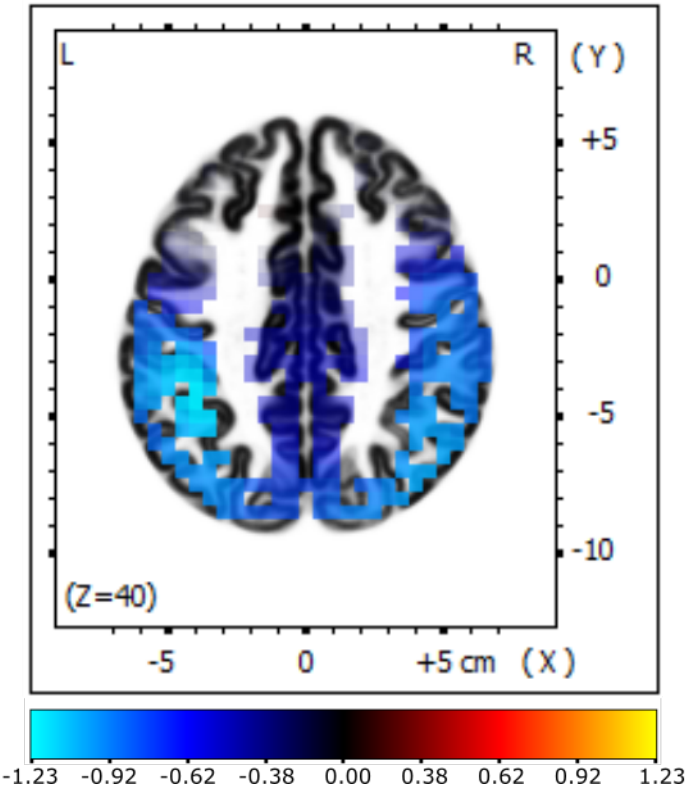

Figure 4.7: Difference plot of activity for the rest recording before and after CES. Negative values (blue scale) indicate that the activity at the recordings prior to CES was greater than activity after CES. Positive values (red scale) indicate the post-recording to have greater activity than the recording prior to CES.

Prior to CES the delta activity at rest was mainly located at the inferior frontal gyrus, middle frontal gyrus, and superior temporal gyrus. Subsequent to CES the source activity was primarily located at the precuneus, the postcentral gyrus, the superior parietal lobule, and the inferior frontal gyrus.

None of the other frequency bands were significant when comparing before and after application of CES. For the theta band, the source activity was located primarily at the inferior frontal gyrus and the middle frontal gyrus and less pronounced at the precuneus and superior parietal lobule. For the three beta frequency bands the activity was located at the inferior, superior, and middle frontal gyrus. Alpha band activity was most persistent at the precuneus, however also present at the inferior gyrus, postcentral gyrus, middle frontal gyrus, postcentral gyrus, and the superior parietal lobule (see alpha band activity post CES as example in figure 4.6 and activity in remaining frequency bands in appendix F).

4.2.2 Coherence

No significant differences in coherence between ROIs between arms ($p>0.34$) or between recordings before and after CES ($p>0.40$) were found. Additionally, none of the interactions were significant ($p>0.26$).

For the rest recordings no significant difference was found for time as main effect, however significant interaction between time and connections were found for the theta ($p=0.0030$), delta ($p=0.019$), and alpha ($p=0.0080$) band frequencies. Thus for these three frequency bands the

different connections between the ROIs changed in different manners from the rest recording prior to CES to the recording after CES. Coherence prior and subsequent to CES are illustrated for the delta band in figure 4.8a and 4.8b.

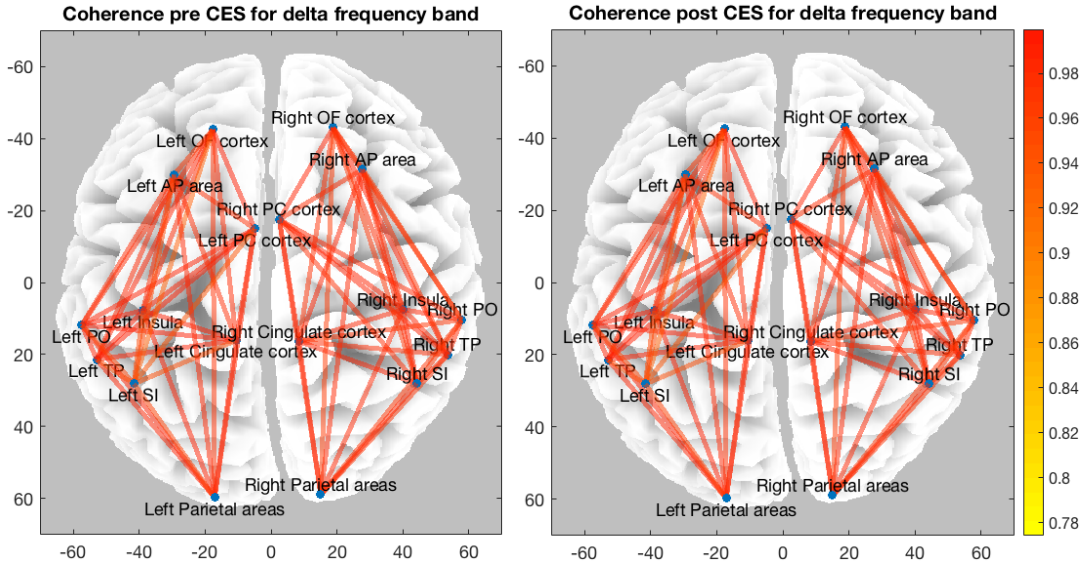

(a) Coherences prior to CES. *(b) Coherences subsequent to CES.*

Figure 4.8: Connections within both hemispheres for the delta band.

For simplicity and clarity, only the largest changes in coherence between before and after CES in the rest recording were investigated further (see additional changes in coherence in appendix F). Large change were defined as correlations between ROIs with a $p<0.05$ without Bonferroni correction found in a paired t-test. For the delta frequency band, the largest changes were between the orbitofrontal cortex and temporal pole, primary somatosensory cortex, and parietal area, all in the contralateral side (see figure 4.9).

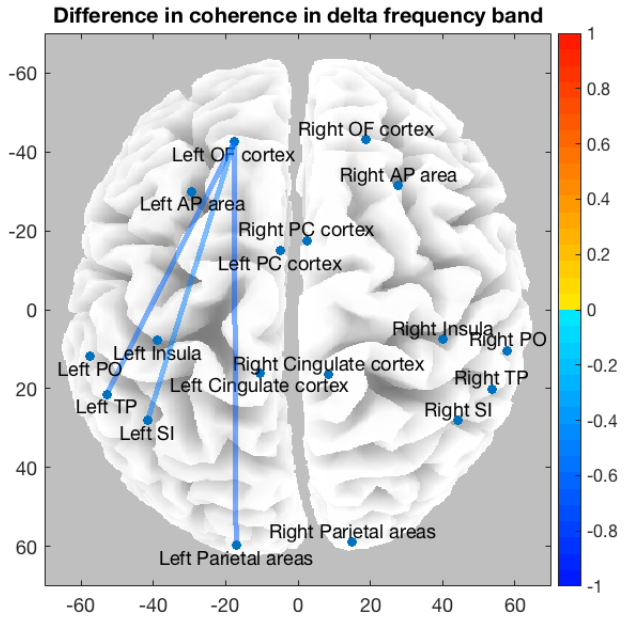

Figure 4.9: Largest differences between coherence before and after CES (lines) for the rest condition in the delta band. Negative values (blue scale) indicate the coherence prior to CES to be larger than subsequent to CES and positive values (red scale) indicate larger coherence values subsequent to CES. OF=orbitofrontal, AP=anterolateral prefrontal, PC=perigenual cingulate, PO=parietal operculum, TP=temporal pole, and SI=primary somatosensory cortex.

For the theta frequency band, raw coherence prior and subsequent to CES are presented in figure 4.10a and 4.10b. The largest change in coherence was between the orbitofrontal cortex and parietal area in the contralateral side (see figure 4.11).

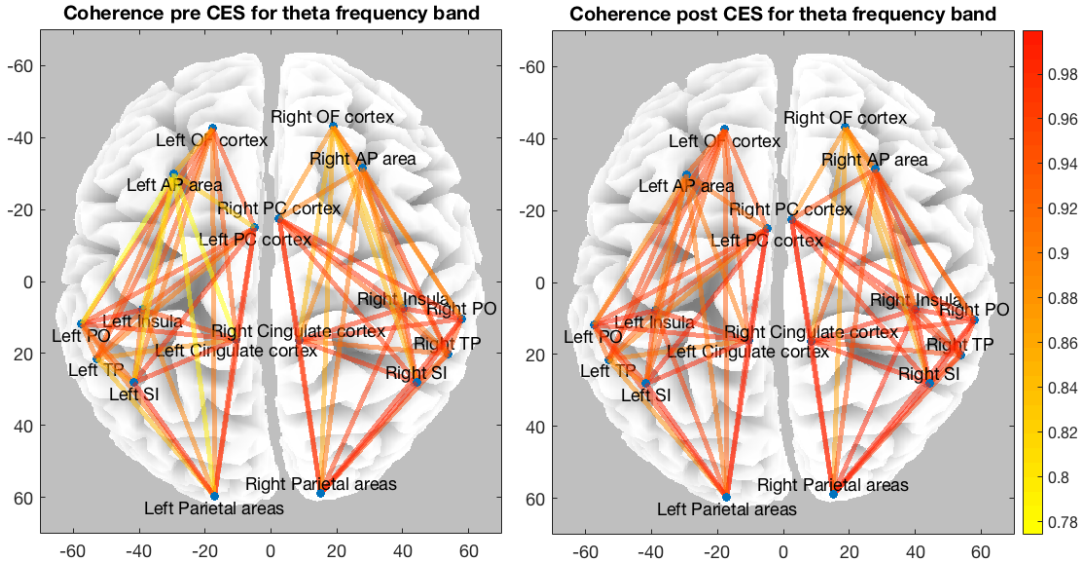

(a) Coherences prior to CES. *(b) Coherences subsequent to CES.*

Figure 4.10: Connections within both hemispheres for the theta band.

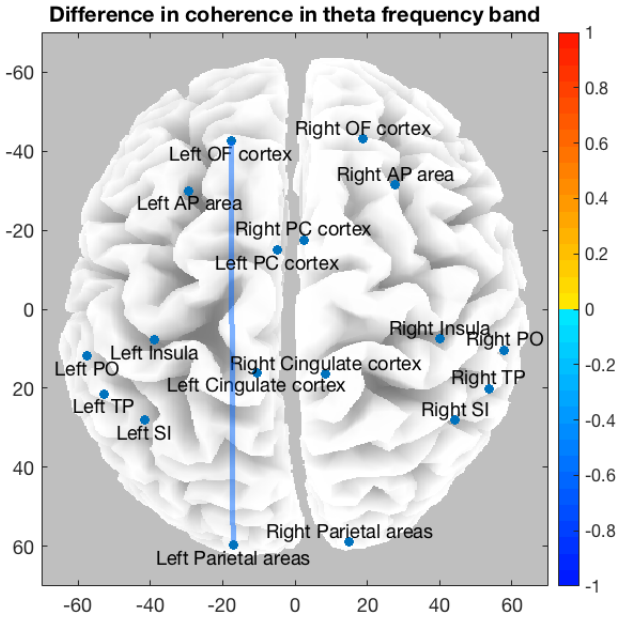

Figure 4.11: Largest differences between coherence before and after CES for the rest condition in the theta band. Negative values (blue scale) indicate the coherence prior to CES to be larger than subsequent to CES and positive values (red scale) indicate larger coherence values subsequent to CES. OF=orbitofrontal, AP=anterolateral prefrontal, PC=perigenual cingulate, PO=parietal operculum, TP=temporal pole, and SI=primary somatosensory cortex.

For the alpha frequency band, the largest changes in coherence were between the parietal area and orbitofrontal cortex, and perigenual cingulate cortex, both in the contralateral side (see figure 4.13). Coherence prior and subsequent to CES are presented in figure 4.12a and 4.12b.

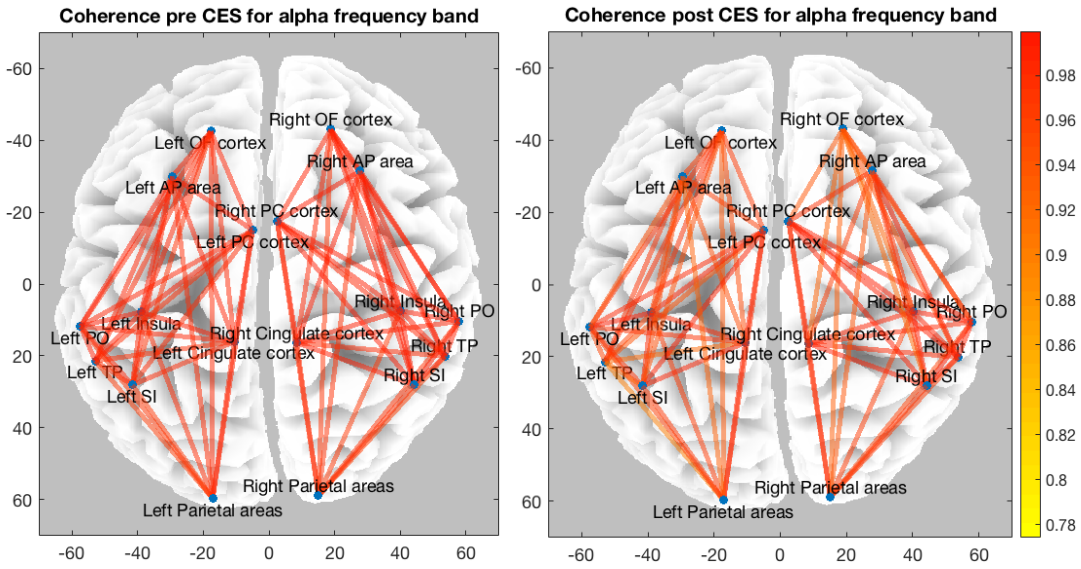

(a) Coherences prior to CES. *(b) Coherences subsequent to CES.*

Figure 4.12: Connections within both hemispheres for the alpha band.

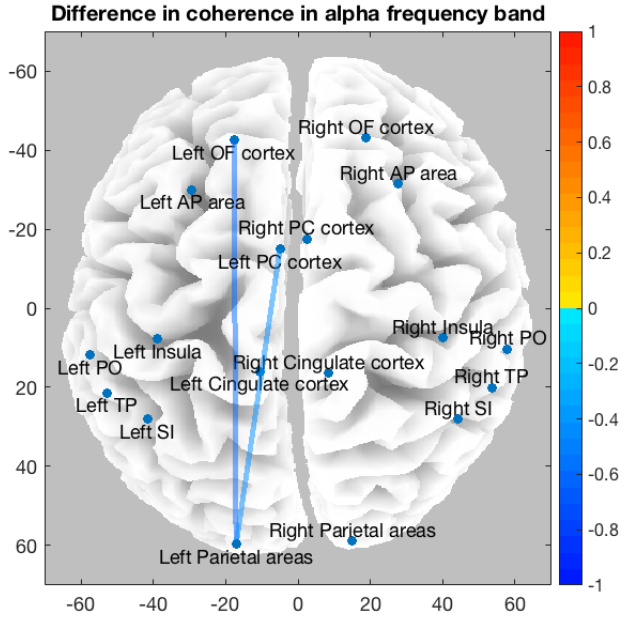

Figure 4.13: Largest differences between coherence before and after CES for the rest condition in the alpha band. Negative values (blue scale) indicate the coherence prior to CES to be larger than subsequent to CES and positive values (red scale) indicate larger coherence values subsequent to CES. OF=orbitofrontal, AP=anterolateral prefrontal, PC=perigenual cingulate, PO=parietal operculum, TP=temporal pole, and SI=primary somatosensory cortex.

4.3 Correlation between coherence and perception increase

To investigate whether the changes in resting state connectivity was correlated to the psychophysical changes in pain perception, relational plots for the frequency bands; delta, theta, and alpha are presented for the largest connections (see figures 4.14, 4.15, and 4.16).

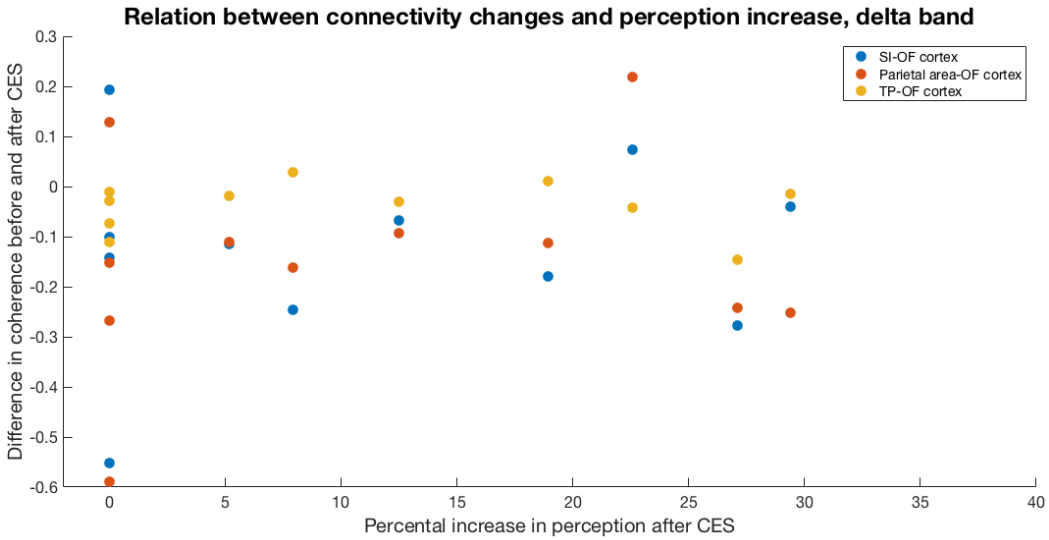

Figure 4.14: Relation between percentage increase in perception after CES and difference in coherence for the rest condition before and after CES in the delta band for all subjects individually. A negative difference indicates a decrease in coherence when comparing before and after CES. SI=primary somatosensory cortex, OF=orbitofrontal, TP=temporal pole.

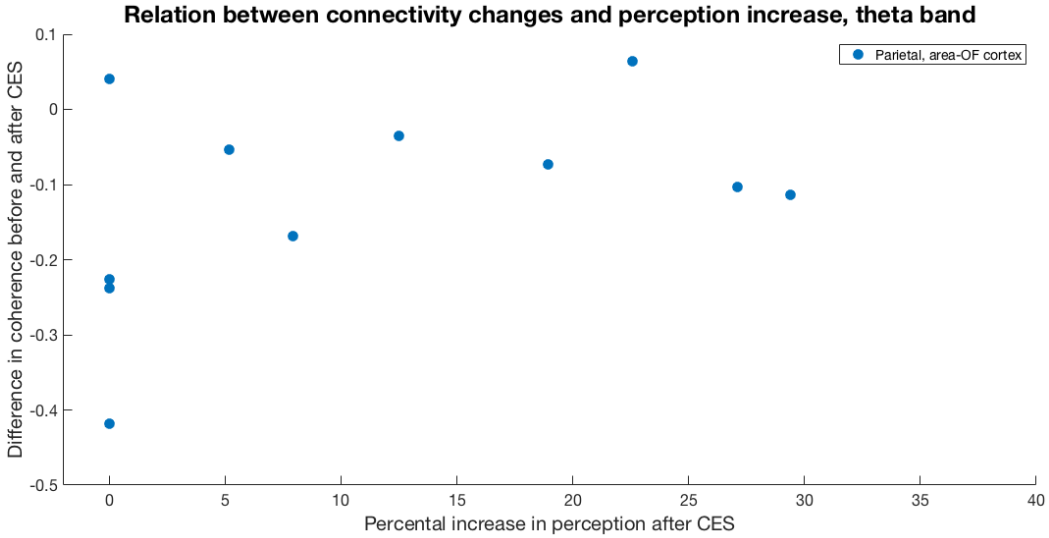

Figure 4.15: Relation between percentage increase in perception after CES and difference in coherence for the rest condition before and after CES in the theta band for all subjects individually. A negative difference indicates a decrease in coherence when comparing before and after CES. OF=orbitofrontal.

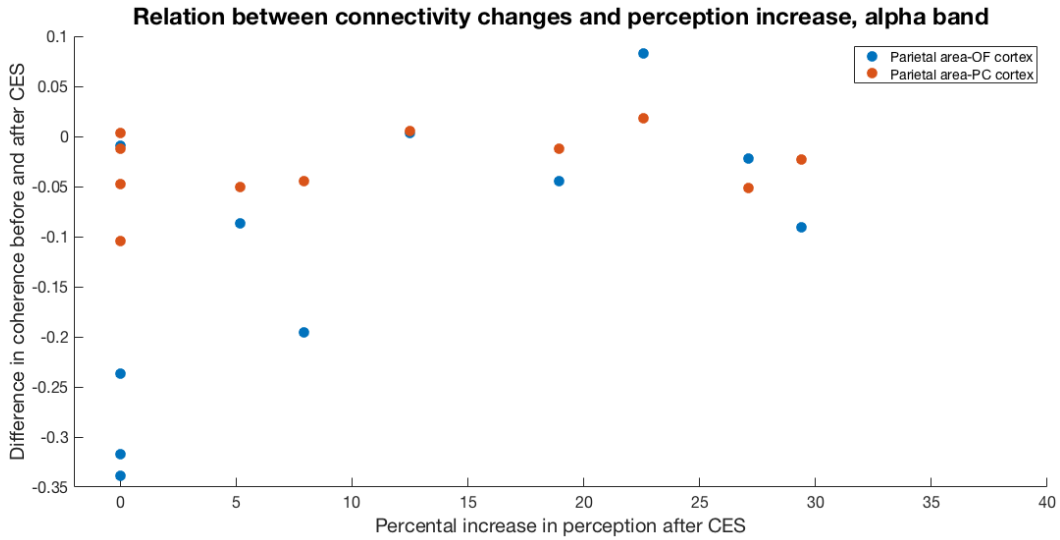

Figure 4.16: Relation between percentage increase in perception after CES and difference in coherence for the rest condition before and after CES in the alpha band for all subjects individually. A negative difference indicates a decrease in coherence when comparing before and after CES. OF=orbitofrontal, PC=perigenual cigulate.

In addition to the plots, correlation coefficients for each of the bands and connections were computed, showing a significant correlation between difference in connectivity between the parietal areas and the orbitofrontal cortex before and after CES and the increase in perception (p=0.041), in the contralateral hemisphere. No other significant correlation between connectivity changes and changes in pain perception were found (p<0.19, see table 4.3).

Table 4.3: Table of correlation coefficients and corresponding p-values for the tested relations between coherence changes and psychophysical perception increase after CES.

Relation tested	**Correlation coefficient**	**p-value**
$\boldsymbol{\delta}$: Primary somatosensory cortex - Orbitofrontal cortex	0.11	0.74
$\boldsymbol{\delta}$: Parietal area - Orbitofrontal cortex	0.17	0.62
$\boldsymbol{\delta}$: Temporal pole - Orbitofrontal cortex	-0.080	0.82
$\boldsymbol{\theta}$: Parietal area - Orbitofrontal cortex	0.43	0.19
$\boldsymbol{\alpha}$: Parietal area - Orbitofrontal cortex	0.62	0.041
$\boldsymbol{\alpha}$: Parietal area - Perigenual cingulate cortex	0.29	0.39

Chapter 5

Discussion

The psychophysical results indicated a non-significant increase in normalized VAS score during single pinpricks. A similar trend was seen for the normalized VAS score during continuous pinprick stimulation, although the normalized condition and control arm converged during the last minute. For the recordings during continuous pinprick stimuli, no significant changes in source activity and coherence between nine regions of interest, defined based on literature, were found when comparing before and after CES. Both source analysis of EEG activity and coherence analysis revealed significant changes in the rest condition when comparing before and after CES. The source activity was significantly changed for the delta band within the inferior parietal lobule and postcentral gyrus. The activity decreased after CES. Analysis of the resting state coherence revealed a significant interaction between time and connections between regions of interest for both the delta, theta, and alpha bands. This means the application of CES have had a different affect on different connections between regions. There was significant correlation between the increase in perception and difference in coherence between the parietal area and orbitofrontal cortex in the alpha band before and after CES.

5.1 Psychophysical results

Normalized VAS scores for single pinprick stimuli showed a trend towards a larger VAS subsequent to CES for the conditioned arm, increasing within the first 10 minutes, slightly decreasing till 20 minutes, after which it increased again until 50 minutes after CES. This sensitization effect could however not be shown statistically. The increase in normalized VAS at 100-150 % of the VAS at baseline was similar to findings of Xia et al. [2016a], who found an increase of VAS of between 100 and slightly above 150 % baseline using a pinprick of 30 g (25.6 g in the present study). The stimulation paradigm of the present study and that of Xia et al. [2016a] was both 10 Hz pulses applied for 50 seconds, however different pulse shapes were used. Xia et al. [2016a] used rectangular pulses of 1 millisecond, while an increasing form of the exponential current decay pulse was used in the present study.

The average increase in sensitivity found by Xia et al. [2016b] for the 10 Hz pulse was 27 %, whereas in the present study the average increase in pain perception at the conditioned arm compared to control was 14 %. The findings by Xia et al. [2016b] showing no significant difference in sensitivity increase for the 10, 100, and 200 Hz stimuli applied for 50 seconds, five times one second, and five times 0.5 seconds, indicates the frequency of the pulse to have less effect on the results, and thus suggests the differences in sensitivity increase between the present study and conventional HFS studies to be primarily due to the stimulation pulse shape. The pulse shape was chosen based on the results of Hennings et al. [2005b] and Hugosdottir et al. [in press], suggesting the exponential current decay pulse to better activate nociceptive fibres selectively when stimulating at detection threshold. A preliminary study comparing conventional HFS and the exponential current decay pulse indicated the exponential current decay pulse to better induce heterotopic hyperalgesia than conventional HFS with square pulses. However, the results of Hugosdottir et al. [in press] does not guarantee the usefulness of the exponential current decay pulse in LTP-like pain induction and at higher intensities and the conclusion of the preliminary study was limited by the number of subjects (n=3). Klein et al. [2004] found a perception threshold of 0.11 ($\pm$0.06) mA in average for the rectangular pulse shape, while the average perception threshold for the exponential current decay pulse in the present study was 0.054 ($\pm$0.031) mA. A lower perception threshold found in the

present study compared to previous studies may indicate better selective activation of nociceptive fibres although these findings could also be due to the longer pulse duration. The average stimulation intensity was lower than the intensity used by Xia et al. [2016a] at 2.63 ($\pm$1.80) mA, for a 10 Hz square pulse stimulation in 50 seconds with intensities of 10 times detection threshold. In the present study, the average VAS score during CES was just above pain threshold (average VAS = 3.25). The pain perception during CES was lower than what has been previously found, as Xia et al. [2016a] found pain scores between 60 and 90 (scale = 0-100, 30 indicating pain).

Apart from the pulse shape, the method of standardizing the intensity of applied CES may have influenced the results and effect of applied CES. Despite an individual CES intensity targeting a VAS of 4 indicating pain, the electrical stimulation was not perceived as painful for all subjects. This may indicate that standardizing the CES intensity to VAS score, is less optimal. It could additionally be an issue of the staircase method used. Since only two descending and two ascending steps were used, the step sizes may have been too large in the first steps, leading to a skewed average of the four steps. The procedure was used in an attempt to minimize the amount of stimuli given prior to CES and thus minimize possible sensitization due to these stimuli. A VAS score of 4 could possibly have been more accurately reached if additional ascending and descending steps had been included in the stair case method or by use of the method of limits, with a relatively small step size, starting from the perception threshold. The stimuli applied for the intensity determination were done manually and thus the stimuli were not applied with a constant interstimuli interval. The random interstimuli interval could to some degree have limited the possible habituation to the stimuli, however some habituation has likely occurred. The stimuli were applied with a relatively low average frequency, since the multiplication factor was manually adjusted for each stimulus. Low frequency stimulation at 1 Hz have previously been used to induce the counterpart to LTP, LTD [Cooke and Bliss, 2006, Klein et al., 2004, Rottmann et al., 2010]. However, the length of the trains used and the time of stimulation to induce LTD was substantially greater than what was achieved in the present study. Klein et al. [2004] and Rottmann et al. [2010] used long trains of 1000 and 1200 pulses, corresponding to approximately 15 and 20 minutes of stimulation, respectively. It is thus not assumed that LTD could have been inducted during the intensity determination within the present study, since the average number of stimuli given was 26.36 (in trains of 5 pulses), corresponding to a total of 13.18 seconds.

No relation was identified between the perception threshold and the multiplication factor used (see figure F.4 in appendix F). Similar results were found by Xia et al. [2016b], who did not observe any statistical difference in pinprick sensitivity between CES paradigms although an initial difference was found for pain perception during CES. These results indicate that a sufficient fixed multiple of perception threshold is difficult to set. It has however been sufficient for the conventional HFS to induce significant increase in pain perception using a fixed multiple of the perception threshold [Klein et al., 2008, Xia et al., 2016a].

For the continuous pinprick stimulation, a larger difference between the baseline measurement prior to CES and the measurement subsequent to CES was seen within the first minute of stimulation for the condition arm. However, after the first minute the difference decreased, which was likely due to the windup effect of continuous stimulation, exceeding the possible sensitization due to CES. Additionally, peripheral sensitization to pinprick stimulation has likely been induced and maintained from the first to the second block of continuous pinprick, as the AUC before and after CES was significantly different in time for both arms.

5.2 Source reconstruction and coherence analysis

For both the source reconstruction and coherence analysis, significant differences were found only for the rest condition. It was expected that a continuous stimuli would result in changes in activity compared to control as Schulz et al. [2015] found changes in cortical oscillations when stimulating with a tonic thermode in 10 minutes. Different responses would be expected for different kinds of stimulation (thermal and mechanical), since these responses are mediated by different nociceptive fibres [van den Broeke et al., 2016b]. However, constant stimuli over a time period was expected to

show some similarities in the pain processing. It is speculated that the non-significant changes in source activity and coherence for the continuous pinprick stimulation may be due to the stimulation method itself. The method was chosen in an attempt to achieve a relatively stable pain perception. The perception ratings increased over the three minutes period, however no greater fast fluctuations in ratings were seen, resulting in a stable scoring. Since the pinprick stimulation was phasic in nature, the stability of the rating may not correspond to the obtained brain responses. It is possible that an ERP analysis approach would have been more suitable for this phasic stimuli. It would though require a trigger signal synchronized to the pinprick stimuli.

The activity in the EEG recordings during continuous pinprick stimuli for both the control and condition arm, and resting state prior to CES was located in areas associated with pain processing. These areas include the primary somatosensory cortex (superior parietal lobule and postcentral gyrus) and somatosensory association cortex (precuneus) [Damasio, 2014]. In addition, other areas related to the stimuli and the experiment in general were found active, such as the auditory association cortex (superior temporal gyrus), and supplementary motor cortex (superior frontal gyrus) [Damasio, 2014].

The resting state recordings showed a significant interaction between time and connections of ROI in the delta, theta and alpha bands. This means the connections and thus the coherence between ROI changed differently over time. The connections that had significantly changed after CES (without Bonferroni correction), showed a decrease in coherence. In the delta band, decreased coherence was detected between the orbitofrontal cortex and the primary somatosensory cortex, the parietal areas, and the temporal pole. For the theta band decreased coherence was detected between the orbitofrontal cortex and the parietal area, while two connections with decreased coherence was detected for the alpha band; between the parietal area and the orbitofrontal, and perigenual cingulate cortex. The connection between the parietal areas and the orbitofrontal cortex, was for the alpha band significantly correlated to the increase in VAS, showing a greater change in coherence with greater increase in VAS ratings. All of these decreases in coherence were detected within the contralateral hemisphere. Changes in resting state connectivity were also found after induction of experimental pain by capsaicin in Martel et al. [2017] although in the beta band. The connection between primary motor cortex and cuneus were different between responders and non-responders (measured by increased motor responses from transcranial magnetic stimulation) after pain induction [Martel et al., 2017]. González-Roldán et al. [2016] and Gram et al. [2017] likewise investigated changes in connectivity during rest. Where Gram et al. [2017] did not find changes in connectivity between patients with and without postoperative pain, González-Roldán et al. [2016] an increased coherence in the left hemisphere in the theta and beta3 bands compared to pain free controls. The fact that these findings does not correspond with the findings in this study could possibly be explained by the fact that González-Roldán et al. [2016] compares fibromyalgia patients with healthy controls whereas this study compares a condition and control arm on the same subject. Even though it has been found that several areas overlap when comparing experimentally induced LTP-like pain and chronic pain, mechanisms, brain responses, and changes in those responses does differ [Friebel et al., 2011], which may account for the differences between findings of González-Roldán et al. [2016] and the present study.

Since significant changes were found for the resting state coherence, it is speculated that the inability to detect significant changes in the EEG recordings during continuous pinprick may be caused by influence of non-pain related factors, making it difficult to detect changes in the pain processing. An example of such a possible contamination could be arm and minor eyes movements in order to continuously rate the perception on the VAS meter. Even though VAS scoring and thereby movement of the arm activated several motor areas, these are activated in the contralateral side to stimuli activated areas, and believed to have less influence. Additionally, the processes involved in the constant conscious evaluation of pain perception may have influenced the recordings to a degree where pain processing related changes could not be seen.

The results of changes in connectivity within the resting state recordings should however be viewed in the light of insignificant psychophysical results. The psychophysical data does not indicate an induction of LTP-like pain, raising the question of whether resting state results are due to different

mechanisms. Brain signals are affected by cognitive and emotional states. [Friebel et al., 2011] These cognitive states such as the degree of concentration, the attention to stimuli and the expectation of pain cannot be controlled and may influence the brain signal and could have changed between the first and second block of EEG recording.

It is additionally important, in relation to the differences seen in the rest recordings before and after CES, to note that power affects functional connectivity analysis [Friston, 2011, Stam and van Straaten, 2012] and that changes in coherence cannot necessarily be interpreted as a strengthening in coupling between two regions of interest as it may merely be an expression of a change in the distribution of activity around those regions. This may be the reason for the changes seen in connectivity for the delta band, since a significant change in activity distribution was present in this frequency band. However, this is less likely the case for the alpha and theta bands since no significant difference in source activity was present for these frequencies. In addition to an amplitude change, coherence can be affected by changes in phase [Sakkalis, 2011].

5.3 Limitations

The VAS results indicate that LTP-like increase in pain perception was not induced in all subjects. The normalized data however showed a tendency towards sensitization, though with a large variation between subjects. The large inter-subject variation may indicate that the number of subjects (n=11) has been insufficient to show significant changes in perception. A power analysis performed with the standard deviation of these initial 11 subjects revealed the need of 28 subjects in order obtain a power of 90 % and a confidence interval of 95 %. Thus the inability to show significant sensitization due to CES may be due to limitations in the number of subjects. Apart from not having a sufficient amount of subjects, the subjects' ability to rate the perception may have influenced the results. Several subjects were naive to VAS and some degree of adjustment to the scale and expectation could have happened between the recordings before and after CES. The scoring is also affected by the instructions to VAS, which was consistent between subjects, but may not have been identical to instruction given in other LTP-studies. van den Broeke and Mouraux [2014b] and van den Broeke and Mouraux [2014a] used a numerical rating scale (NRS) ranging from 0 to 100, with 50 indicating the pain threshold. The NRS has been considered more intuitive, to have higher compliance and thus be easier for subjects to use compared to VAS [Fillingim et al., 2016]. However, both scales are widely used standards and have both been described as easy to use [Fillingim et al., 2016]. In order to avoid the possible bias of subjects' naiveness to VAS, a training period could be introduced prior to experimentation, making sure the subjects were familiar and comfortable with the scoring system and consistent for identical stimuli intensities.

Coherence is sensitive to volume conduction which may limit the results of such an analysis. However, to account for this issue source reconstruction was performed prior to coherence computations, minimizing but not eliminating the effect of volume conduction [Bastos and Schoffelen, 2015]. Source reconstruction may influence the correlations between source-based signals and thus biasing the results to some extend [Stam and van Straaten, 2012]. Another approach to account for volume conduction could be to use a phase-based connectivity measure, such as the imaginary part of coherence. Such measures are however unable to detect interactions with near zero-phase difference and may not find all relevant interactions. [Bastos and Schoffelen, 2015]

Chapter 6

Conclusion

Significant changes in connectivity were observed for the EEG rest recording. At rest, connectivity decreased from before CES to after CES for three connection in the delta band, two in the alpha band, and for one connection in the theta band. The significant changes observed in the delta band might be due to a difference in activity distribution as this had significantly changed after CES. Within the alpha band, the decrease in coherence between the parietal areas and the orbitofrontal cortex was significantly correlated to the increase in pain perception subsequent to CES. This indicates that the cortical interconnection was affected and to some extend related to the increase in pain perception. Even though significant changes were found for coherence in the resting state, these changes may not be due to induced LTP-like increase in pain perception, expressed as heterotopic hyperalgesia, as the psychophysical results were non-significant. However, a trend towards increased perception subsequent to CES, applied as an increasing exponential current decay pulse, was found. The lack of significant changes in VAS score could be due to the fact that CES was not perceived as painful for all subjects and thus the C-fibre activation may not have been intense enough to induce LTP-like increase in pain perception. A small sample size and variation in instructions between studies additionally limits the findings. Like for the psychophysical VAS scores, changes in cortical interactions for EEG recorded during continuous pinprick were non-significant.

With additional subjects, and with a more sufficient determination of CES intensity it is likely that several cortical interactivity changes in experimentally induced LTP-like pain could contribute to the analysis and understanding of cortical pain processing and central sensitization.

References

Baillet, Mosher, and Leahy, **2001**. Sylvain Baillet, John C. Mosher, and Richard M. Leahy. *Electromagnetic brain mapping.* IEEE Signal Processing Magazine, 18(6), 14–30, 2001. ISSN 10535888. doi: 10.1109/79.962275.

Bastos and Schoffelen, **2015**. André M Bastos and Jan-Mathijs Schoffelen. *A Tutorial Review of Functional Connectivity Analysis Methods and Their Interpretational Pitfalls.* Frontiers in systems neuroscience, 9, 1–23, 2015. ISSN 1662-5137. doi: 10.3389/fnsys.2015.00175.

Becker, Bondegaard Thomsen, Olsen, Sjøgren, Bech, and Eriksen, **1997**. Niels Becker, Annemarie Bondegaard Thomsen, Alf Kornelius Olsen, Per Sjøgren, Per Bech, and Jørgen Eriksen. *Pain epidemiology and health related quality of life in chronic non-malignant pain patients referred to a Danish multidisciplinary pain center.* Pain, 73, 393–400, 1997. ISSN 0304-3959. doi: S0304395997001267[pii].

Bliss and Collingridge, **1993**. T. V. Bliss and G. L. Collingridge. *A synaptic model of memory: long-term potentiation in the hippocampus.* Nature, 361(6407), 31–39, 1993. ISSN 0028-0836. doi: 10.1038/361031a0.

Peter H. Boeijinga. Electroencephalography. In *Encyclopedia of Psychopharmacology*, pages 462–471. 2010. ISBN 978-3-642-36171-5. doi: 10.1007/978-3-642-36172-2.

Bowyer, **2016**. Susan M. Bowyer. *Coherence a measure of the brain networks: past and present.* Neuropsychiatric Electrophysiology, 2, 1, 2016. ISSN 2055-4788. doi: 10.1186/s40810-015-0015-7.

Breivik, Collett, Ventafridda, Cohen, and Gallacher, **2006**. Harald Breivik, Beverly Collett, Vittorio Ventafridda, Rob Cohen, and Derek Gallacher. *Survey of chronic pain in Europe: Prevalence, impact on daily life, and treatment.* European Journal of Pain, 10(4), 287–333, 2006. ISSN 10903801. doi: 10.1016/j.ejpain.2005.06.009.

Cao and Slobounov, **2010**. C. Cao and S. Slobounov. *Alteration of Cortical Functional Connectivity as a Result of Traumatic Brain Injury Revealed by Graph Theory, ICA, and sLORETA Analyses of EEG Signals.* IEEE Trans Neural Syst Rehabil Eng., 18(1), 11–19, 2010. ISSN 1946-6242. doi: 10.1124/dmd.107.016501.CYP3A4-Mediated.

Cao, Guo, and Su, **2015**. K. Cao, Y. Guo, and Steven W. Su. *A review of motion related EEG artifact removal techniques.* 2015 Ninth International Conference on Sensing Technology, pages 600–604, 2015. ISSN 21568073. doi: 10.1109/ICSensT.2015.7438469.

Case, Zhang, Mundahl, Datta, Nelson, Gupta, and He, **2017**. Michelle Case, Huishi Zhang, John Mundahl, Yvonne Datta, Stephen Nelson, Kalpna Gupta, and Bin He. *Characterization of functional brain activity and connectivity using EEG and fMRI in patients with sickle cell disease.* NeuroImage: Clinical, 14, 1–17, 2017. ISSN 22131582. doi: 10.1016/j.nicl.2016.12.024.

Chen, Ros, and Gruzelier, **2013**. Jean Lon Chen, Tomas Ros, and John H. Gruzelier. *Dynamic changes of ICA-derived EEG functional connectivity in the resting state.* Human Brain Mapping, 34(4), 852–868, 2013. ISSN 10659471. doi: 10.1002/hbm.21475.

Clark, Brown, Jones, and El-Deredy, **2008**. Jennifer A. Clark, Christopher A. Brown, Anthony K P Jones, and Wael El-Deredy. *Dissociating nociceptive modulation by the duration of pain anticipation from unpredictability in the timing of pain.* Clinical Neurophysiology, 119(12), 2870–2878, 2008. ISSN 13882457. doi: 10.1016/j.clinph.2008.09.022.

Cooke and Bliss, **2006**. S. F. Cooke and T. V. P. Bliss. *Plasticity in the human central nervous system.* Brain, 129(7), 1659–1673, 2006. ISSN 00068950. doi: 10.1093/brain/awl082.

Hanna Damasio. Exterior Description of a Normal Dolichocephalic Brain. In *Human Brain Anatomy in Computerized Images*, chapter 2, pages 11–30. Oxford University Press, 2014.

Dowman, **2001**. Robert Dowman. *Attentional set effects on spinal and supraspinal responses to pain.* Psychophysiology, 38(3), 451–64, 2001. ISSN 0048-5772. doi: 10.1017/S0048577201991395.

Eriksen, Jensen, Sjøgren, Ekholm, and Rasmussen, **2003**. Jørgen Eriksen, Marianne K. Jensen, Per Sjøgren, Ola Ekholm, and Niels K. Rasmussen. *Epidemiology of chronic non-malignant pain in Denmark.* Pain, 106(3), 221–228, 2003. ISSN 03043959. doi: 10.1016/S0304-3959(03)00225-2.

Fillingim, Loeser, Baron, and Edwards, **2016**. Roger B. Fillingim, John D. Loeser, Ralf Baron, and Robert R. Edwards. *Assessment of Chronic Pain: Domains, Methods, and Mechanisms.* Journal of Pain, 17(9), T10–T20, 2016. ISSN 15288447. doi: 10.1016/j.jpain.2015.08.010.

Fraschini, Demuru, Crobe, Marrosu, Stam, and Hillebrand, **2016**. Matteo Fraschini, Matteo Demuru, Alessandra Crobe, Francesco Marrosu, Cornelis J. Stam, and Arjan Hillebrand. *The effect of epoch length on estimated EEG functional connectivity and brain network organisation.* Journal of Neural Engineering, 13(3), 2016. ISSN 1741-2560. doi: 10.1088/1741-2560/13/3/036015.

Friebel, Eickhoff, and Lotze, **2011**. Ulrike Friebel, Simon B. Eickhoff, and Martin Lotze. *Coordinate-based meta-analysis of experimentally induced and chronic persistent neuropathic pain.* NeuroImage, 58(4), 1070–1080, 2011. ISSN 10538119. doi: 10.1016/j.neuroimage.2011.07.022.

Friston, **2011**. Karl J. Friston. *Functional and Effective Connectivity: A Review.* Brain Connectivity, 1(1), 13–36, 2011. ISSN 2158-0022. doi: 10.1089/brain.2011.0008.

Garcia-Larrea and Peyron, **2013**. Luis Garcia-Larrea and Roland Peyron. *Pain matrices and neuropathic pain matrices: A review.* Pain, 154(Suppl. 1), S29–S43, 2013. ISSN 03043959. doi: 10.1016/j.pain.2013.09.001.

González-Roldán, Cifre, Sitges, and Montoya, **2016**. Ana M. González-Roldán, Ignacio Cifre, Carolina Sitges, and Pedro Montoya. *Altered Dynamic of EEG Oscillations in Fibromyalgia Patients at Rest.* Pain medicine, 17(6), 224–224, 2016. ISSN 1526-4637. doi: 10.1093/pm/pnw023.

Gram, Erlenwein, Petzke, Falla, Przemeck, Emons, Reuster, Olesen, and Drewes, **2017**. M. Gram, J. Erlenwein, F. Petzke, D. Falla, M. Przemeck, M. I. Emons, M. Reuster, S. S. Olesen, and A. M. Drewes. *Prediction of postoperative opioid analgesia using clinical-experimental parameters and electroencephalography.* European Journal of Pain, 21(2), 264–277, 2017. ISSN 15322149. doi: 10.1002/ejp.921.

Grech, Cassar, Muscat, Camilleri, Fabri, Zervakis, Xanthopoulos, Sakkalis, and Vanrumste, **2008**. Roberta Grech, Tracey Cassar, Joseph Muscat, Kenneth Camilleri, Simon Fabri, Michalis Zervakis, Petros Xanthopoulos, Vangelis Sakkalis, and Bart Vanrumste. *Review on solving the inverse problem in EEG source analysis.* Journal of NeuroEngineering and Rehabilitation, 5(25), 2008. ISSN 1743-0003. doi: 10.1186/1743-0003-5-25.

Hansen, Klein, Magerl, and Treede, **2007**. Niels Hansen, Thomas Klein, Walter Magerl, and Rolf-Detlef Treede. *Psychophysical Evidence for Long-Term Potentiation of C-Fiber and A$\boldsymbol{\delta}$ - Fiber Pathways in Humans by Analysis of Pain Descriptors.* J Neurophysiol., 97, 2559–2563, 2007. doi: 10.1152/jn.01125.2006.

Henderson and Di Pietro, **2016**. Luke A Henderson and Flavia Di Pietro. *How do neuroanatomical changes in individuals with chronic pain result in the constant perception of pain?* Pain Management, 6(2), 147–159, 2016. ISSN 1758-1877. doi: 10.1002/9780470015902.a0003656.pub2.

Hennings, Arendt-Nielsen., Christensen, and Andersen, **2005a**. K. Hennings, L. Arendt-Nielsen., S.S. Christensen, and O.K. Andersen. *Selective activation of small-diameter motor fibres using exponentialiy rising waveforms: a theoretical study.* Medical & Biological Engineering & Computing, 43, 493–500, 2005.

Hennings, Arendt-Nielsen, and Andersen, **2005b**. Kristian Hennings, Lars Arendt-Nielsen, and Ole K. Andersen. *Orderly activation of human motor neurons using electrical ramp prepulses.* Clinical Neurophysiology, 116(3), 597–604, 2005. ISSN 13882457. doi: 10.1016/j.clinph.2004.09.011.

Henrich, Magerl, Klein, Greffrath, and Treede, **2015**. Florian Henrich, Walter Magerl, Thomas Klein, Wolfgang Greffrath, and Rolf Detlef Treede. *Capsaicin-sensitive C- and A-fibre nociceptors control long-term potentiation-like pain amplification in humans.* Brain, 138(9), 2505–2520, 2015. ISSN 14602156. doi: 10.1093/brain/awv108.

Hugosdottir, Mørch, Andersen, Helgason, and Arendt-Nielsen. R. Hugosdottir, C.D. Mørch, O.K. Andersen, T. Helgason, and L. Arendt-Nielsen. *Evaluating the Ability of Non-Rectangular Electrical Pulse Forms to Preferentially Activate Nociceptive Fibers by Comparing Perception Thresholds.*

Huishi Zhang, Sohrabpour, Lu, and He, **2016**. Clara Huishi Zhang, Abbas Sohrabpour, Yunfeng Lu, and Bin He. *Spectral and spatial changes of brain rhythmic activity in response to the sustained thermal pain stimulation.* Human Brain Mapping, 37(8), 2976–2991, 2016. ISSN 10970193. doi: 10.1002/hbm.23220.

Iannetti and Mouraux, **2010**. G. D. Iannetti and a. Mouraux. *From the neuromatrix to the pain matrix (and back).* Experimental Brain Research, 205(1), 1–12, 2010. ISSN 00144819. doi: 10.1007/s00221-010-2340-1.

John R. Iversen, Alejandro Ojeda, Tim Mullen, Markus Plank, Joseph Snider, Gert Cauwenberghs, and Howard Poizner, *2014*. John R. Iversen, Alejandro Ojeda, Tim Mullen, Markus Plank, Joseph Snider, Gert Cauwenberghs, and Howard Poizner. Causal analysis of cortical networks involved in reaching to spatial targets. In *Engineering in Medicine and Biology Society. 36th Annual International Conference of the IEEE*, pages 4399–4402, 2014. ISBN 9781424479290. doi: 10.1109/EMBC.2014.6944599.

Jatoi, Kamel, Malik, Faye, and Begum, **2014**. Munsif Ali Jatoi, Nidal Kamel, Aamir Saeed Malik, Ibrahima Faye, and Tahamina Begum. *A survey of methods used for source localization using EEG signals.* Biomedical Signal Processing and Control, 11(1), 42–52, 2014. ISSN 17468108. doi: 10.1016/j.bspc.2014.01.009.

Ji, Kohno, Moore, and Woolf, **2003**. Ru Rong Ji, Tatsuro Kohno, Kimberly A. Moore, and Clifford J. Woolf. *Central sensitization and LTP: Do pain and memory share similar mechanisms?* Trends in Neurosciences, 26(12), 696–705, 2003. ISSN 01662236. doi: 10.1016/j.tins.2003.09.017.

Jutzeler, Curt, and Kramer, **2015**. Catherine R. Jutzeler, Armin Curt, and John L K Kramer. *Effectiveness of High-Frequency Electrical Stimulation Following Sensitization With Capsaicin.* Journal of Pain, 16(7), 595–605, 2015. ISSN 15288447. doi: 10.1016/j.jpain.2015.03.005.

Kadam and Bhalerao, **2010**. P. Kadam and S. Bhalerao. *Sample size calculation.* International journal of Ayurveda Research, 1(1), 55–57, 2010. doi: 10.4103/0974-7788.59946.

Kirschstein and Köhling, **2009**. Timo Kirschstein and Rüdiger Köhling. *What is the Source of the EEG?* Clinical EEG and Neuroscience, 40(3), 146–149, 2009. ISSN 1550-0594. doi: 10.1177/155005940904000305.

Klein, Magerl, Hopf, Sandkühler, and Treede, **2004**. Thomas Klein, Walter Magerl, Hanns-Christian Hopf, Jürgen Sandkühler, and Rolf-Detlef Treede. *Perceptual Correlates of Nociceptive Long-Term Potentiation and Long-Term Depression in Humans.* Journal of Neuroscience, 24(4), 964–971, 2004. ISSN 0270-6474. doi: 10.1523/JNEUROSCI.1222-03.2004.

Klein, Magerl, and Treede, **2006**. Thomas Klein, Walter Magerl, and Rolf-Detlef Treede. *Perceptual correlate of nociceptive long-term potentiation (LTP) in humans shares the time course of early-LTP.* J Neurophysiol., 96(6), 3551–3555, 2006. ISSN 0022-3077. doi: 10.1152/jn.00755.2006.

Klein, Stahn, Magerl, and Treede, **2008**. Thomas Klein, Simon Stahn, Walter Magerl, and Rolf-Detlef Treede. *The role of heterosynaptic facilitation in long-term potentiation (LTP) of human pain sensation.* Pain, 139(3), 507–519, 2008. ISSN 03043959. doi: 10.1016/j.pain.2008.06.001.

Kuner and Flor, **2017**. Rohini Kuner and Herta Flor. *Structural plasticity and reorganisation in chronic pain.* Nature Reviews Neuroscience, 18(1), 20–30, 2017. ISSN 1471-003X. doi: 10.1038/nrn.2016.162.

Lang, Klein, Magerl, and Treede, **2007**. Stefanie Lang, Thomas Klein, Walter Magerl, and Rolf-Detlef Treede. *Modality-specific sensory changes in humans after the induction of long-term potentiation (LTP) in cutaneous nociceptive pathways.* Pain, 128(3), 254–263, 2007. ISSN 03043959. doi: 10.1016/j.pain.2006.09.026.

Lelic, Mørch, Hennings, Andersen, and M. Drewes, **2012**. D. Lelic, C. D. Mørch, K. Hennings, O. K. Andersen, and A. M. Drewes. *Differences in perception and brain activation following stimulation by large versus small area cutaneous surface electrodes.* European Journal of Pain, 16 (6), 827–837, 2012. ISSN 10903801. doi: 10.1002/j.1532-2149.2011.00063.x.

Lelic, Olesen, Hansen, Valeriani, and Drewes, **2014**. D. Lelic, S. S. Olesen, T. M. Hansen, M. Valeriani, and A. M. Drewes. *Functional reorganization of brain networks in patients with painful chronic pancreatitis.* European journal of pain, 18, 968–977, 2014. ISSN 1532-2149. doi: 10.1002/j.1532-2149.2013.00442.x.

Mahjoory, Nikulin, Botrel, Linkenkaer-Hansen, Fato, and Haufe, **2017**. Keyvan Mahjoory, Vadim V Nikulin, Loic Botrel, Klaus Linkenkaer-Hansen, Marco M Fato, and Stefan Haufe. *Consistency of EEG source localization and connectivity estimates.* NeuroImage, 152, 071597, 2017. ISSN 10538119. doi: 10.1101/071597.

Maihöfner, Jesberger, Seifert, and Kaltenhäuser, **2010**. Christian Maihöfner, Florian Jesberger, Frank Seifert, and Martin Kaltenhäuser. *Cortical processing of mechanical hyperalgesia: A MEG study.* European Journal of Pain, 14(1), 64–70, 2010. ISSN 10903801. doi: 10.1016/j.ejpain.2009.02.007.

Manresa, Neziri, Curatolo, Arendt-Nielsen, and Andersen, **2013**. José A. Biurrun Manresa, Alban Y. Neziri, Michele Curatolo, Lars Arendt-Nielsen, and Ole K. Andersen. *Reflex receptive fields are enlarged in patients with musculoskeletal low back and neck pain.* Pain, 154(8), 1318–1324, 2013. ISSN 03043959. doi: 10.1016/j.pain.2013.04.013.

Manresa, Finnerup, Johannesen, Biering-Sørensen, Jensen, Arendt-Nielsen, and Andersen, **2014**. José Alberto Biurrun Manresa, Nanna Susanne Brix Finnerup, Inger Lauge Johannesen, Fin Biering-Sørensen, Troels Staehelin Jensen, Lars Arendt-Nielsen, and Ole Kæseler Andersen. *Central sensitization in spinal cord injured humans assessed by reflex receptive fields.* Clinical Neurophysiology, 125(2), 352–362, 2014. ISSN 13882457. doi: 10.1016/j.clinph.2013.06.186.

Martel, Harvey, Houde, Balg, Goffaux, and Léonard, **2017**. Marylie Martel, Marie-Philippe Harvey, Francis Houde, Frédéric Balg, Philippe Goffaux, and Guillaume Léonard. *Unravelling the*

effect of experimental pain on the corticomotor system using transcranial magnetic stimulation and electroencephalography. Experimental Brain Research, 235(4), 1223–1231, 2017. ISSN 14321106. doi: 10.1007/s00221-017-4880-0.

Martini, Nath, and Bartholomew, **2012**. Frederic H. Martini, Judi L. Nath, and Edwin F. Bartholomew. *Anatomy and Physiologi*. 2012. ISBN 9780321709332. doi: 10.1080/13613320802110217.

Michel and Murray, **2012**. Christoph M. Michel and Micah M. Murray. *Towards the utilization of EEG as a brain imaging tool*. NeuroImage, 61(2), 371–385, 2012. ISSN 10538119. doi: 10.1016/j.neuroimage.2011.12.039.

Michel, Murray, Lantz, Gonzalez, Spinelli, and Grave De Peralta, **2004**. Christoph M. Michel, Micah M. Murray, Göran Lantz, Sara Gonzalez, Laurent Spinelli, and Rolando Grave De Peralta. *EEG source imaging*. Clinical Neurophysiology, 115(10), 2195–2222, 2004. ISSN 13882457. doi: 10.1016/j.clinph.2004.06.001.

Mohr, Leyendecker, Mangels, Machner, Sander, and Helmchen, **2009**. C. Mohr, S. Leyendecker, I. Mangels, B. Machner, T. Sander, and C. Helmchen. *Central representation of cold-evoked pain relief in capsaicin induced pain: An event-related fMRI study*. Pain, 139(2), 416–430, 2009. ISSN 03043959. doi: 10.1016/j.pain.2008.05.020.

Navarro, Vivó, and Valero-Cabré, **2007**. X. Navarro, Meritxell Vivó, and Antoni Valero-Cabré. *Neural plasticity after peripheral nerve injury and regeneration*. Progress in Neurobiology, 82(4), 163–201, 2007. ISSN 03010082. doi: 10.1016/j.pneurobio.2007.06.005.

Niso, Bruña, Pereda, Gutiérrez, Bajo, Maestú, and Del-Pozo, **2013**. Guiomar Niso, Ricardo Bruña, Ernesto Pereda, Ricardo Gutiérrez, Ricardo Bajo, Fernando Maestú, and Francisco Del-Pozo. *HERMES: Towards an integrated toolbox to characterize functional and effective brain connectivity*. Neuroinformatics, 11(4), 405–434, 2013. ISSN 15392791. doi: 10.1007/s12021-013-9186-1.

Pascual-Marqui, **2002**. R. D. Pascual-Marqui. *Standardized low resolution brain electromagnetic tomography (sLORETA): technical details*. Methods & Findings in Experimental & Clinical Pharmacology, 24D, 1–16, 2002. ISSN 0379-0355. doi: 841[pii].

Pascual-Marqui, **2015a**. Roberto D. Pascual-Marqui. *LORETA; Low Resolution Electromagnetic Tomography, Standardized & exact & Zero-error forever*, 2015. URL http://www.uzh.ch/keyinst/loreta.

Pascual-Marqui, **2015b**. Roberto D. Pascual-Marqui. *Statistical testing implemented in the KEY-LORETA software : Non-parametric randomization tests , aka Statistical non- Parametric Mapping (SnPM) methodology*, 2015.

Pascual-Marqui, **2015c**. Roberto D. Pascual-Marqui. *sLORETA. eLORETA. Functional connectivity tutorial*, 2015c.

Pesarin and Salmaso, **2010**. Fortunato Pesarin and Luigi Salmaso. *The permutation testing approach: a review*. Statistica, 70(4), 481–509, 2010. ISSN 1973-2201. doi: 10.6092/issn.1973-2201/3599.

Petrini, Hennings, Li, Negro, and Arendt-Nielsen, **2014**. Laura Petrini, Kristian Hennings, Xi Li, Francesco Negro, and Lars Arendt-Nielsen. *A human experimental model of episodic pain*. International Journal of Psychophysiology, 94(3), 496–503, 2014. ISSN 18727697. doi: 10.1016/j.ijpsycho.2014.07.013.

Pfau, Klein, Putzer, Pogatzki-Zahn, Treede, and Magerl, **2011**. Doreen B. Pfau, Thomas Klein, Daniel Putzer, Esther M. Pogatzki-Zahn, Rolf-Detlef Treede, and Walter Magerl. *Analysis of hyperalgesia time courses in humans after painful electrical high-frequency stimulation identifies a possible transition from early to late LTP-like pain plasticity.* Pain, 152(7), 1532–1539, 2011. ISSN 03043959. doi: 10.1016/j.pain.2011.02.037.

Reches, Nir, Shram, Dickman, Laufer, Shani-Hershkovich, Stern, Weiss, Yarnitsky, and Geva, **2016**. A. Reches, R.-R. Nir, M. J. Shram, D. Dickman, I. Laufer, R. Shani-Hershkovich, Y. Stern, M. Weiss, D. Yarnitsky, and A. B. Geva. *A novel electroencephalography-based tool for objective assessment of network dynamics activated by nociceptive stimuli.* European Journal of Pain, 20(2), 250–262, 2016. ISSN 15322149. doi: 10.1002/ejp.716.

Rottmann, Jung, and Ellrich, **2010**. Silke Rottmann, Kerstin Jung, and Jens Ellrich. *Electrical low-frequency stimulation induces long-term depression of sensory and affective components of pain in healthy man.* European Journal of Pain, 14(4), 359–365, 2010. ISSN 10903801. doi: 10.1016/j.ejpain.2009.06.001.

Sakkalis, **2011**. V. Sakkalis. *Review of advanced techniques for the estimation of brain connectivity measured with EEG/MEG.* Computers in Biology and Medicine, 41(12), 1110–1117, 2011. ISSN 00104825. doi: 10.1016/j.compbiomed.2011.06.020.

Sandkühler, **2000**. Jürgen Sandkühler. *Learning and memory in pain pathways.* Pain, 88(2), 113–118, 2000. ISSN 03043959. doi: 10.1016/S0304-3959(00)00424-3.

Sandkühler, **2007**. Jürgen Sandkühler. *Understanding LTP in pain pathways.* Molecular pain, 3 (9), 2007. ISSN 1744-8069. doi: 10.1186/1744-8069-3-9.

Sandkühler, **2009**. Jürgen Sandkühler. *Models and mechanisms of hyperalgesia and allodynia.* Physiol Rev, 89, 707–758, 2009. doi: 10.1152/physrev.00025.2008.

Sandkühler and Gruber-Schoffnegger, **2012**. Jürgen Sandkühler and Doris Gruber-Schoffnegger. *Hyperalgesia by synaptic long-term potentiation (LTP): An update.* Current Opinion in Pharmacology, 12(1), 18–27, 2012. ISSN 14714892. doi: 10.1016/j.coph.2011.10.018.

Saeid Sanei and J. A. Chambers. Introduction to EEG. In *EEG Signal Processing*, chapter 1, pages 1–35. John Wiley & Sons, 2007. ISBN 9780199985906. doi: 10.1093/med/9780199985906.003.0001.

Schulz, May, Postorino, Tiemann, Nickel, Witkovsky, Schmidt, Gross, and Ploner, **2015**. Enrico Schulz, Elisabeth S. May, Martina Postorino, Laura Tiemann, Moritz M. Nickel, Viktor Witkovsky, Paul Schmidt, Joachim Gross, and Markus Ploner. *Prefrontal gamma oscillations encode tonic pain in humans.* Cerebral Cortex, 25(11), 4407–4414, 2015. ISSN 14602199. doi: 10.1093/cercor/bhv043.

Sekihara, Sahani, and Nagarajan, **2005**. Kensuke Sekihara, Maneesh Sahani, and Srikantan S. Nagarajan. *Localization bias and spatial resolution of adaptive and non-adaptive spatial filters for MEG source reconstruction.* NeuroImage, 25(4), 1056–1067, 2005. ISSN 10538119. doi: 10.1016/j.neuroimage.2004.11.051.

Sekihara, Owen, Trisno, and Nagarajan, **2011**. Kensuke Sekihara, Julia P. Owen, Stephan Trisno, and Srikantan S. Nagarajan. *Removal of spurious coherence in MEG source-space coherence analysis.* IEEE Transactions on Biomedical Engineering, 58(11), 3121–3129, 2011. ISSN 00189294. doi: 10.1109/TBME.2011.2162514.

Stam and Straaten, **2012**. C. J. Stam and E. C. W. van Straaten. *The organization of physiological brain networks.* Clinical Neurophysiology, 123(6), 1067–1087, 2012. ISSN 13882457. doi: 10.1016/j.clinph.2012.01.011.

Staud, **2006**. Roland Staud. *Biology and therapy of fibromyalgia: pain in fibromyalgia syndrome.* Arthritis research & therapy, 8(3), 2006. ISSN 1478-6362. doi: 10.1186/ar1950.

Sun, Lim, Kwok, and Bezerianos, **2014a**. Yu Sun, Julian Lim, Kenneth Kwok, and Anastasios Bezerianos. *Functional cortical connectivity analysis of mental fatigue unmasks hemispheric asymmetry and changes in small-world networks.* Brain and Cognition, 85(1), 220–230, 2014. ISSN 02782626. doi: 10.1016/j.bandc.2013.12.011.

Sun, Lim, Meng, Kwok, Thakor, and Bezerianos, **2014b**. Yu Sun, Julian Lim, Jianjun Meng, Kenneth Kwok, Nitish Thakor, and Anastasios Bezerianos. *Discriminative Analysis of Brain Functional Connectivity Patterns for Mental Fatigue Classification.* Annals of Biomedical Engineering, 40(10), 2084–2094, 2014. ISSN 15739686. doi: 10.1007/s10439-014-1059-8.

Taesler and Rose, **2016**. Philipp Taesler and Michael Rose. *Prestimulus Theta Oscillations and Connectivity Modulate Pain Perception.* Journal of Neuroscience, 36(18), 5026–5033, 2016. ISSN 0270-6474. doi: 10.1523/JNEUROSCI.3325-15.2016.

Trans Cranial Technologies Ltd., **2012**. Trans Cranial Technologies Ltd. *Cortical Functions Reference*, 2012. URL http://www.trans-cranial.com/local/manuals/cortical{_}functions{_}ref{_}v1{_}0{_}pdf.pdf.

Broeke, Geene, Van Rijn, Wilder-Smith, and Oosterman, **2014**. E. N. van den Broeke, N. Geene, C. M. Van Rijn, O. H. G. Wilder-Smith, and J. Oosterman. *Negative expectations facilitate mechanical hyperalgesia after high-frequency electrical stimulation of human skin.* European Journal of Pain, 18(1), 86–91, 2014. ISSN 10903801. doi: 10.1002/j.1532-2149.2013.00342.x.

Broeke and Mouraux, **2014a**. Emanuel N. van den Broeke and André Mouraux. *High-frequency electrical stimulation of the human skin induces heterotopical mechanical hyperalgesia, heat hyperalgesia, and enhanced responses to nonnociceptive vibrotactile input.* Journal of neurophysiology, 111(8), 1564–73, 2014. ISSN 1522-1598. doi: 10.1152/jn.00651.2013.

Broeke and Mouraux, **2014b**. Emanuel N. van den Broeke and André Mouraux. *Enhanced brain responses to C-fiber input in the area of secondary hyperalgesia induced by high-frequency electrical stimulation of the skin.* Journal of neurophysiology, 112(9), 2059–66, 2014. ISSN 1522-1598. doi: 10.1152/jn.00342.2014.

Broeke, Van Rijn, Manresa, Andersen, Arendt-Nielsen, and Wilder-Smith, **2010**. Emanuel N. van den Broeke, Clementina M. Van Rijn, José A. Biurrun Manresa, Ole K. Andersen, Lars Arendt-Nielsen, and Oliver H. G. Wilder-Smith. *Neurophysiological correlates of nociceptive heterosynaptic long-term potentiation in humans.* Journal of Neurophysiology, 103(4), 2107–2113, 2010. ISSN 0022-3077. doi: 10.1152/jn.00979.2009.

Broeke, Heck, Rijn, and Wilder-Smith, **2011**. Emanuel N. van den Broeke, Casper H. van Heck, Clementina M. van Rijn, and Oliver H. G. Wilder-Smith. *Neural correlates of heterotopic facilitation induced after high frequency electrical stimulation of nociceptive pathways.* Molecular pain, 7(28), 2011. ISSN 1744-8069. doi: 10.1186/1744-8069-7-28.

Broeke, Koeslag, Arendsen, Nienhuijs, Rosman, Rijn, Wilder-Smith, and Goor, **2013**. Emanuel N. van den Broeke, Lonneke Koeslag, Laura J. Arendsen, Simon W. Nienhuijs, Camiel Rosman, Clementina M. van Rijn, Oliver H. G. Wilder-Smith, and Harry van Goor. *Altered cortical responsiveness to pain stimuli after high frequency electrical stimulation of the skin in patients with persistent pain after inguinal hernia repair.* PLoS ONE, 8(12), 2013. ISSN 19326203. doi: 10.1371/journal.pone.0082701.

Broeke, Mouraux, Groneberg, Pfau, Treede, and Klein, **2015**. Emanuel N. van den Broeke, Andre Mouraux, Antonia H. Groneberg, Doreen B. Pfau, Rolf-Detlef Treede, and Thomas Klein. *Characterizing pinprick evoked brain potentials before and after experimentally-induced secondary*

hyperalgesia. Journal of neurophysiology, 114, 2672–2681, 2015. ISSN 1522-1598. doi: 10.1152/jn.00444.2015.

Broeke, Lambert, Huang, and Mouraux, **2016a**. Emanuel N. van den Broeke, Julien Lambert, Gan Huang, and André Mouraux. *Central Sensitization of Mechanical Nociceptive Pathways Is Associated with a Long-Lasting Increase of Pinprick-Evoked Brain Potentials.* Frontiers in Human Neuroscience, 10, 2016. ISSN 1662-5161. doi: 10.3389/fnhum.2016.00531.

Broeke, Lenoir, and Mouraux, **2016b**. Emanuel N. van den Broeke, Cédric Lenoir, and André Mouraux. *Secondary hyperalgesia is mediated by heat-insensitive A-fibre nociceptors.* The Journal of Physiology, 594(22), 6767–6776, 2016. ISSN 00223751. doi: 10.1113/JP272599.

Diessen, Numan, Dellen, Kooi, Boersma, Hofman, Lutterveld, Dijk, Straaten, Hillebrand, and Stam, **2015**. E. van Diessen, T. Numan, E. van Dellen, A. W. van der Kooi, M. Boersma, D. Hofman, R. van Lutterveld, B. W. van Dijk, E. C W van Straaten, A. Hillebrand, and C. J. Stam. *Opportunities and methodological challenges in EEG and MEG resting state functional brain network research.* Clinical Neurophysiology, 126(8), 1468–1481, 2015. ISSN 18728952. doi: 10.1016/j.clinph.2014.11.018.

Vo and Drummond, **2016**. L. Vo and P. D. Drummond. *Involvement of alpha2-adrenoceptors in inhibitory and facilitatory pain modulation processes.* European Journal of Pain, 20(3), 386–398, 2016. ISSN 15322149. doi: 10.1002/ejp.736.

Rotz, Kometer, Dornbierer, Gertsch, Salomé Gachet, Vollenweider, Seifritz, Bosch, and Quednow, **2017**. Robin von Rotz, Michael Kometer, Dario Dornbierer, Jürg Gertsch, M. Salomé Gachet, Franz X. Vollenweider, Erich Seifritz, Oliver G. Bosch, and Boris B. Quednow. *Neuronal oscillations and synchronicity associated with gamma-hydroxybutyrate during resting-state in healthy male volunteers.* Psychopharmacology, 2017. ISSN 0033-3158. doi: 10.1007/s00213-017-4603-z.

Wartolowska, **2011**. Karolina Wartolowska. *How neuroimaging can help us to visualise and quantify pain?* European Journal of Pain Supplements, 5(2), 323–327, 2011. ISSN 17543207. doi: 10.1016/j.eujps.2011.08.012.

Weidner, Schmidt, Schmelz, Hilliges, Handwerker, and Torebjörk, **2000**. C. Weidner, R. Schmidt, M. Schmelz, M. Hilliges, H. O. Handwerker, and H. E. Torebjörk. *Time course of post-excitatory effects separates afferent human C fibre classes.* The Journal of physiology, 527 (1), 185–191, 2000. ISSN 0022-3751. doi: 10.1111/j.1469-7793.2000.00185.x.

Woolf, **2011**. Clifford J. Woolf. *Central sensitization: Implications for the diagnosis and treatment of pain.* Pain, 152(3), S2–S15, 2011. ISSN 0304-3959. doi: 10.1016/j.pain.2010.09.030.

Xia, Mørch, Matre, and Andersen, **2016a**. W. Xia, C. D. Mørch, D. Matre, and O. K. Andersen. *Exploration of conditioned pain modulation effect on long-term potentiation-like pain amplification in humans.* European Journal of Pain (, 2016. ISSN 15322149. doi: 10.1002/ejp.968.

Xia, Mørch, and Andersen, **2016b**. Weiwei Xia, Carsten Dahl Mørch, and Ole Kæseler Andersen. *Exploration of the conditioning electrical stimulation frequencies for induction of long-term potentiation-like pain amplification in humans.* Experimental Brain Research, 234(9), 2479–2489, 2016. ISSN 14321106. doi: 10.1007/s00221-016-4653-1.

Yao, **2001**. Dezhong Yao. *A method to standardize a reference of scalp EEG recordings to a point at infinity.* Physiological Measurement, 22, 693–711, 2001. ISSN 0967-3334. doi: 10.1088/0967-3334/22/4/305.

Appendix A

Long-term potentiation

Long-term potentiation (LTP) is a persistent strengthening of synapses that outlast the duration of the conditioning stimulus for a minimum of 30 minutes and up to several months. The increased synaptic strength characterizing LTP is mediated by several molecular mechanisms [Cooke and Bliss, 2006]. The N-methyl-D-aspartate (NMDA) receptors can act as a molecular detector of coincident pre- and post-synaptic activity. This mechanism accounts for the associativity characteristics of LTP, where a nerve can be potentiated by a weak stimulus not strong enough by itself, because of a simultaneous strong stimulus. [Bliss and Collingridge, 1993]

During resting state or low level activity the NMDA receptor channel is blocked by magnesium ions (MG^{2+}). Two events must occur simultaneously to open the NMDA channels. Both L-glutamate released into the synaptic cleft from the pre-synaptic terminal must be bound to the NMDA receptor and MG^{2+} must be expelled. The magnesium blockage is voltage dependent and the MG^{2+} is only expelled when the post-synaptic cell is sufficiently depolarized. The sufficient depolarization of the post-synaptic membrane is mediated by $\boldsymbol{\alpha}$-amino-3-hydroxy-5-methyl-4-isoxazolepropionic (AMPA) receptor channels, which open for sodium influx when L-glutamate in the synaptic cleft is bound to the receptor. When depolarization results in removal of MG^{2+} from the NMDA channel and L-glutamate is bound to the NMDA receptor the channels open. The opening of the NMDA channels allows an influx of sodium and calcium (Ca^{2+}) ions. [Cooke and Bliss, 2006]

This calcium influx is considered the initial step of LTP induction by activation of several calcium sensitive enzymes proposed to mediate the persistent modifications of synaptic strength. Inhibitor studies on animal slice preparations of the hippocampus have found several kinases to play a role in LTP induction. Introducing inhibitors of Ca^{2+}/Phospholipid-dependent protein kinase (PKC), resulted in a blockage of LTP induction indicating the activation of this enzyme to be necessary for LTP induction, however not sufficient. PKC is considered to be especially involved in the transition from short term potentiation (STP) to LTP. Inhibiting Ca^{2+}/calmodulin-dependent protein kinase (CAMKII) impaired the ability to exhibit LTP. The fact that the LTP induction is not completely blocked is suggested to be caused by the autophosphorylation of the enzyme. The autophosphorylation does not require calcium, since it is a process where the enzyme is phophorylated (addition of a phosphoryl group $\boldsymbol{(PO_3)^-}$ to the protein, changes the structure of the protein) by itself. This has further led to the suggestion of CaMKII to act as a molecular memory mechanism by detecting previous calcium releases. Other enzymes possibly involved in the induction of LTP are cyclic adenosine monophosphate (cAMP)-dependent protein kinase (PKA) and protein tyrosine kinase. These are considered to have a possible role because of their relation to the NMDA receptor activation. The level of cAMP is positively correlated to NMDA activation and NMDA receptor activation also leads to tyrosine phoshorylation of specific kinases. [Bliss and Collingridge, 1993]

Apart from the activation of enzymes other calcium sensitive mechanisms are activated as a result of calcium influx. These mechanisms include altered gene expression by transcription factor (protein binding to DNA) signaling to the cell nucleus and local phosphorylation of receptors resulting in altered receptor properties. [Cooke and Bliss, 2006] The gene transcription and protein synthesis may contribute to synaptic remodeling. This remodeling include possible increase in the amount of receptors and dendritic spines at the synapse, thus increasing the post-synaptic response to pre-synaptic activity [Kuner and Flor, 2017]. The protein kinases are also suggested to be involved, since some of them are regulated through the gene transcription. [Bliss and Collingridge, 1993]

Pre-synaptic modifications, resulting in an increased release of L-glutamate per impulse, also

influence the synaptic strengthening and potentiation. This is thought to be mediated by an intercellular signal released post-synapticly. However, the specific messenger mechanisms are not completely understood. Both arachidonic acid and nitric oxide (NO) has been proposed as messengers. Arachidonic acid is a fatty acid [Martini et al., 2012] that is released into the extracellular medium from cultured neurons as a response to NMDA receptor activation. It may act to increase the pre-synaptic release of L-glutamate and to depress L-glutamate uptake in glial cells. [Bliss and Collingridge, 1993] NO is a lipid soluble gas, mostly present in the brain, that can diffuse through lipid membranes activating enzymes inside the cell, which in turn promotes second messengers [Martini et al., 2012]. NO increases the frequency of small excitatory post-synaptic potentials in hippocampal cultures and LTP has been observed to be blocked by administration of NO synthase inhibitors. [Bliss and Collingridge, 1993] Even though, these two substances have been considered probable candidates their time course of action does not correspond with the time course of LTP. One possible messenger could be potassium, which is released from the postsynaptic site during the LTP inducing stimulation in a degree that to some extend follow the level of NMDA receptor activation. This extracellular potassium could provide signal to the pre-synaptic terminal by interaction with glutamate receptors. [Bliss and Collingridge, 1993]

Appendix B

Electroencephalography

Electroencephalography (EEG) is a widely used method for the study of brain dynamics. It is a measure of currents originating from synaptic excitation of dendrites of pyramidal neurons in the cortex. [Sanei and Chambers, 2007] Pyramidal neurons have rounded pyramid shaped somas. From the pointy end of the soma long apical dendrites emerge, while shorter basal dendrites emerge from the rounded end of the soma. Due to this structure and the perpendicular positioning of the apical dendrites relative to the cortical surface, the electrical dipole generated between apical and basal dendrites becomes detectable. Whether the recorded scalp potential is negative or positive depends on the depth of synaptic input and the excitatory or inhibitory nature of the input. For excitatory synapses, superficial excitation results in a negative scalp potential, while a deep excitation will cause positive scalp potentials. The opposite is the case for inhibitory synapses. [Kirschstein and Köhling, 2009]

The resulting electrical potentials generated by pyramidal cells are often recorded by electrodes at the scalp. The head consists of several tissue layers, all contributing to an attenuation of the electrical signal produced at the dendrites. The skull attenuates the signal the most and about 100 times more than soft tissue. Due to tissue composition, attenuation, and the introduction of noise within the brain and at the scalp, the surface EEG recording can only reflect a summation of extracellular potentials of large populations of neurons that are simultaneously active. [Sanei and Chambers, 2007] Consequently, the spatial resolution of the EEG is distorted, however the EEG has a high temporal resolution, making it a particular interesting tool when analyzing time variant interconnections of the brain [Stam and van Straaten, 2012].

The EEG signal is mostly sinusoidal in shape and in the microvolt range. The signal is often subdivided into five major brain waves characterized by frequency ranges. Each frequency band is associated with a state of alertness. [Sanei and Chambers, 2007]

- Alpha (9-12 Hz): relaxed awareness [Sanei and Chambers, 2007]
  - Alpha-1 (9-10 Hz)
  - Alpha-2 (10-12 Hz)
- Beta (14-26 Hz): active thinking, attention, focus, problem solving [Sanei and Chambers, 2007]
  - Beta-1 (13-17 Hz)
  - Beta-2 (18-20 Hz)
  - Beta-3 (21-30 Hz)
- Delta (1-4 Hz): deep sleep [Sanei and Chambers, 2007]
- Theta (5-8 Hz): drowsiness, unconscious material, creative inspiration, meditation [Sanei and Chambers, 2007]
- Gamma (30-100 Hz)

[Boeijinga, 2010]

Appendix C

Pilot studies

For the EEG connectivity analysis it was desired to record a total of 3-5 minutes, during continuous stimulation. In order to achieve a reliable and stable EEG response over the entire period of recording it was important that any sensitization of the skin area due to the effect of windup was limited. If the skin sensitized over the timespan of recording the perception of the stimulation would become more intense and the brain activity would be affected and thus might not have the same properties over the entire recording, which would in a great degree limit the analysis and the results thereof. Consequently, a pilot study was performed in order to investigate whether pinprick stimulation was suitable as continuous stimulation for the EEG recording.

An additional pilot study was performed in order to investigate which pulse shape and stimuli configuration to use for the conditional electrical stimulation (CES). It is known that five bursts of 1 second of rectangular pulses (2 ms) applied with a frequency of 100 Hz and with a burst interval of 10 s can be used to induce LTP-like increase in pain perception in healthy subjects [Klein et al., 2004]. It was shown by Hugosdottir et al. [in press] that an increasing form of the exponential current decay was the pulse shape amongst a number of different shapes that showed best potential towards selective activation of thin fibres. Selective thin fibre activation could be an indication of better induction of LTP-like pain.

The second pilot study showed inconsistent results in relation to the pulse shape, where a clear effect was observed for two subjects for the increasing form of exponential current decay, however the third subject did not respond. The missing response from one of the subjects could be due to a too low intensity of the applied CES, to induce detectable LTP-like increase in pain perception. Consequently, a third pilot study was conducted to consider standardization of the intensity of CES in relation to VAS scores.

In total three pilot studies were conducted with the following aims:

1. To identify a suitable protocol for continuous pinprick
2. To test the increasing form of the exponential current decay pulse with an exponential trailing phase for induction of LTP-like pain amplification
3. To investigate the method of standardizing the intensity of CES in relation to VAS scoring

Pilot 1

The purpose of the first pilot study was to test the possibility of performing continuous pinprick stimulation without considerably sensitizing the skin.

Materials

- Marker
- Pinprick stimulator (6.4 g)
- VAS meter (Aalborg university)
- Computer with AVel Electrical Pain Stimulation (Aalborg University)

Setup

The subject was seated comfortably in a chair with the arms resting on a table in a supine position. The VAS meter was places between the subject's hands.

Procedure

The first pilot study consisted of one session using both arms, one for each protocol. In one protocol the marked area on the arm was stimulated in a total of five minutes divided into blocks of one minute stimulation and one minute break. The second protocol consisted of three minutes continuous stimulation. In both protocols VAS was continuously scored during periods of stimulation. It was randomized which arm was used for which protocol. A circle with a diameter of 40 mm was drawn on the subjects medial lower arm and served as a marker of the stimulation site (see figure C.1). Pinpricks were applied on the peripheral boarder of the electrode placement and continuously rated by the subject on a VAS ranging from 0 to 10, where 0 was no sensation, 3 was the pain threshold and 10 was unbearable pain

Figure C.1: Mark of stimulation site in the pilot study

Analysis

For each minute the VAS was recorded and average VAS score was calculated. Subsequently the average scores and VAS tendencies throughout the two protocols were compared.

Results

The protocol containing five blocks of one minute stimulation and one minute break, showed a clear tendency towards sensitization of the skin, especially at the third, fourth, and fifth minute of stimulation. The average VAS score within these minutes increased well above the average score of the first minute for both subjects. For the protocol of three minutes continuous stimulation, the increase in VAS score from the first minute of stimulation to the third minute was not as pronounced as for the protocol containing one minute breaks (see figure C.2). However, the score was slightly higher at the initial minute for the continuous three minute protocol compared to the five minute protocol.

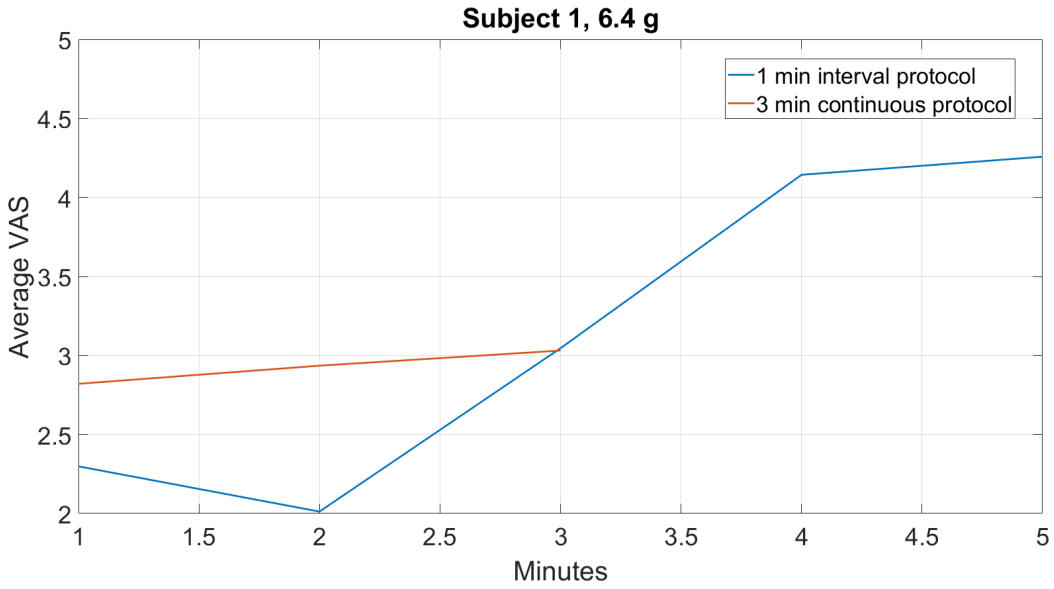

(a) The average VAS score for subject 1.

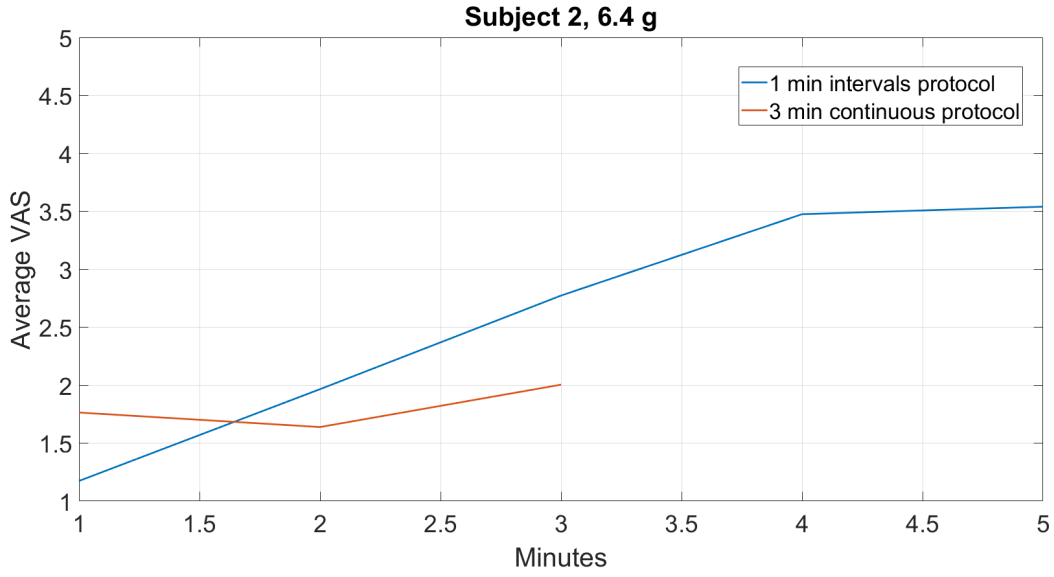

(b) The average VAS score for subject 2.

Figure C.2: Results of the two investigated pinprick protocols. Average VAS scores for each minute of stimulation. The blue line is VAS scores for the protocol containing five blocks of one minute stimulation followed by a one minute break. The red line is VAS scores for three minutes continuous stimulation protocol.

Pilot 2

The purpose of the second pilot study was to test if stimulation with an increasing form of the exponential current decay pulse with an exponential trailing phase was able to induce LTP-like increase in pain perception in a similar fashion as the conventional HFS [Klein et al., 2004]. In addition different pinprick weights were tested.

Materials

- Marker and tape
- Pinprick stimulator (6.4 g, 12.8 g, 25.6 g, and 50.1 g)
- VAS meter (Aalborg University)
- Computer with AVel Electrical Pain Stimulation (Aalborg University)

- Pin-electrode (cutaneous punctuate electrode, Aalborg University)
- Stimulator (Digitimer DS5)

Setup

The subject was seated comfortably in a chair with the arms resting on a table in a supine position. Electrodes were placed with the periphery 5 cm distal to the cubital fossa on both arms (see figure C.3). The VAS meter was placed between the subject's hands.

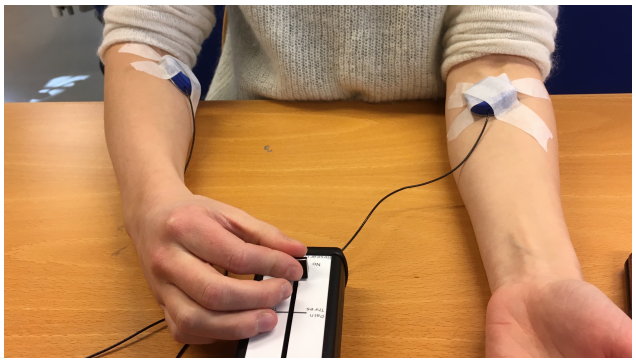

Figure C.3: Experimental setup. The electrodes were placed on both arms with the periphery 5 cm distal to the cubital fossa and the VAS meter between the subject's hands.

Procedure

The pilot study consisted of two sessions. In both sessions, the subject was stimulated with test stimuli before and after application of CES. The placement of the electrode was marked beforehand. Continuous pinprick stimuli (6.4 g) for three minutes was applied 45 minutes prior and 35 minutes subsequent to CES on both the conditioning and control arm. Single pinprick stimulation (12.8 g, 25.6 g, and 50.1 g) was applied in random order 10 and 20 minutes before, and 10, 20, and 30 minutes after CES (see figure C.4). For each measurement the single pinprick was rated on a VAS and performed three times on the peripheral boarder of the electrode placement with each weight, both on the conditioning and control arm. The VAS ranged from 0 to 10, where 0 was no sensation, 3 was the pain threshold and 10 was unbearable pain.

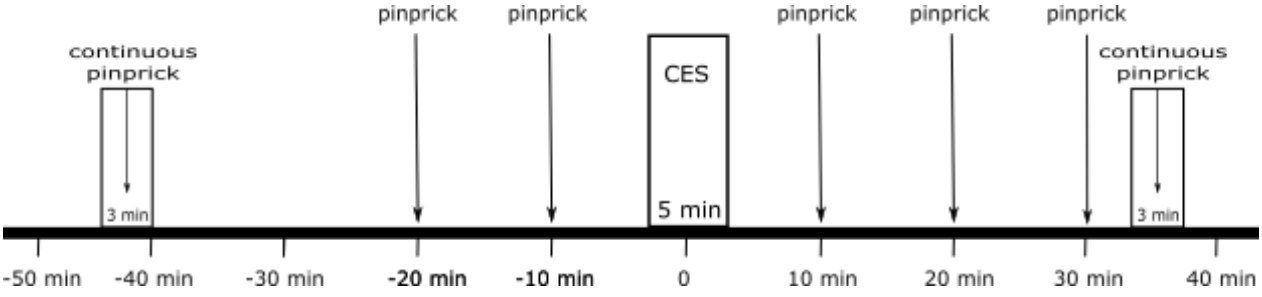

Figure C.4: The procedure time line of the pilot study. Three minutes of continuous pinprick was performed 45 minutes prior to CES and 35 minutes after CES. Test stimuli consisting of single pinprick stimulation with three different weights was performed 10 and 20 minutes prior to CES and 10, 20 and 30 minutes subsequent to CES.

In one session CES was applied as HFS described in Xia et al. [2016a] (100 Hz, 1 millisecond square waves, 5 times 1 second with 9 second in between) while the CES in the other session was applied as an increasing form of the exponential current decay with an exponential trailing phase (10 Hz, 50 ms). Before applying CES, the detection threshold was determined using the method of limits (three ascending and three descending, step size of 5 %) and the intensity was set to ten or two times the detection threshold for the square waves and the increasing exponential current decay, respectively. During threshold detection and CES, a similar electrode was placed on the control

arm, however no electrical stimulation was applied through this electrode, to account for possible electrode effect.

Analysis

An average of each minute of the VAS measured from the condition arm during the continuous pinprick was calculated and compared to the average of each minutes from the control arm.

For the single pinprick stimuli an average of the three measurements performed at 10, and 20 minutes prior to and 10, 20, and 30 minutes subsequent to CES were averaged for each weight and normalized to the control arm.

Results

For subject one and subject three, the increasing exponential current decay pulse had the most effect on sensitization, measured by single pinprick (see figures C.5a and C.5c). For subject two, Klein's paradigm showed the best effect (see figure C.5b).

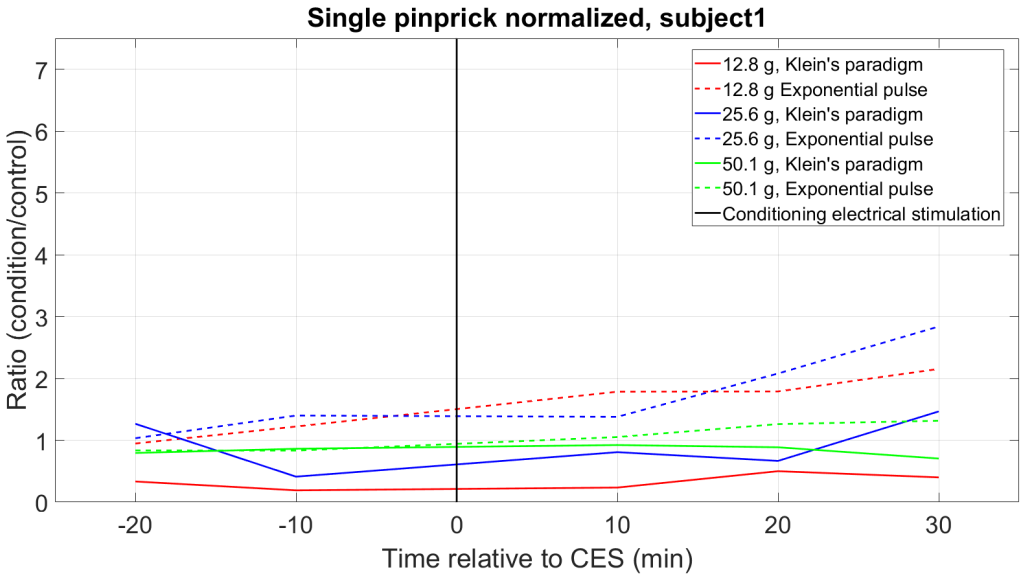

(a) Results for single pinpricks with different weights for subject 1

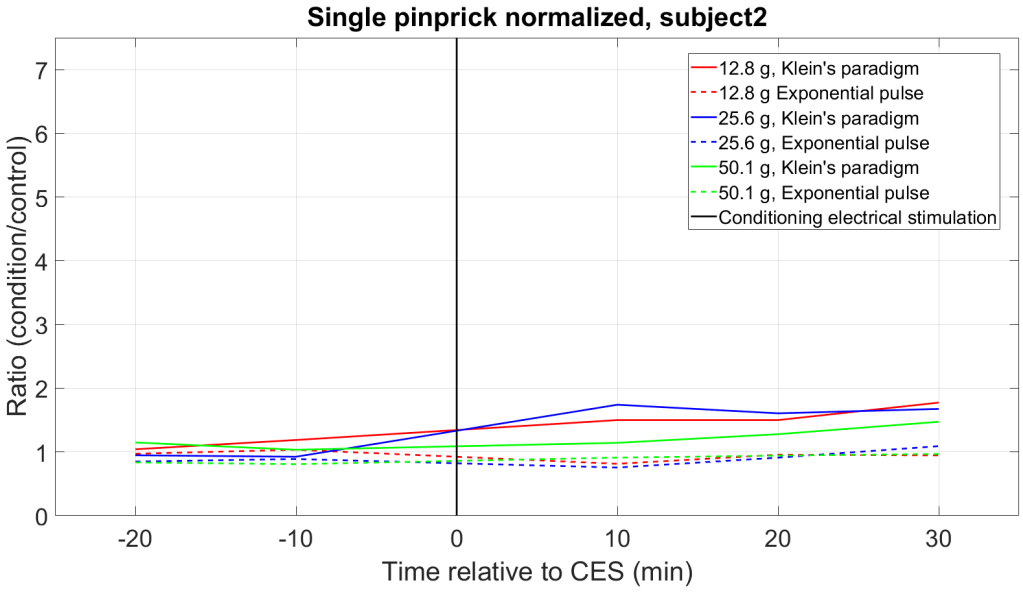

(b) Results for single pinprick stimuli with different weights for subject 2

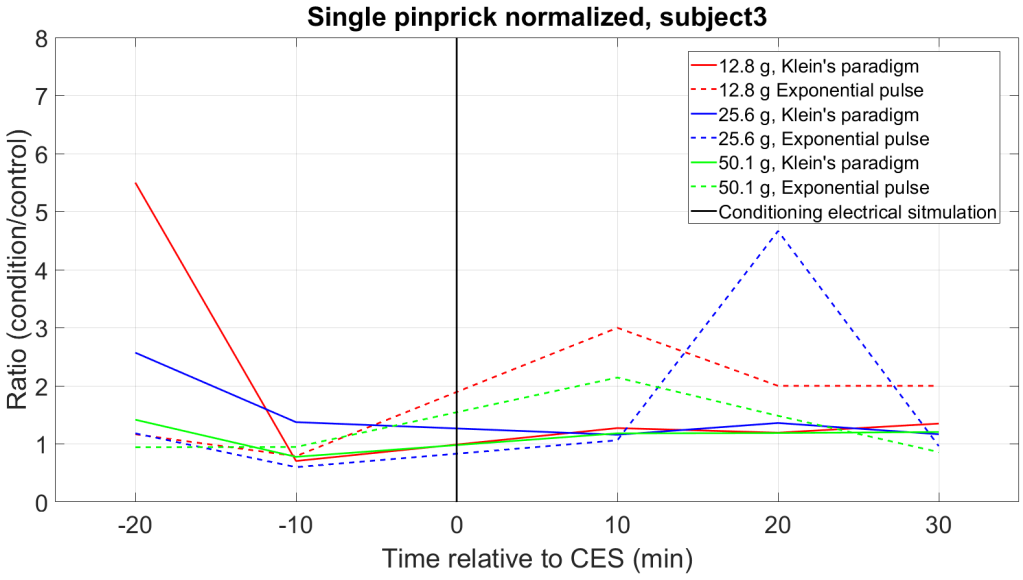

(c) Results for single pinprick stimuli with different weights for subject 3

Figure C.5: Normalized to the control arm. Black vertical line indicates the time of CES.

In general the 25.6 g pinprick weight seemed most suitable in order to show an increased sensitivity after electrical stimulation with the increasing exponential current decay for all subjects (see figure C.6).

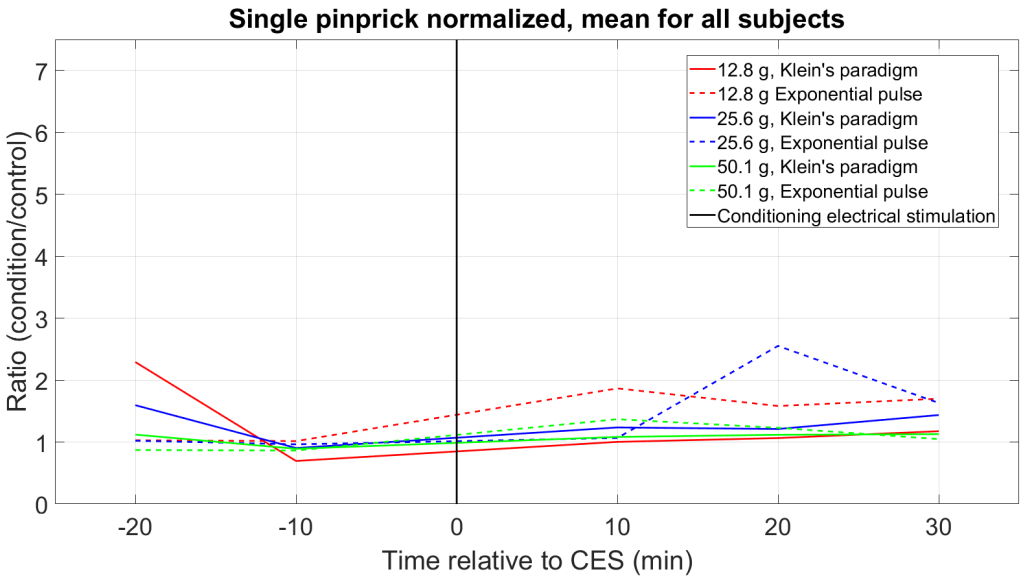

Figure C.6: Results for single pinprick stimuli with different weights, average for all subjects, normalized to control arm. Black vertical line indicates time of CES.

For both paradigms, before and after electrical stimulation, the three minutes continuous pinprick did not show habituation towards the last minute. Opposed to Klein's paradigm, the stimulation with the increasing form of the exponential current decay with an exponential trailing phase showed a difference between before and after stimulation (see figure C.7).

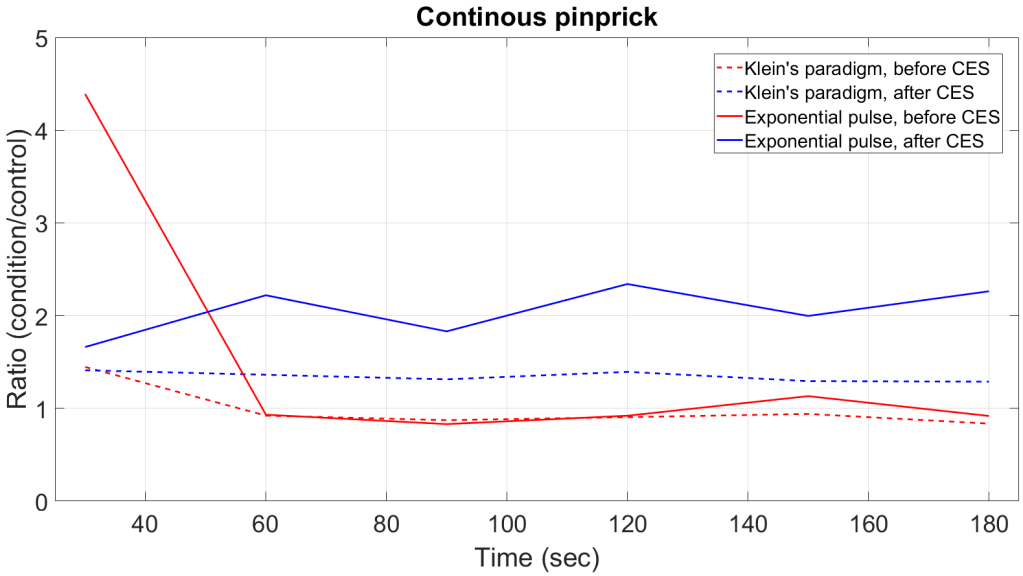

Figure C.7: Results for continuous three minutes pinprick, average for all subjects, normalized to control arm.

Pilot 3

Purpose

The purpose of the third pilot study was to investigate the effect of using VAS scores to standardize the applied intensity of CES, when using a charge balanced increasing form of the exponential current decay (10 Hz, 50 seconds).

Materials

- Marker and tape
- Pinprick stimulator (12.8 g)
- VAS meter (Aalborg University)
- Computer with AVel Electrical Pain Stimulation (Aalborg University)
- Pin-electrode (cutaneous punctuate electrode, Aalborg University)
- Stimulator (Digitimer DS5)

Setup

The subject was seated in a chair with arms placed on a table in a supine position and with the VAS meter between the arms. The pin-electrodes were placed with the periphery 5 cm distal to cubital fossa one on each arm. One arm served as condition and the other as control. Only the electrode placed on the conditioned arm was connected to the electrical stimulator.

Procedure

The third pilot study consisted of one session. Test stimuli were applied 10, and 20 minutes prior to the CES and 10, 20, and 30 minutes subsequent to CES (see figure C.8). The test stimulation consisted of five single pinprick stimuli applied on the peripheral boarder of the electrode placement. Each of the five pinpricks were rated by the subject on a VAS ranging from 0 to 10, where 0 was no sensation, 3 was the pain threshold and 10 was unbearable pain.

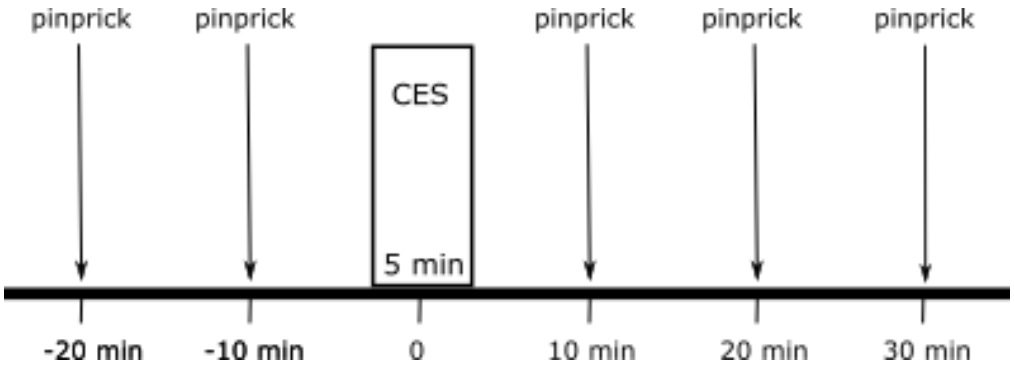

Figure C.8: Time line over the procedure of the third pilot study. Five pinprick stimuli were applied 10, and 20 minutes prior to CES. Additionally five pinpricks were applied 10, 20, and 30 minutes after the application of CES.

The CES paradigm consisted of a 10 Hz increasing exponential current decay, with an exponential trailing phase for charge balance [Hugosdottir et al., in press] applied for 50 seconds. Prior to CES the perception threshold was determined through the method of limits (three ascending and three descending, with a step size of 5 %). Subsequent to threshold detection, the intensity used for CES was determined. The subject was instructed to rate the VAS of a three second stimulation with the same pulse shape. The target intensity was an intensity corresponding to a VAS score in the interval of 6 and 7.

Analysis

The five VAS scores for the single pinprick test stimuli were averaged for each time point and each arm. Subsequently the VAS for the conditioning arm was normalized to the control arm.

Results

LTP-like increase in pain perception was induced in both subjects, however a more pronounced increase in VAS score was observed for subject 1. The general tendency for the two subjects were an increase in sensitivity from 10 minutes after CES to 20 minutes after and the level remained increased at 30 minutes subsequent to CES (see figure C.9).

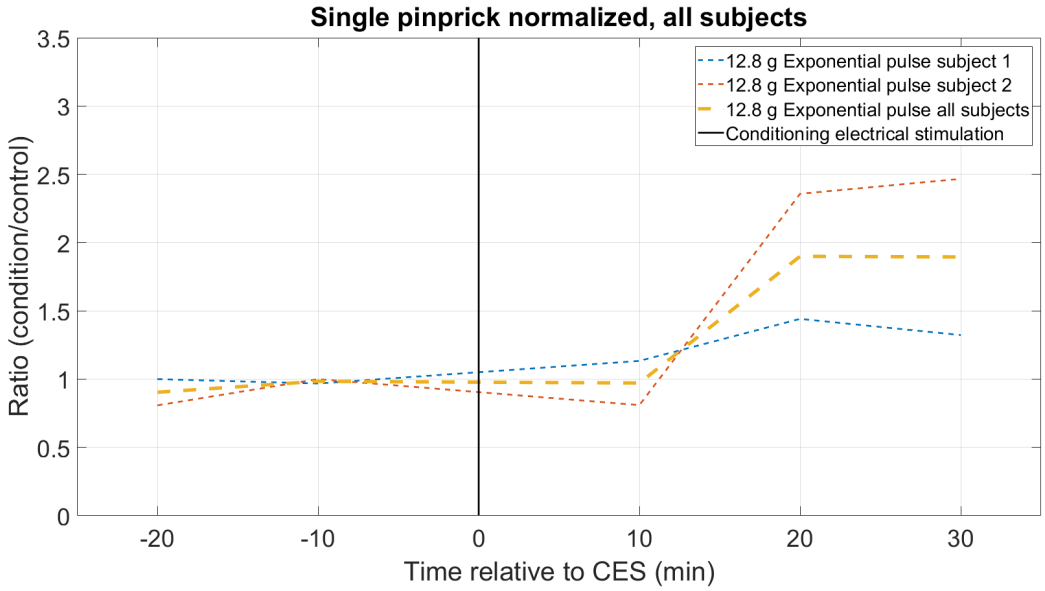

Figure C.9: The ratio between the VAS of the conditioned and control arm. The blue graph is results for subject 1 the red for subject 2 and the yellow is an average of both subjects.

Appendix D

Standard operating procedure

The following is a description of the materials and methods used in the experiment. Key words to instruct the subjects are marked with **bold font**. The methods described regards experimental preparations, introduction to VAS, pinprick stimulation, EEG recording and conditional electrical stimulation (CES) (see figure D.1).

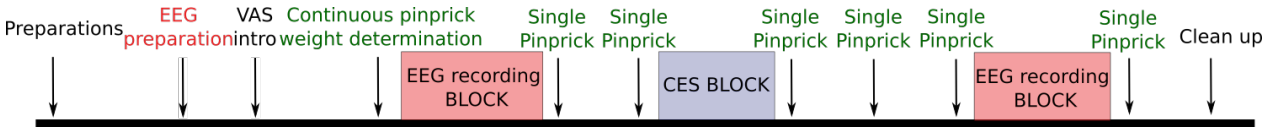

Figure D.1: Time line for the experiment including the different methods used.

Materials

- Cutaneous pin electrode (Aalborg University)
- Electrical stimulator (Digitimer DS5)
- Pinprick stimulators (6.4 g, 12.8 g, 25.6 g)
- Marker
- Tape
- Visual analog scale meter (VAS, digital, connected via DAQ-board)
- EEG-cap
- EEG-gel
- Syringe for EEG-gel application
- Alkoswaps
- Perception button
- Computer with AVel Electrical Pain Stimulation (Aalborg University)
- Computer with g.recorder (Guger technologies medical engineering)

Preparation

Before the subject arrives, the equipment is set up. VAS and EEG amplifier are connected to computers and the EEG cap with active electrodes is connected to the amplifier. The pin electrode and the pinpricks are cleaned with alko-swaps. The sex, age and hand of dominance of the subject is noted in the case report file in the beginning of the experiment (CRF, see appendix E).

Introduction to the visual analog scale

The subject is introduced to the visual analog scale (VAS) in the beginning of the experiment. On the VAS meter the **bottom** is defined as **no perception**. The marked line on the meter defines the **border between perception and pain** and the top of the scale is defined as the **worst imaginable pain** (see figure D.2).

Figure D.2: VAS meter used for sensory/pain scoring during the experiment. The bottom of the scale is defined as ***no perception****, the line indicates the* ***border between perception and pain*** *and the top of the scale is defined as the* ***worst imaginable pain***

Pinprick stimulation procedures

Three pinprick stimulation procedures are used in the experiment, one for the determination of pinprick weight to be used in the continuous pinprick procedure during EEG recording and a single pinprick procedure for evaluation of perception in the heterotopic zone (see green area in figure D.3).

Determination of weight for continuous pinpricks

Prior to the beginning of the experiment, the weight for continuous pinprick stimulation is determined. Pinpricks with weights of 6.4 g, 12,8 g and 25,6 g are applied in a random order. Each of the weights are applied as ten stimuli with a frequency of 0.5 Hz within the continuous pinprick areas (see dark green area on figure D.3), while the subject rates the **overall perception** (one score for all ten stimuli). This is repeated until each weight have been tested three times. VAS is noted in the CRF after each period of ten stimuli and the VAS meter is reset. The weight that produces a response between 3-4 on the VAS is selected for the following continuous pinprick procedure. If none of the pinprick weights are rated to a VAS above 3, the heaviest weight of 25.6 g is selected.

Continuous pinprick stimuli

The subject is instructed to **rate** the stimuli **continuously** on the VAS. **If the perception change, the rating should change accordingly.** Each arm is stimulated continuously for three minutes with a frequency of 0.5 Hz within the continuous pinprick areas (see dark green area on figure D.3). The weight of the pinprick stimulator is the weight found most appropriate during determination of weight for continuous pricks. The continuous pinprick stimulation is recorded with the program; *AVel Electrical Pain Stimulation 2.02* (Aalborg University), in the mode *Cond. Stim.*, where the *PostStim Ack.* is set to 140 seconds. The electrical stimulator is turned off during the measurements. The three minute measurements, one for each arm, are subsequently saved in the subject folder.

Single pinprick stimuli

The subject is instructed to **rate** the stimuli on the VAS **after each prick** and to **reset** the VAS-meter between each stimulus. Each arm is stimulated eight times with a 25.6 g pinprick, within the single prick areas (see light green area on figure D.3). For each arm the eight pinprick stimuli are randomly applied to the two areas and it is randomized which arm is stimulated first. The VAS is noted in the CRF after each stimulus.

Figure D.3: Stimulation sites. The stimulation area is places with the periphery 5 cm distal to the cubical fossa. The red area is the stimulation site for CES and the yellow dots represent the electrode pins. The green areas are used for pinprick simulation. Dark green area is the stimulation site for continuous pinprick, and light green is the stimulation site for single pinprick stimuli.

Conditioning electrical stimulation

Prior to application of CES the subject is familiarized to the stimulation, the perception threshold is determined and the intensity that should be used for CES is determined. The electrodes are placed on the subject just prior to the first instruction and removed immediately after CES has been applied (see figure D.4).

The pin electrode is placed with the periphery 5 cm distal to the cubical fossa on the beforehand marked electrode area (see red area on figure D.3).

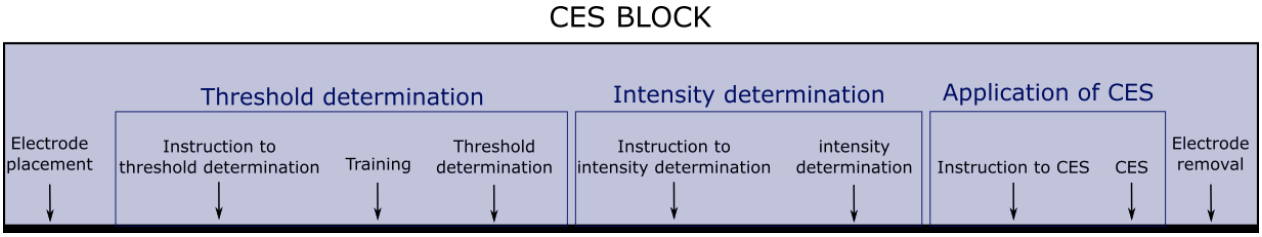

Figure D.4: Elaborated time line for the CES block.

Threshold determination

The subject is instructed in the use of the perception button and to the method of limits. Each time the step is ascending the subject is instructed to **push the button** when the stimulation **is felt**. For each descending step the subject is instructed to **push the button** when the stimulation **is no longer felt**. Firstly, the subject is familiarized to the stimulation through training. The training is a method of limits training of two ascending and descending measurements. The subject is during the training instructed to **feel a few stimuli** before pushing the button. Subsequent to training, the perception threshold is determined through three ascending and descending measurements with a step size of 5 % and starting at 10 μA. Both the training and threshold determination is performed with the program; *AVel Electrical Pain Stimulation 2.02* (Aalborg University). The program is in the *Find Threshold* mode, the *Stim Intensity* is set to 10 μA and *Pattern* is set to *File* and a file containing a single pulse of the increasing exponential current decay is imported.

Intensity determination

Prior to the determination of stimulation intensity, the subject is instructed to **rate each applied stimulus** on the VAS meter. The subject is told when to expect each of the stimuli. The intensity determination is performed through an up-down staircase method. The stimulation intensity is initially set to the determined perception threshold and is increased in steps of 50 % until a VAS of 4 or above is reached. The intensity is subsequently decreased in steps of 20 % until the subject rates the VAS to be below 4. The process is repeated once more with the ascending step size set to 10 % and the descending step size set to 5 %. The average intensity of the two ascending and descending measures is noted in the CRF and used for CES. The program *AVel Electrical Pain Stimulation 2.02* (Aalborg University) is used for the intensity determination and the mode is set to *Test Stim*. The pattern used is a file containing half a second of 10 Hz exponential current decay pulses. The intensity is changed by manually changing the *Ths.Factor*.

Application of conditioning electrical stimulation

Before application of CES, the subject is instructed to **continuously rate** the stimulation and is told that the stimulation **may be painful**. CES is applied for 50 seconds with an intensity corresponding to the intensity found through intensity determination. The stimulation is administered with the program *AVel Electrical Pain Stimulation 2.02* (Aalborg University) in mode *Cond. Stim.* The *PostStim Ack.* is set to 10 seconds, in order to acquire the VAS for a total of 60 seconds (50 second stimulation and 10 seconds after the stimulation is completed).

Electroencephalography

The experiment contains two EEG recording blocks, one prior to and one subsequent to CES. Each EEG block contains a rest recording and two three recordings during continuous pinprick stimulation, one for each arm (see figure D.5). EEG is recorded with g.recorder software, g.HIamp amplifier and g.GAMMAsys EEG cap (Guger technologies medical engineering).

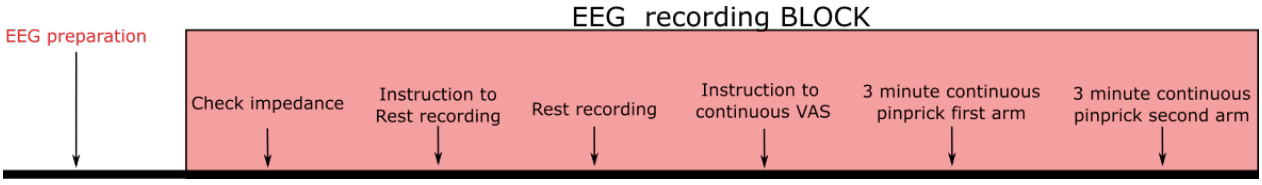

Figure D.5: Elaborated time line for the EEG block.

Preparation

The EEG cap is in accordance with the 10-20 system. The reference is placed on the right ear lope and put on immediately after the cap is placed upon the subjects head. The EEG-setup is loaded from the file "*LtpExperimentSpring2017*". Subsequently, gel is applied to the impedance and ground electrode and the remaining electrodes while measuring the impedance. The preparation is finalized when impedance on all electrodes is below 30 k$\mathbf{\Omega}$.

Recording

Initially, in each block of EEG recording the impedance is checked to make sure it is below 30 k$\mathbf{\Omega}$. Subsequently EEG is recoded during rest for five minutes. The subject is instructed to **not move or talk** and **look at a fixed point straight ahead**. In addition EEG is recorded during three minutes continuous pinprick stimulation. The subject is instructed to **look at the VAS** and **only move the hand used for rating** the stimuli. The stimulation should be **rated continuously**. The software is set to record and uses approximately 30 seconds to settle, after which point the initiation of recording the data of interest is marked as a *start event*, by pushing the *s* key. To mark the ending of a recording the *e* key is used to make an *end event*. When the end event has been set, the recording is stopped and saved.

Clean up

After the session, the equipment is disconnected and the EEG cap is thoroughly cleaned with water.

Appendix E

Case report file

For each subject, the case report file is filled out. Red text marked the field to fill out.

SubjectX

Table E.1: Check for exclusion criteria.

Criteria		
	yes	no
Neuropathic diseases		
Heart diseases		
Diseases in arms		
Chronic pain		
Caffeine		
Painkillers		
Nicotine		
Medication		

Table E.2: Subject information.

Subject information	
Age:	
Sex:	
Dominant arm:	
Condition arm:	
Height:	
Weight:	

Table E.3: Files to save inclusive corresponding intended file names.

Files		
Folder with subject files	Folder name	*"subjectX"*
Rest pre CES **EEG**:	File name	*"subjectX_pre_rest"*
Continuous pinprick pre CES **EEG**:	File name	*"subjectX_pre_cont_condition_eeg"*
	File name	*"subjectX_pre_cont_control_eeg"*
Continuous pinprick pre CES **VAS**:	File name	*"subjectX_pre_cont_condition"*
	File name	*"subjectX_pre_cont_control"*
VAS during CES:	File name	*"subjectX_CES"*
Rest post CES **EEG**:	File name	*"subjectX_post_rest"*
Continuous pinprick post CES **EEG**:	File name	*"subjectX_post_cont_condition_eeg"*
	File name	*"subjectX_post_cont_control_eeg"*
Continuous pinprick post CES **VAS**:	File name	*"subjectX_post_cont_condition"*
	File name	*"subjectX_post_cont_control"*

Table E.4: Notation of pinprick perception during determination of weights.

Pinprick determination							
Weight (g)	**VAS right arm**			**VAS left arm**			**Average**
6.4							
12.8							
25.6							

Table E.5: Notation of perception threshold.

Perception threshold determination	
Threshold	

Table E.6: Notation of intensity, multiplication factor, and number of stimuli given during the determination of CES intensity.

Intensity determination - 0.5 sec pulse ('halfSec'), aim at VAS 4					
Multiplication factor step size	0.5 - up	0.2 -down	0.1 - up	0.05 - down	**Average**
Multiplication factor					
Intensity					
Number of stimuli					

Table E.7: Notation of single pinprick stimuli ratings.

VAS for single pinprick										
Time relative to CES	**arm**	**test1**	**test2**	**test3**	**test4**	**test5**	**test6**	**test7**	**test8**	**Average**
-20	R									
	L									
-10	R									
	L									
10	R									
	L									
20	R									
	L									
30	R									
	L									
50	R									
	L									

Table E.8: Notation of possible comments.

Comments
Comments on experiment

Appendix F

Additional results

Demographic data for the subjects are presented in table F.1

Table F.1: Demographic data

	mean (± standard deviation)
Age (years)	24.73 (± 1.68)
Height (cm)	173.91 (± 10.22)
Weight (kg)	71.27 (± 13.34)
	Part
Female (%)	63.64
Right arm dominant (%)	100

Psychophysical data

Results (non-normalized) for average VAS scores for the single pinprick test stimuli are presented in figure F.1, while non-normalized average VAS scores during continuous pinprick stimulation are presented in figure F.2.

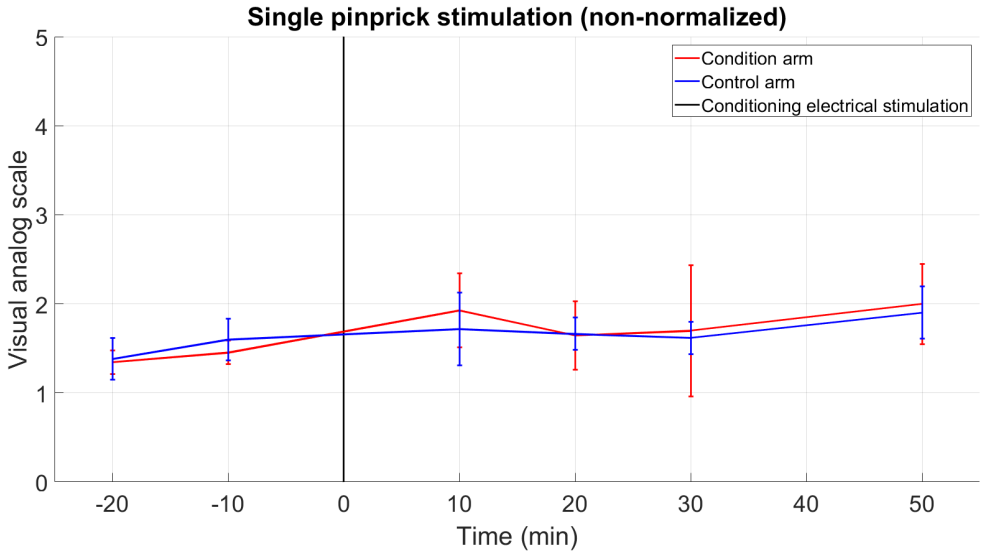

Figure F.1: Non-normalized results for single pinprick data.

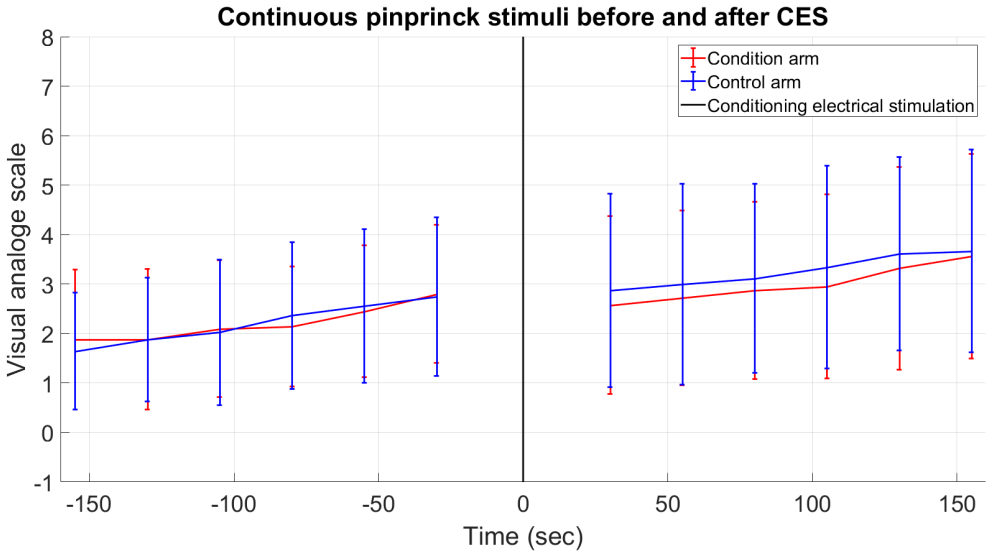

Figure F.2: Non-normalized results for continuous pinprick data.

Subjects rated the perception of the applied CES and in figure F.3 the time course of the ratings for each subject are represented.

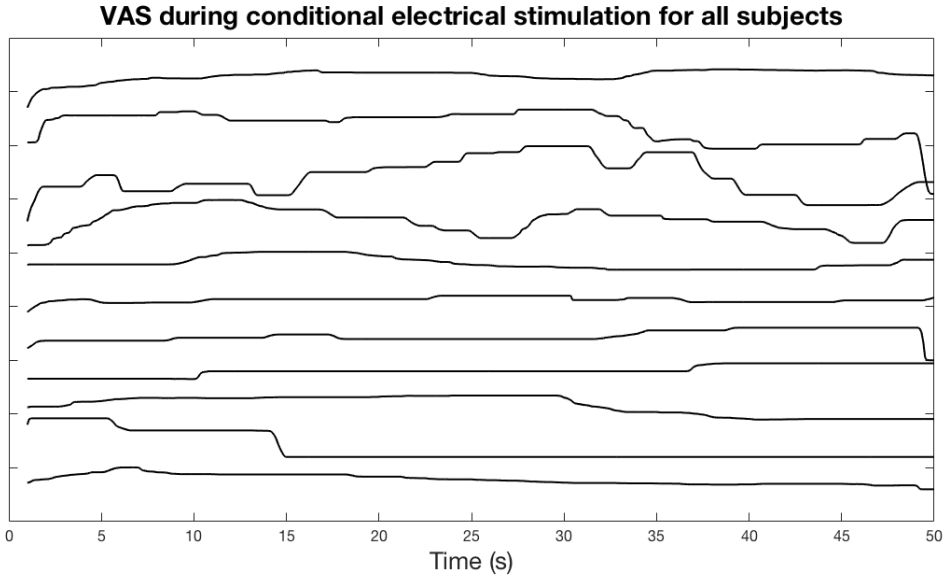

Figure F.3: Tendencies in visual analog ratings for all subjects (with offset)

Relation between perception threshold and multiplication factor

The multiplication factor was not related to the perception threshold. This is illustrated in figure F.4, where no clear relation can be seen.

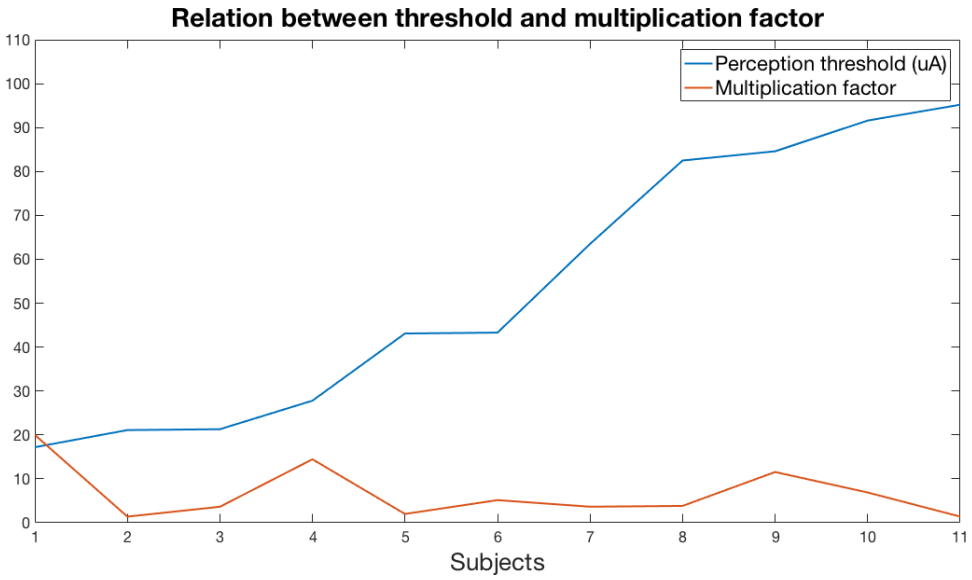

Figure F.4: Relation between perception threshold and multiplication factor

EEG data

Source reconstruction

The overall source activity for the six frequency bands (delta, theta, alpha, beta1, beta2, and beta3) are presented in figures F.5, F.7, F.8, F.9, F.10, and F.11, respectively. This activity is the overall activity for all subjects both before and after CES. As significant changes in source activity was observed for the delta band during resting state, the activity for comparison is presented for rest both before and after CES in figure F.6.

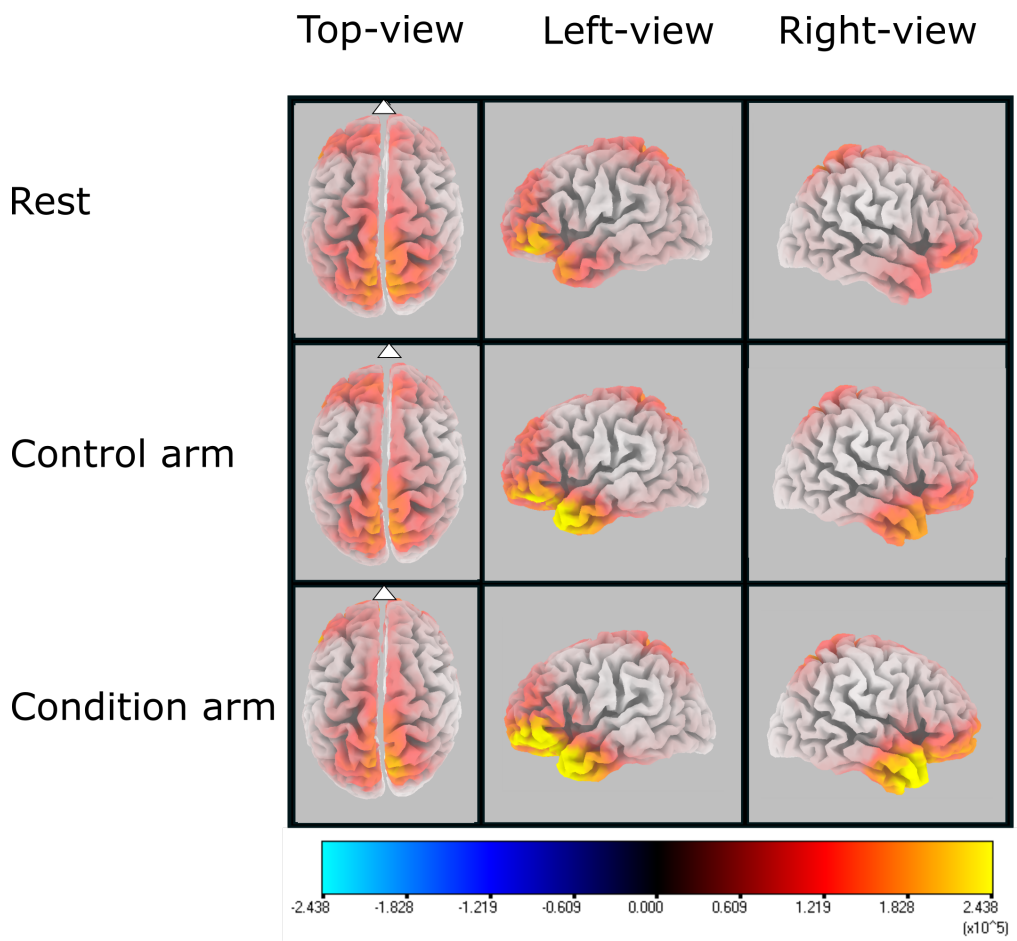

Figure F.5: Average source activity for all three conditions (rest, and continuous pinprick on control and conditioned arm), for all subjects before and after CES, in the delta band.

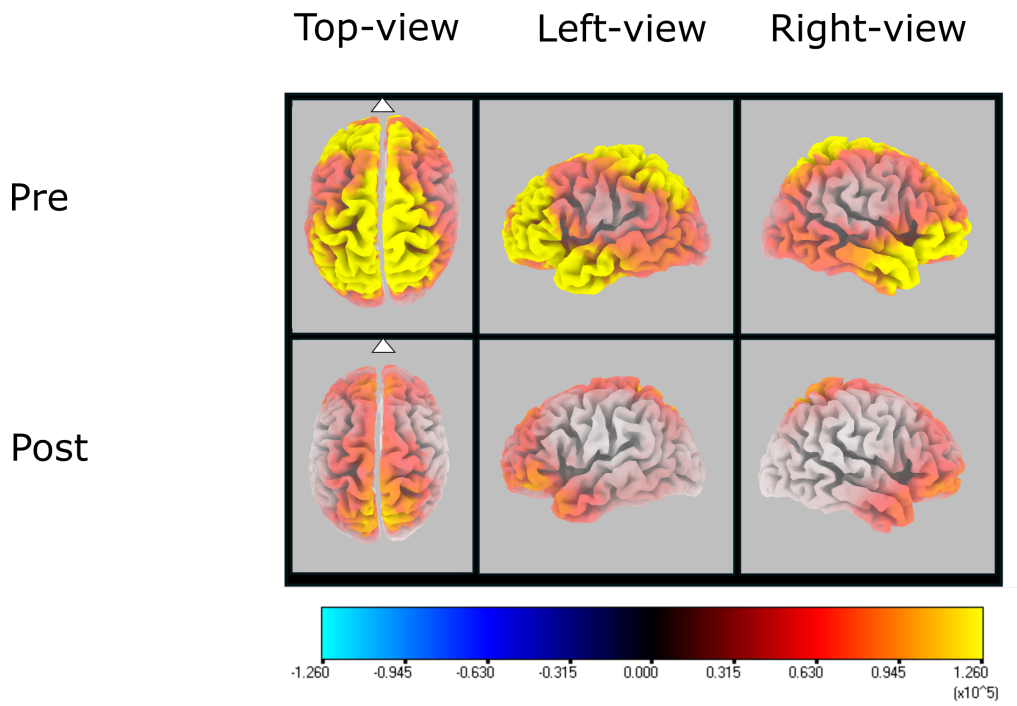

Figure F.6: Average source activity at rest for all subjects before (pre) and after (post) CES in the delta band.

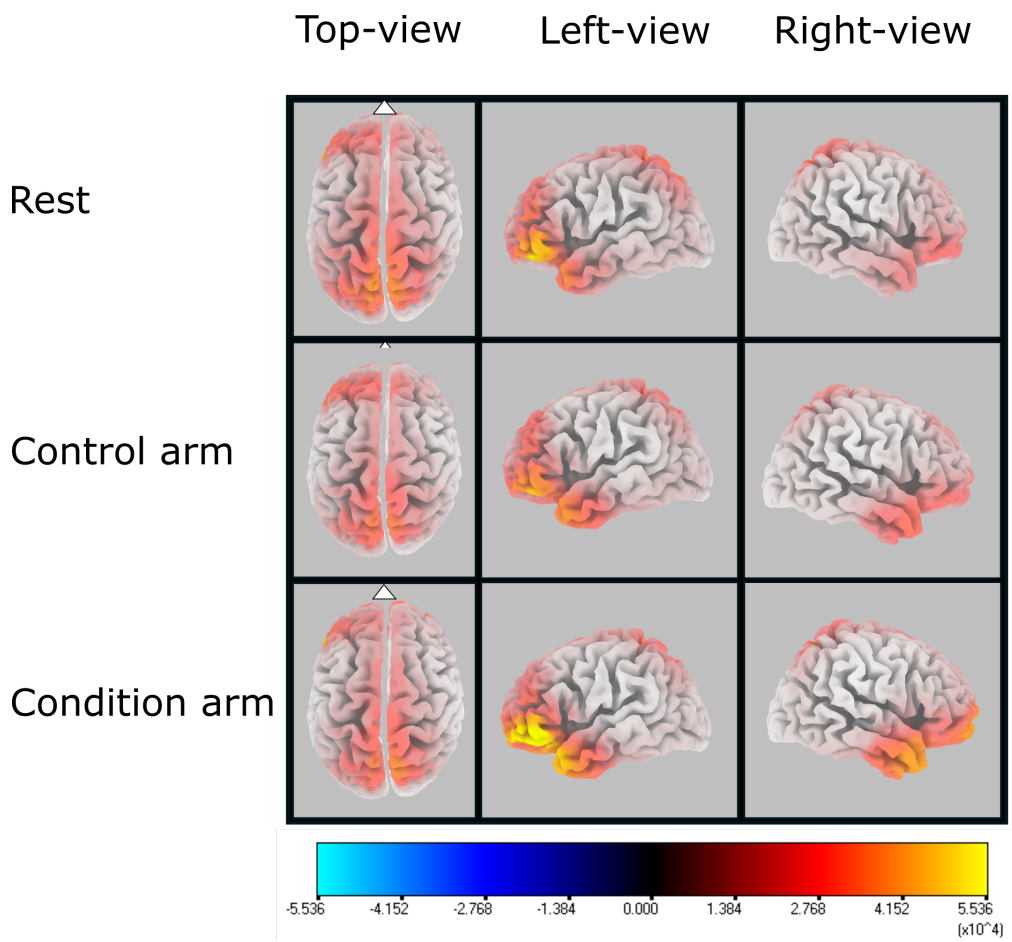

Figure F.7: Average source activity for all three conditions (rest, and continuous pinprick on control and conditioned arm), for all subjects before and after CES, in the theta band.

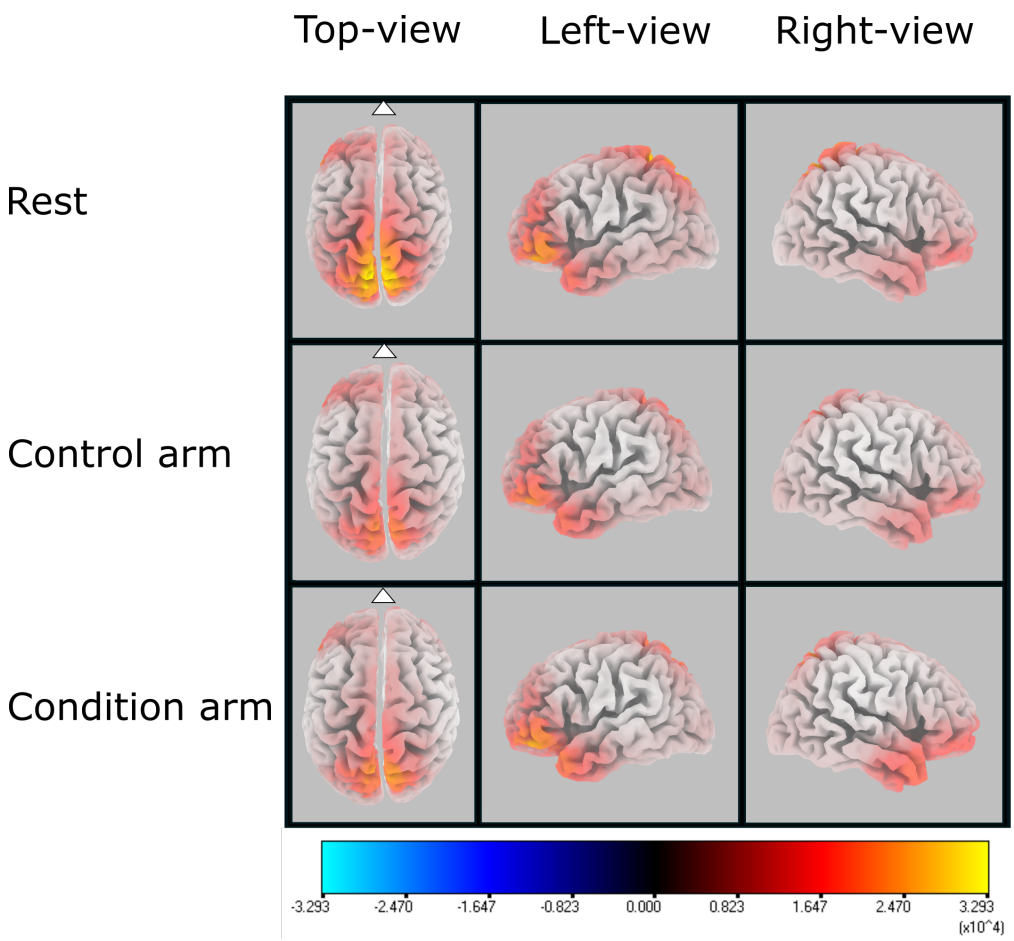

Figure F.8: Average source activity for all three conditions (rest, and continuous pinprick on control and conditioned arm), for all subjects before and after CES, in the alpha band.

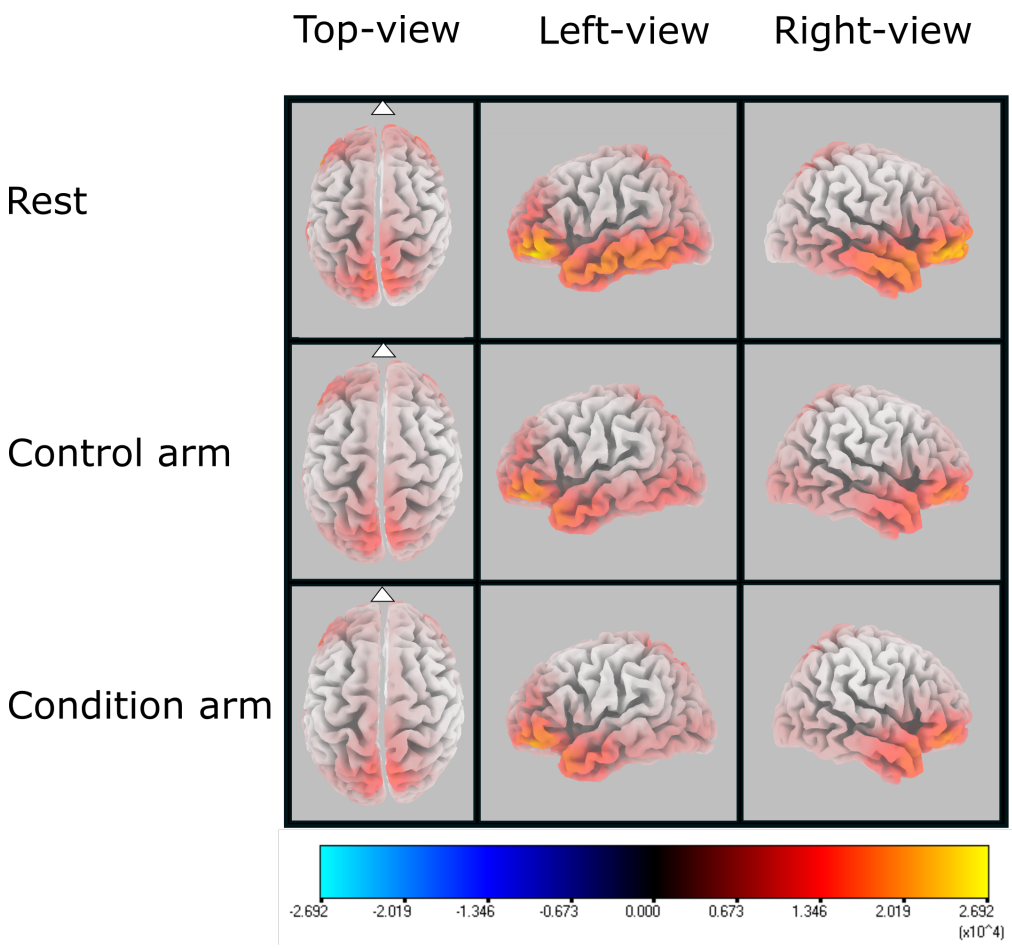

Figure F.9: Average source activity for all three conditions (rest, and continuous pinprick on control and conditioned arm), for all subjects before and after CES, in the beta1 band.

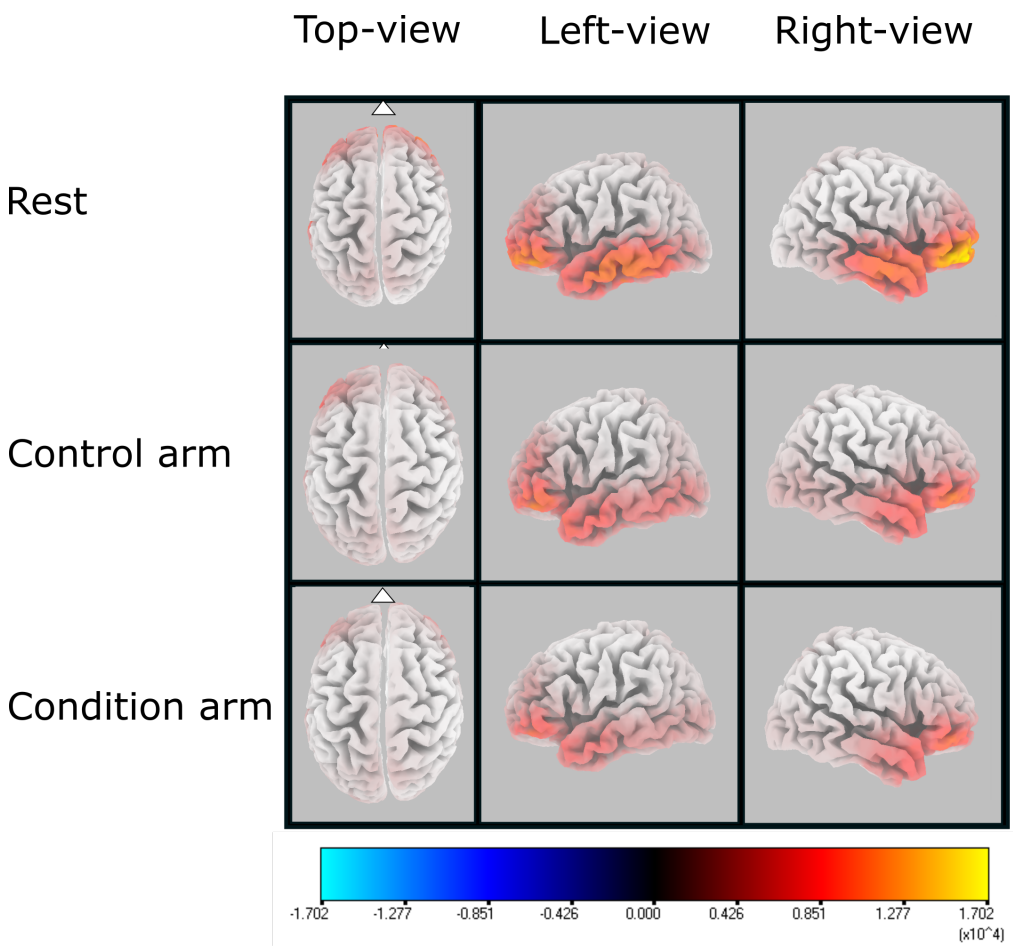

Figure F.10: Average source activity for all three conditions (rest, and continuous pinprick on control and conditioned arm), for all subjects before and after CES, in the beta2 band.

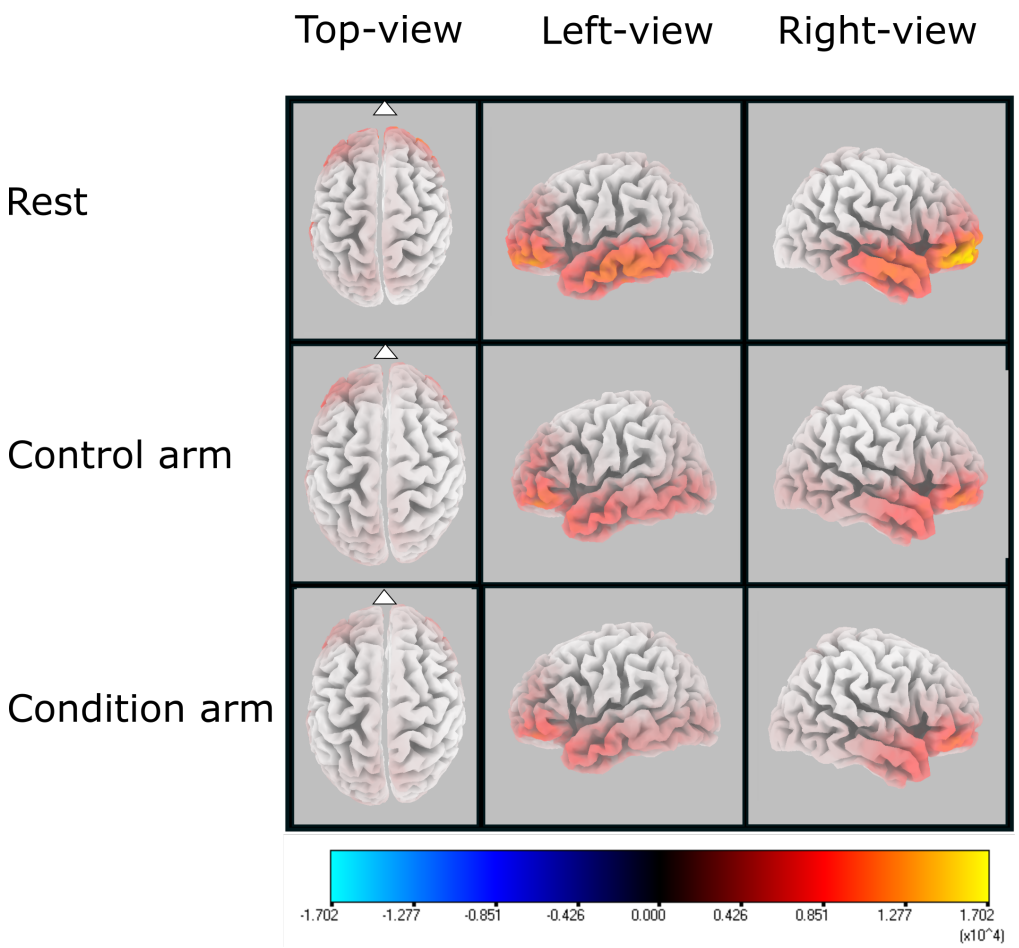

Figure F.11: Average source activity for all three conditions (rest, and continuous pinprick on control and conditioned arm), for all subjects before and after CES, in the beta3 band.

Coherence

Differences in coherence between before and after CES for all connections between regions of interest (within each hemisphere) is presented for the delta, theta, and alpha band in figure F.12, F.13, and F.14, respectively

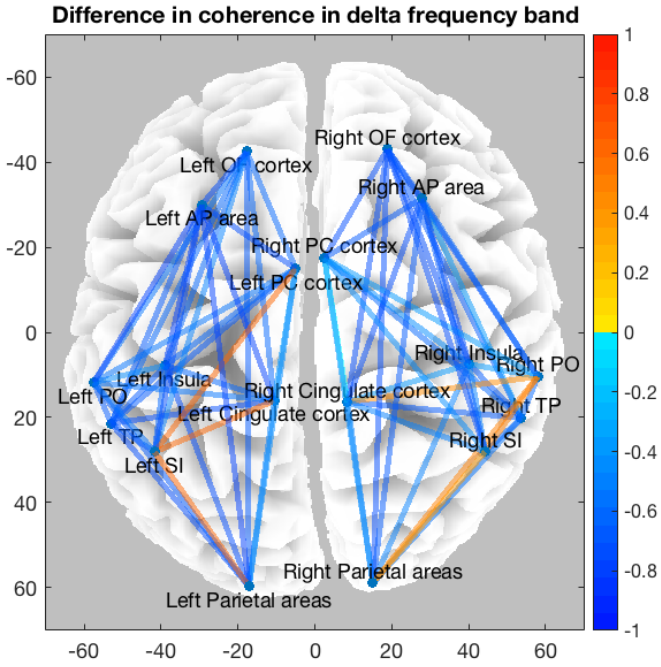

Figure F.12: Differences between coherence before and after CES (lines) for the rest condition in the delta band. Negative values (blue scale) indicate the coherence prior to CES to be larger than subsequent to CES and positive values (red scale) indicate larger coherence values subsequent to CES. OF=orbitofrontal, AP=anterolateral prefrontal, PC=perigenual cingulate, PO=parietal operculum, TP=temporal pole, and SI=primary somatosensory cortex.

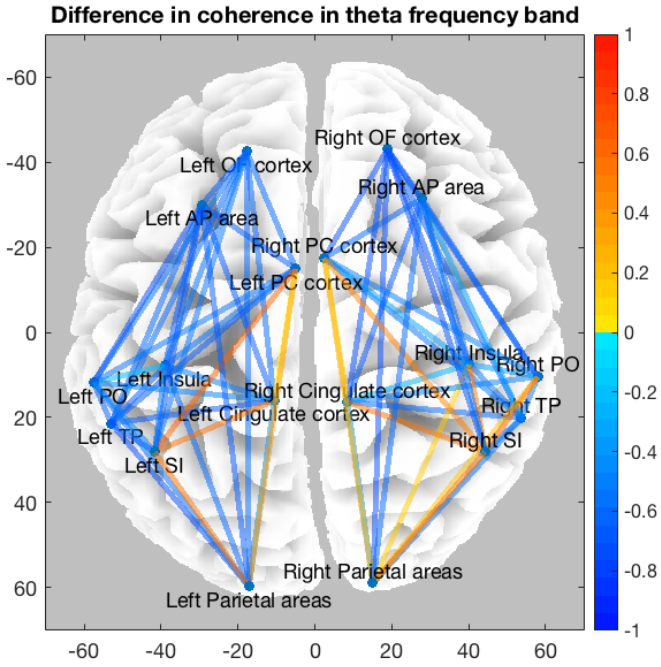

Figure F.13: Differences between coherence before and after CES for the rest condition in the theta band. Negative values (blue scale) indicate the coherence prior to CES to be larger than subsequent to CES and positive values (red scale) indicate larger coherence values subsequent to CES. OF=orbitofrontal, AP=anterolateral prefrontal, PC=perigenual cingulate, PO=parietal operculum, TP=temporal pole, and SI=primary somatosensory cortex.

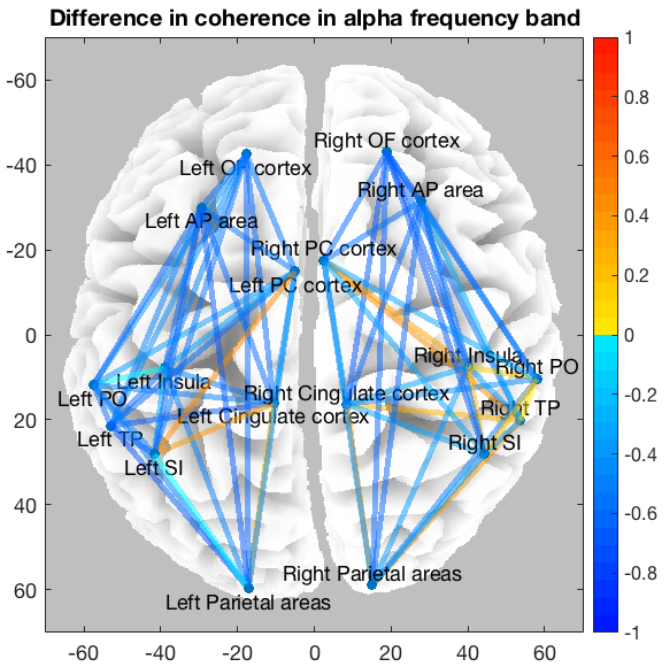

Figure F.14: Differences between coherence before and after CES for the rest condition in the alpha band. Negative values (blue scale) indicate the coherence prior to CES to be larger than subsequent to CES and positive values (red scale) indicate larger coherence values subsequent to CES. OF=orbitofrontal, AP=anterolateral prefrontal, PC=perigenual cingulate, PO=parietal operculum, TP=temporal pole, and SI=primary somatosensory cortex..

Appendix G

Connectivity analysis and source reconstruction

In relation to the choice of connectivity method the methods previously used together with source reconstruction was compared (see table G.1).

Table G.1: Previously used connectivity measures with source reconstruction

Source reconstruction method	**ICA**	**Connectivity method**	**Separate analysis**	**Frequency bands**	**Pros/cons**	**Reference**
eLORETA	no	Phase locking value	yes	$\boldsymbol{\theta}$, $\boldsymbol{\gamma}$	-	Taesler and Rose [2016]
	no	Lagged phase syncronisation	no	$\boldsymbol{\delta}$, $\boldsymbol{\theta}$, $\boldsymbol{\alpha 1}$, $\boldsymbol{\alpha 2}$, $\boldsymbol{\beta 1}$, $\boldsymbol{\beta 2}$	-	von Rotz et al. [2017]
sLORETA	no	Coherence	yes	$\boldsymbol{\delta}$, $\boldsymbol{\theta}$, $\boldsymbol{\alpha}$, $\boldsymbol{\beta 1}$, $\boldsymbol{\beta 2}$, $\boldsymbol{\beta 3}$	-	González-Roldán et al. [2016]
	yes	Graph theory and ICA	no	-	Investigates the whole range of frequencies compared with eg. coherence	Cao and Slobounov [2010]
sLORETA on IC's	yes	Graph teory and directed partial coherence*	no	$\boldsymbol{\alpha}$	Lower number of validated components when performing source reconstruction of IC's	Chen et al. [2013]
eLORETA, weighted MNE and LCMV**	no	Phase slope index	no	$\boldsymbol{\alpha}$	More robust than Granger causality but less consistent across subjects	Mahjoory et al. [2017]
	no	Imaginary part of coherence	no	$\boldsymbol{\alpha}$	More robust than coherence but less consistent across subjects	Mahjoory et al. [2017]
LORETA	yes	Granger causality	no	-	-	Huishi Zhang et al. [2016]

cLORETA	yes	Short-time directed transfer function	no	1-50 Hz	Quantifies information tranfer for each frequency, opposite to Granger causality	Iversen et al. [2014]
Minimum norm estimate	yes	Graph theory and partial directed coherence	both	low-α	-	Sun et al. [2014a]
	yes	Directed partial coherence	no	low-α	-	Sun et al. [2014b]

*Cross-correlation in the band-power spectrum, **MNE: minimum-norm estimate and LCMV: linearly-constrained minimum-variance beamforming

Methods for source reconstruction

In order to choose which method to use for source reconstruction existing methods were compared in relation to advantages and limitations. Additionally, it was investigated whether an existing toolbox or software was available for method implementation. The identified methods and description of these are presented in table G.4.

Table G.4: Description of the assumptions, advantages and limitations of different source reconstruction methods.

Method	**Methodology and assumptions**	**Advantages**	**Limitations**	**Available software**
The minimum norm solution (MNS)	Tries to solve the inverse problem by current estimation through linear combination of lead fields [Jatoi et al., 2014]. General estimate for a 3D source distribution in absence of a priori information. Assumes the current distribution to have minimum overall intensity. [Michel et al., 2004]	- Good initial result [Jatoi et al., 2014]. - A priori information can increase the performance [Jatoi et al., 2014]. - Modifications of the method exists, introducing weighting for better estimations [Michel et al., 2004].	- The assumption of overall minimum intensity may not be valid [Michel et al., 2004]. - Favors weak and localized activation patterns [Michel et al., 2004]. - Deep sources are incorrectly projected to the surface [Michel et al., 2004, Jatoi et al., 2014, Grech et al., 2008] - Performs worse than LORETA and weighted minimum norm solutions [Jatoi et al., 2014, Michel et al., 2004].	Yes

Low resolution tomography algorithm (LORETA)	Combines lead-field normalization with laplacian operators, selecting the solution with a smooth spatial distribution by minimization of the laplacian of weighted sources [Michel et al., 2004, Grech et al., 2008]. Assumes neighbouring neurons to be simultaneous and synchronously activated [Jatoi et al., 2014].	- Performs well on boundary and deep sources [Jatoi et al., 2014, Grech et al., 2008]. - High time resolution and computationally efficiency [Jatoi et al., 2014]. - Validated on experimental data [Jatoi et al., 2014]. - Fewer ghost sources and better localization error than shrinking LORETA-FOCUSS when performed subsequent to regularization [Grech et al., 2008].	- Low spatial resolution [Jatoi et al., 2014, Michel et al., 2004, Grech et al., 2008]. - Regularization cause increase in spatial blurring [Jatoi et al., 2014], however without regularization the method is highly noise dependent [Michel et al., 2004]. - Assumption may not necessarily be applicable in all situations [Michel et al., 2004]. - Not well suited for focal sources and may introduce spurious activity [Grech et al., 2008].	Yes
Standardized LORETA (sLORETA)	Based on the assumption of standardization of current density, considering both biological and noise variance. The biological variance is assumed to be independent and uniformly distributed resulting in a linear method with exact zero-localization error. [Jatoi et al., 2014]	- Performs well on both boundary and deep sources [Jatoi et al., 2014]. - Computationally efficient and validated on experimental data [Jatoi et al., 2014]. - Performs well on single sources [Grech et al., 2008]. - Performs better than the MNS, especially in the presence of noise [Jatoi et al., 2014]. - Localization error is lower than LORETA and shrinking LORETA-FOCUSS and when regularized, outperforms these other methods in terms of ghost sources [Grech et al., 2008].	- Has trouble recovering multiple sources, at overlap of point-spread function of sources [Jatoi et al., 2014]. - Low spatial resolution and regularization increases spatial blurring [Jatoi et al., 2014].	Yes

Exact LORETA (eLORETA)	Attempts to minimize the localization error by more adequate selection of the weight matrix. Weigh deep sources higher and is standardized, implying the theoretically expected variance to be of unity. [Jatoi et al., 2014]	- Provides exact localization with zero error in the presence of both external and biological noise [Jatoi et al., 2014]. - Standardized method [Jatoi et al., 2014]. - Computationally effective and validated on experimental data [Jatoi et al., 2014].	- Poor spatial resolution and spatial blurring increases when performing regularization [Jatoi et al., 2014].	Yes
Focal under determined system solution (FOCUSS)	High-resolution non-parametric technique performed with recursive steps of calculations with the help of MNS [Jatoi et al., 2014].	- Stable output and handles non-uniquely identified localized energy-sources [Jatoi et al., 2014]. - Better spatial resolution [Jatoi et al., 2014].	- Can be highly unstable if data is noisy [Baillet et al., 2001]. - Large computational load and time [Jatoi et al., 2014]. - Initialization dependent [Grech et al., 2008].	No
The Multiple signal classification (MUSIC): Recursive/ RAP MUSIC	Based on the projection of dipoles at each grid point against a signal subspace. Sources are localized to the best signal subspace projection. [Jatoi et al., 2014]	- Low localization error. - Performs better in the presence of few clustered sources [Grech et al., 2008].	- Complex computation [Jatoi et al., 2014]. - Estimation may include random error and noise [Jatoi et al., 2014]. - Will fail in the presence of noise, whenever two sources are strongly correlated [Baillet et al., 2001]. - Not validated on experimental data [Jatoi et al., 2014].	No

Shrinking LORETA-FOCUSS	Iterative adjustments to the solution space in order to increase source resolution [Grech et al., 2008, Jatoi et al., 2014]. Assumes neuronal sources are focal and sparse [Grech et al., 2008].	- Low localization and energy error [Jatoi et al., 2014]. - Able to reconstruct a three-dimensional source distribution [Grech et al., 2008]. - Smaller localization and energy error compared to LORETA, LORETA-FOCUSS [Jatoi et al., 2014], and weighted MNS [Grech et al., 2008]. - Superior to LORETA, weighted MNS and sLORETA, in term of ghost sources, when no regularization is performed [Grech et al., 2008]. - 10 times faster than the normally combined LORETA-FOCUSS, however slower than the individual algorithms [Grech et al., 2008].	- Complex algorithm which needs more computational power and time [Jatoi et al., 2014]. - Inferior performance if the assumption does not hold. [Grech et al., 2008]	No
Weighted minimum norm (WMN)-LORETA	WMN is used to initialize the LORETA algorithm [Jatoi et al., 2014].	- Smaller error and better resolution than the two methods alone [Jatoi et al., 2014].	- More complex, which increases the computational time [Jatoi et al., 2014]. - Only been validated on somatosensory evoked potentials [Jatoi et al., 2014]	No
Recursive sLORETA-FOCUSS		- More efficient computation and better localization than any of the methods alone and the sLORETA-FOCUSS [Jatoi et al., 2014].	- Only been validated on simulated data [Jatoi et al., 2014].	No

Beamforming	IntroduceS spatial filtering on the data from a sensor array to discriminate signals from regions of interest and signals originating elsewhere [Baillet et al., 2001]. Assumes orthogonality between distinct sources [Baillet et al., 2001].	- Adaptive method [Baillet et al., 2001]. - Generally produces more focally concentrated SNR maps than eLORETA and weighted MNS [Mahjoory et al., 2017]. - Most consistent across toolboxes [Mahjoory et al., 2017].	- The correlated nature of neuronal activity may limit the performance [Baillet et al., 2001]. - Elaborating constraint in order to minimize signal attenuation and possible cancellation reduces the degrees of freedom and makes the method less adaptive [Baillet et al., 2001]. - May produce an output simply due to noise in the absence of signal [Baillet et al., 2001].	Yes

Appendix H

Standardized low resolution tomography analysis

The sLORETA algorithm for source reconstruction was firstly introduced by Pascual-Marqui [2002] and has been widely used since [Grech et al., 2008, Jatoi et al., 2014].

The scalp electric potentials measured at the electrodes ($\boldsymbol{\phi}$) are defined as the lead field ($\mathbf{K}$) multiplied by the current density ($\mathbf{J}$) added some arbitrary constant (c). The arbitrary constant is within the sLORETA algorithm however eliminated by the use of average reference transformation of $\boldsymbol{\phi}$ and $\mathbf{K}$ (see equation **(H.1)**). [Pascual-Marqui, 2002]

$$\boldsymbol{\phi} = \boldsymbol{K} \cdot \boldsymbol{J} \tag{H.1}$$

Where $\boldsymbol{\phi}$ is the scalp electric potentials, $\boldsymbol{K}$ is the lead field matrix, $\boldsymbol{J}$ is the current density. [Pascual-Marqui, 2002]

From the Bayesian formulation of the inverse problem the function to minimize can be derived (see equation **(H.2)**). The function is minimized with respect to $\mathbf{J}$, when the scalp electric potentials ($\boldsymbol{\phi}$), the lead field matrix ($\mathbf{K}$), and the regularization parameter ($\boldsymbol{\alpha}$) are known.

$$\boldsymbol{F} = ||\boldsymbol{\phi} - \boldsymbol{K} \cdot \boldsymbol{J}||^{\mathbf{2}} + \boldsymbol{\alpha}||\boldsymbol{J}||^{\mathbf{2}} \tag{H.2}$$

Where $\boldsymbol{\phi}$ is the scalp electric potentials, $\boldsymbol{K}$ is the lead field matrix, $\boldsymbol{J}$ is the current density, and $\boldsymbol{\alpha}$ is the regularization parameter. [Pascual-Marqui, 2002]

The minimum solution is obtained at $\hat{\boldsymbol{J}} = \mathbf{T} \cdot \boldsymbol{\phi}$ where $\mathbf{T} = \mathbf{K}^{\boldsymbol{T}} \cdot [\mathbf{K} \cdot \mathbf{K}^{\boldsymbol{T}} + \boldsymbol{\alpha} \cdot \mathbf{H}]^{+}$, with $\mathbf{H}$ being the average reference operator. [Pascual-Marqui, 2002]

In order to standardize the current density estimate ($\hat{\boldsymbol{J}}$) the variance should be estimated. The sLORETA algorithm takes both the actual source variance and the noise variance into account, according to the assumption of standardization of the current density [Jatoi et al., 2014]. The actual source variance $\boldsymbol{S_J}$ is a priori and equal to the identity matrix, while the variance due to noisy measurements is equal to $\boldsymbol{\alpha} \cdot \boldsymbol{H}$. The regularization parameter is usually set to the average variance of electrode noise [Sekihara et al., 2005]. Based on the assumption that the activity of the actual source is uncorrelated to the measurement noise and uniformly distributed across the brain, the electric potential variance can be described by equation **(H.3)**. [Pascual-Marqui, 2002]

$$\boldsymbol{S_\phi} = \boldsymbol{K} \cdot \boldsymbol{S_J} \cdot \boldsymbol{K^T} + \boldsymbol{S_\phi^{noise}} = \boldsymbol{K} \cdot \boldsymbol{K^T} + \boldsymbol{\alpha} \cdot \boldsymbol{H} \tag{H.3}$$

Where $\boldsymbol{S_\phi}$ is the electric potential variance, K is the lead field matrix, $\boldsymbol{S_J}$ is the actual source variance, H is the average reference operator, and $\boldsymbol{S_\phi^{noise}}$ is the electric potential variacne due to noise ($\boldsymbol{S_\phi^{noise}} = \boldsymbol{\alpha} \cdot \boldsymbol{H}$)

Based on the linear relation of the minimization, the variance of the current density can thus be expressed as; $\boldsymbol{S_j} = \boldsymbol{T} \cdot \boldsymbol{S_\phi} \cdot \boldsymbol{T^T} = \boldsymbol{K^T} \cdot [\boldsymbol{K} \cdot \boldsymbol{K^T} + \boldsymbol{\alpha} \cdot \boldsymbol{H}]^{+} \cdot \boldsymbol{K}$. Consequently the estimates of standardized current density power calculated in sLORETA are defined in equation **(H.4)**

$$\boldsymbol{ESCD} = \hat{\boldsymbol{J}}_{\boldsymbol{l}}^{\boldsymbol{T}} \cdot [\boldsymbol{S_J}]_{\boldsymbol{ll}}{}^{\mathbf{-1}} \cdot \hat{\boldsymbol{J}}_{\boldsymbol{l}} \tag{H.4}$$

with ESCD being estimate of standardized current density and l defined as the l'th voxel. [Pascual-Marqui, 2002]